

IN THE UNITED STATES DISTRICT COURT
FOR THE WESTERN DISTRICT OF TEXAS
SAN ANTONIO DIVISION

JACQUELINE ONOFRE, INDIVIDUALLY
AND A/N/F OF LUKE ONOFRE and
HANNAH ONOFRE, MINORS
V.

C.R. ENGLAND and
PAUL JOHNSON

§
§
§
§
§
§
§

CIVIL ACTION NO. 5:15-cv-000425-DAE

AFFIDAVIT OF RICHARD V. BARATTA, Ph.D., P.E.

STATE OF TEXAS

COUNTY OF HARRIS

BEFORE ME, the undersigned authority, personally came and appeared Richard V. Baratta, Ph.D., P.E. who, being first duly sworn did depose and state:

1. I have Bachelor's degrees in biomedical engineering and mathematics, a Master's degree in biomedical engineering, and a PH D. in biomedical engineering, all from Tulane University in New Orleans, Louisiana. I received my Ph.D. in 1989 and have worked in the field of biomechanics since that time. I am also a traffic accident reconstruction expert, having completed a course in traffic accident investigation at Northwest University in Illinois and being accredited by the Accreditation Commission for Traffic Accident Reconstructionists (ACTAR). I am a registered professional engineer in a number of states, including Texas. A true and correct copy of my *curriculum vitae* is attached to the response to the motion to strike my testimony.

2. Biomechanics is the application of principles of mechanics or engineering to problems in medicine and biology. Simply stated, the field of biomechanics involves the study of how human tissue behaves under various loads. As one might expect, much of the literature in the field of biomechanics relates to the study of accidents and other events and how they result in injury to human tissue. The field of biomechanics is widely accepted in the medical community and is a course taught in medical school.

3. From 1990-1997, I was affiliated with Tulane University School of Engineering, training engineering students in orthopedic biomechanics and research. From 1991 to 2004, I was employed by the LSU School of Medicine at New Orleans, performing research in orthopedics, training

orthopedic residents on biomechanics and tissue mechanics, and teaching physical therapy students, and attaining the position of tenured Professor of Orthopedic Surgery. In 2005, I taught a biomechanical course under the auspices of the American Academy of Orthopedic Surgeons, which was an update course for those physicians seeking to become board certified in the field of orthopedics.

4. I have been qualified as an expert in biomechanics and accident reconstruction approximately seventy times in trial and twelve times in arbitration.

5. My opinions in the instant case are based upon generally accepted principles in biomechanics and biomedical engineering and are supported by studies that have been conducted in these fields. It is a generally accepted principle in the field of biomechanics that scientific testing has proven that disc herniations are generally the result of a slow degenerative process and not due to trauma unless the traumatic event results in fracture to the bone or significant hyper flexion and compression with forceful torsion beyond the parameters of normal physiologic motion.

6. Attached hereto as Exhibit "A" is an excerpt from a treatise titled Trauma Biomechanics: Introduction to Accident Injury. This is a widely accepted authoritative treatise in the field of biomechanics. The excerpt shows that there is generally no causal relationship between impact and disc rupture—which includes disc herniations and protrusions—as ruptures are generally the result of a slow degenerative process.

7. Attached as Exhibit "B" is an excerpt from a chapter on injury to the thoraco-lumbar spine and pelvis, by Albert I. King, who is a widely regarded researcher in the field of biomechanics. This chapter is part of a treatise titled Accidental Injury: Biomechanics and Prevention, edited by Alan Nahum and John Melvin, both highly regarded researchers in the fields of injury biomechanics. In the chapter, King discusses studies which have been done on cadavers to determine the relationship between disc rupture and impact loading on the spine and which have led to the conclusion that disc ruptures do not occur as the result of a single loading event, unless there are associated massive bony injuries to the spine. King discusses the fact that earlier researchers have concluded that the vertebral body always broke before the adjacent disc incurred visible damage. Even loads causing fracture of the vertebral body did not result in herniation or excessive bulging. There are only two reports of disc rupture due to a single loading event in the literature, both involving the lumbar spine and significant hyper flexion and compression with forceful torsion, meaning that the lumbar spine of the cadaver would have been doubled over, pushed down and twisted all at the same time. I am unaware of any peer-reviewed literature in which an

author has been able to replicate a cervical disc herniation in the absence of a fracture.

8. Attached hereto as Exhibit "C" is an excerpt from Biomechanics of Musculoskeletal Injury by William Whiting and Ronald Zernicke. This is another widely accepted treatise in the field of biomechanics. Notably, nowhere in the section on lumbar spine injury mechanisms is there a discussion of herniations in the lumbar spine, as it is not generally accepted that disc herniations in the lumbar spine are related to traumatic injury. While many physicians in practice will relate disc herniations to accidents and other isolated loading events based upon the history given by the patient, actual scientific testing on the lumbar discs of cadavers does not support this theory, as discussed above. Orthopedic surgeons are taught this information as part of their training, but the practicing physician typically is not trying to analyze an accident and its effect on human tissue scientifically. Rather, the primary role of the physician is to diagnose the condition and treat it.

9. In order to render an opinion as a biomechanical and accident reconstruction expert in the instant case, it was necessary for me to try to evaluate the probable forces which were placed upon the human tissue of the occupant of the vehicle during the accident. My review of the photographs as well as the anecdotal information available to me led me to the conclusion that this case involved an event analogous to a sideswipe collision because it resulted in a sliding motion/contact between the vehicles, which simply results in vibrational motions to the Plaintiff's vehicle rather than net motion, as would occur in an "impact." This case does not involve an "impact" because that is something that happens over a very short period of time, unlike the sliding contact in this case. Also, contact between the vehicles was limited to the Plaintiff's lift gate, which would limit the loads transmitted to the body of the vehicle and the occupant.

10. Attached to my affidavit as Exhibits "D" and "E" are published, peer reviewed papers involving the biomechanical study of sideswipe contacts on human subjects, such as the one in this case, which support my conclusions. *Vehicle and Occupant Response in Heavy Truck to Passenger Car Sideswipe Impacts*, by Tanner, Wiechel, and Guenther.

11. Exhibit D, "*Vehicle and Occupant Response in Heavy Truck to Passenger Car Sideswipe Impacts*", shows that occupant accelerations are less than those experienced by the vehicle, and well below those experienced during activities of daily living.

12. Attached to my affidavit as Exhibit "F" is an article entitled "*Passenger Vehicle Occupant Response to Low Speed Impacts Involving a Tractor-*

Semitrailer", which also shows that the vehicle accelerations experienced during sideswipes is well within the levels experienced during daily activities.

14. Attached hereto as Exhibit "G" is an article titled Occupant "Data and Methods for Estimating the Severity of Minor Impacts" that compares the results of many research studies and indicates that subjects do not exhibit symptoms with impacts such as occurred in this accident.

13. Also attached hereto as Exhibit "H" is an article titled "Acceleration Perturbations of Daily Living". This article illustrates that in various activities in daily living, we experience accelerations that are actually much higher than those experienced during low velocity accidents. For example, the article illustrates that being jostled in a crowd can result in accelerations of 8.1g, and plopping down into a chair can involve accelerations of 10.1g.

14. As per my report, a true and correct copy of which is attached here as Exhibit "I", it is my scientific opinion that there were no forces involved in this accident that were sufficient to cause significant hyper-flexion or compression with torsion on the plaintiff's spine. We know that the accident did not cause any type of fracture. Disc herniations based upon a single loading event such as an accident, in the absence of fracture and in the absence of significant hyper-flexion and compression, have not been able to be duplicated in the laboratory research that has been done in the field of biomechanics. Further, no laboratory research has been able to duplicate cervical disc herniations in the absence of a fracture, irrespective of flexion and compression.

15. My analysis did not require an actual view of the scene of the collision, as there do not appear to be any unique properties of the property which would need to be taken into account from a biomechanical standpoint. Likewise, I was able to obtain sufficient information regarding the vehicles in question from the photographs and published resources relating to those vehicles. Further, the use of photographs is a common and accepted method of evaluating accident severity. Attached is Exhibit "J" titled "Evaluating the Uncertainty in Various Measurement Tasks Common to Accident Reconstruction." This article establishes the use of photographs along with other information as accepted and commonly used in the accident reconstruction community.

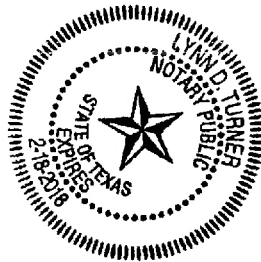
16. In light of the foregoing, it is my opinion that the accident in this case did not result in a high level of g force acceleration/deceleration upon the occupant of the vehicle, with very little if any movement of the body during the crash. The vehicle's suspension system would have absorbed most of the movement forces on the vehicle, and the remaining forces would have been insufficient, particularly in the absence of a compressing force, to have caused any disc herniations.

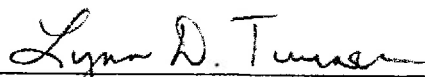
17. It is also my scientific opinion that there were no forces involved in this accident that were sufficient to cause significant hyper-flexion or compression with torsion on Ms. Onofre's spine. We know that the accident itself did not cause any type of fracture. Disc herniations based upon a single loading event such as an accident, in the absence of an acute fracture and in the absence of significant hyper-flexion or compression with forceful torsion, have not been able to be duplicated in the laboratory research that has been done in the field of biomechanics.



RICHARD V. BARATTA, Ph.D.

SWORN TO AND SUBSCRIBED before me, Notary, on this the 8th day of July,
2015.





NOTARY PUBLIC
MY COMMISSION EXPIRES: 2-18-2018

K.-U. Schmitt
P. Niederer
F. Walz

Trauma Biomechanics

Introduction
to Accidental Injury

 Springer

which can result in separation of the posterior elements of the spine, for instance, by ruptures of the supra- and interspinous ligaments. Furthermore, the spinal cord is stretched and might be injured.

Injuries of the soft tissue of the thoracolumbar spine are also often reported after automotive accidents. The soft tissues involved are the intervertebral discs, the various ligaments, the facet joints, the muscles and tendons attached to the vertebral column. A usual complaint of this type of injury is low back pain. Incidents provoking this complaint are manifold, ranging from minor rear-end collisions to severe frontal impacts. In some cases the back pain is associated with disc rupture or disc bulge. However, a causal relationship between an impact and a rupture does usually not exist [King 2002]. Disc ruptures are generally the result of a slow degenerative process.

4.3 Biomechanical response and tolerances

The mechanical performance of the human spine was subject to numerous volunteer, cadaver, animal and dummy tests. Experiments were conducted statically and dynamically (both with and without head impact) utilising different test set-ups (see also section 2.5). Further, the use of so-called functional units is common in spine testing. Here a functional unit usually means a motion segment consisting of two or three vertebrae. Tissue that is not of interest in the study performed (e.g. muscles) is dissected. Analysing the head-neck kinematics, some studies also use larger units that are made of a cadaver head and neck whereas the neck is fixed at its lower end and then mounted on a (mini-) sled. However, it has to be noted that the use of functional units can influence the kinematics significantly. This has to be considered when drawing conclusions from results obtained in such experiments.

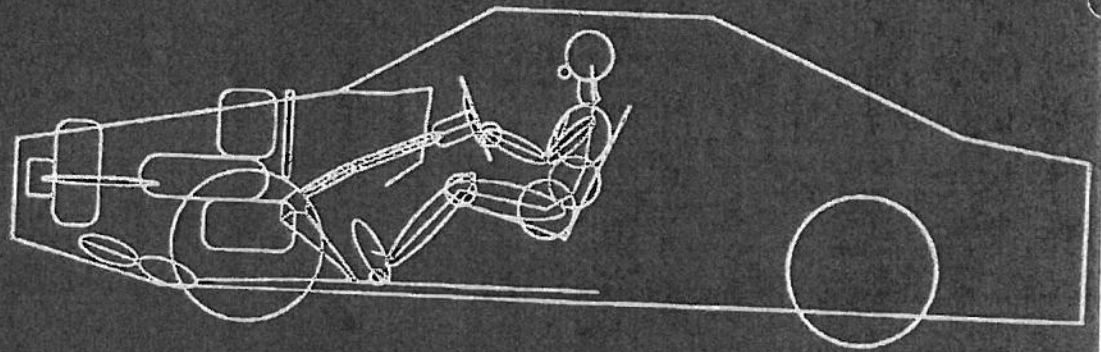
Muscle activity can often not be simulated in experiments, because they are either removed (functional units) or without muscular tonus (cadaver experiments). Only volunteer experiments offer the possibility to measure to some extent muscle activity. Tolerances to other spinal injuries, like for instance vertebral artery lesions, are difficult to assess because a physiological limit of the loading of the structure of interest cannot be defined properly.

Investigating the biomechanical response of the cervical spine, many studies still refer to and rely on tolerance levels based on volunteer and cadaver experiments that were performed in the late nineteen sixties and the

SECOND EDITION

Accidental Injury

BIOMECHANICS
AND
PREVENTION



Alan M. Nahum
John W. Melvin
EDITORS

and Bogduk and Twomey (1987) as well as to a study by King et al (1990). There is some evidence that pain fibers are present in the outer layers of the intervertebral disc annulus. They are found in and around the capsules of the facet joints, extending to the borders of nearby ligaments and tendons.

The biomechanics of soft tissue deformation has also been studied. Stokes (1987) found that the strain of the anterior disc due to an applied compressive load was about 10% along the directions of the annular fibers. In Cavanaugh et al (1996), it was reported that the human facet joint capsule can undergo large deformations, particularly during spinal extension. In fact, during cadaveric experiments on spinal motion segments under static loading, the stretching of the superior lateral corner of certain facet capsules can be easily seen without optical magnification. The stretch can vary over a large range of strain, depending on the geometry of the facets. Table 18.3 shows data provided by Cavanaugh et al given in the form of stretch per unit moment (in N.m). The peak values of the flexion and extension moments applied were 24 and 18 N.m, respectively.

With respect to the third requirement, it is a well-known fact that nociceptors have high thresholds and do not go off unless stimulated vigorously. The large deformations noted in the facet capsules may be large enough but it is nec-

essary to demonstrate this neurophysiologically. Yamashita et al (1990) and Avramov et al (1991) have mapped the distribution of nociceptors and other types of mechanoreceptors in and around the facet joint. They have also shown that spinal load and stretching of the facet capsule can cause the high threshold nociceptors to fire. This work confirms the previously reported facet syndrome by Mooney and Robertson (1976) and others. In fact, facet pain may be responsible for a large proportion of the LBP being reported. This combined neurophysiological and biomechanical technique is being extended to the disc, which appears to be sensitive to a change in the pH of its contents (Nachemson, 1969).

A significant finding of the research by Cavanaugh and colleagues was the lowering of the threshold of the nociceptors in the presence of spinal degeneration or of an inflammatory process. When the facet capsule was artificially inflamed with carrageenan, the nociceptors would fire spontaneously and would fire more rigorously if stimulated (Ozaktay et al 1994). However, the firing of nociceptors is non-adaptive. That is, they will continue to fire until the stimulus is removed, as opposed to other mechanoreceptors that cease to fire even though the stimulus is still acting. Thus, the pain resulting from a mechanical stimulus to a degenerated spine should be a temporary exac-

TABLE 18.3. Maximum tensile facet capsule stretch (%/N.m).

Cadaver no.	Extension tests			Flexion tests		
	X-axis ^a	Y-axis ^b	Z-axis ^c	X-axis	Y-axis	Z-axis
400	7.1	8.7	5.3	0.6	0.2	0.1
464	4.8	5.5	8.2	0.1	0.4	0.3
807	3.3	2.5	6.4	0.4	0.6	0.3
329	7.4	6.3	0.2	0.8	2.6	1.9
455	1.3	3.9	1.3	0.3	1.3	0.3
490	0.8	2.5	4.7	2.2	4.5	1.2
002	0.8	7.4	7.0	1.3	3.5	6.4
117	0.8	6.6	6.6	0.9	7.1	1.3
034	12.4	21.0	21.1	2.0	0.3	3.0
SD	4.0	5.6	6.0	0.7	2.4	2.0
CV	93.8	78.4	88.7	77.5	104.5	122.8

^aThe X-axis is directed anteriorly in the transverse plane.

^bThe Y-axis is directed laterally to the left in the transverse plane.

^cThe Z-axis is directed superiorly, normal to the transverse plane.

A.I. King

18. Injury to the Thoracolumbar Spine and Pelvis

467

ate this neurophysiologi- (1990) and Avramov et al the distribution of noci- es of mechanoreceptors in et joint. They have also ad and stretching of the se the high threshold noci- work confirms the previ- syndrome by Mooney and d others. In fact, facet pain r a large proportion of the l. This combined neuro- omechanical technique is e disc, which appears to be in the pH of its contents

ing of the research by agues was the lowering of ociceptors in the presence n or of an inflammatory et capsule was artificially eenan, the nociceptors usly and would fire more ed (Ozaktay et al 1994) of nociceptors is non- ey will continue to fire removed, as opposed to ors that cease to fire even is still acting. Thus, the mechanical stimulus to a ould be a temporary exac-

erbation of a painful condition. Another aspect of pain is its ability to initiate a vicious cycle of pain that is brought on by the production of neurotransmitters, such as substance P. These transmitters travel to the site of pain and further decrease the threshold of the nociceptor, resulting in more pain. This phenomenon explains the observed cycle of back pain in some individuals whose back pain gets worse day after day until they can no longer get out of bed. Then the cycle is reversed and they recover practically without any treatment. Nevertheless, the exacerbation is still temporary and should last from a few days to a few weeks. Continuous complaints of chronic pain without remission are possibly due to psychological or other physical causes. One such physical cause has been described by Ozaktay et al (1995) and Chen et al (1997). They have shown that the toxic chemical phospholipase A₂ (PLA₂) found in the nucleus pulposus can destroy nerve endings and cause the axons in the nerve root and the dorsal root ganglion to send nociceptor signals up the spinal cord, signaling referred pain in the lower extremities. The sympathetic nervous system can also be involved in the form of abdominal visceral pain at the level of L2-3 for a degenerative disc condition in the lower lumbar spine (Nakamura et al, 1996).

Research into facet pain may have provided an incentive for neurologists and anesthesiologists to treat back pain nonsurgically with facet injections and rhizotomies. There is, however, a predominant majority of physicians who attribute back pain solely to the intervertebral disc. Of course, surgical intervention usually involves the disc and there are no surgical procedures for facet pain. The reimbursement incentive is reinforced by the traditional belief that disc pain is synonymous with low back pain. This indeed is a concept that has outlived its scientific usefulness. While it is true that a degenerated disc can cause pain, it can induce facet pain due to loss of disc height, leading to an increase in facet load, and there are many other causes of back pain. Low back pain is a complex problem that cannot be neatly explained by a single cause. Much research remains to be done, but for minor impact loads the complaint of pain cannot be equated

with permanent injury of the soft tissue involved.

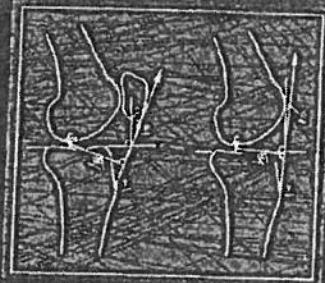
With regard to the relationship between disc rupture and impact loading on the spine, it can be safely said that disc ruptures do not occur as the result of a single loading event, unless there are associated massive bony injuries to the spine. This statement is based on a review of the literature on spinal response by Henzel et al (1968), who indicated that early researchers such as Ruff (1950), Brown et al (1957), and Roaf (1960) observed that the vertebral body always broke before the adjacent disc incurred visible damage. Moreover, Brinckmann (1986) has shown that a severely weakened lumbar disc, with the posterior elements removed, could not be ruptured and hardly even bulged when loaded in compression to 1 kN. Additional loads causing fracture of the vertebral body did not result in herniation or excessive bulging. There are two reports of disc rupture due to a single loading event in the literature. Farfan et al (1970) applied torsional loads to intact lumbar motion segments without any compressive preload and was able to cause posterior and anterior disc ruptures after a rotation averaging 22.9 degrees for normal discs and 15.2 degrees for abnormal discs. They also tested facet joints and facet capsules to failure and found that the average angle at which they failed was 14 and 12 degrees, respectively. This meant that if the facets were allowed to slide over each other or fracture, resulting in a large rotation, then the rupture can occur. Normally, in the presence of a preload of the facets, a single torsional load that does not disrupt the facets or tear the capsules does not cause rupture. The second report is by Adams and Hutton (1982), in which they caused spontaneous rupture of several discs by compressing the spine while it was hyperflexed both laterally and sagittally. If the disc did not rupture on the first try, it was flexed 1 or 2 degrees more and loaded again with the same load. The average angle of flexion was 12.9 degrees, implying that the lumbar spine alone was flexed a total of 64 degrees. The average applied load was 5,449 N (1,225 lb). This situation is again not representative of a realistic loading condition, as it is extremely

ests

Z-axis

0.1
0.3
0.3
1.9
0.3
1.2
6.4
1.3
3.0
2.0
122.8

Biomechanics *of* Musculoskeletal INJURY



William C. Whiting
Ronald F. Zernicke

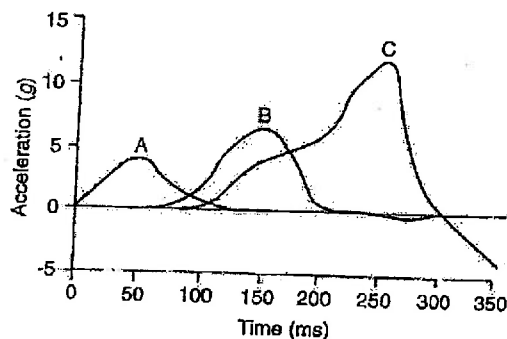


Figure 8.20 Idealized acceleration curves of (A) an impacted vehicle, (B) an occupant's shoulders, and (C) an occupant's head. As the vehicle is impacted (e.g., in an automobile rear-end collision), it accelerates first, reaching a peak acceleration of almost 5 g's (i.e., five times the acceleration of gravity). The vehicle occupant's shoulders reach their peak acceleration of about 7 g's 100 ms later. Finally, the occupant's head reaches its peak acceleration of greater than 12 g's 250 ms after initial impact. This sequential progression of peak accelerations is evidence of both momentum and energy transfers.

Reprinted from Barnsley, Lord, & Bogduk 1994.

forces prior to cervical hyperextension, and cervical structures are prestretched and more predisposed to severe injury.

At first glance, whiplash might appear a simple injury mechanism. However, "in an individual accident there is likely to be a complex interaction between different forces depending upon the speed and direction of impact and the attitude of the head and neck" (Barnsley, Lord, & Bogduk 1994, 288). Many structures can be injured in whiplash accidents. These include structures in the brain, temporomandibular joint, muscles, spinous ligaments, intervertebral disks, vertebral bodies, and facet (zygapophyseal) joints. Various mechanisms and potential injury sites are shown in figure 8.21.

Cervical Spondylosis

The etiology of chronic cervical conditions, such as cervical spondylosis, stands in marked contrast with the potentially catastrophic traumatic injuries just described. While their onset is less dramatic, chronic injuries nonetheless can cause considerable dysfunction. Cervical spondylosis is a general term used to describe degenerative changes in the cervical intervertebral disks and surrounding structures.

As part of the normal aging process, disks lose vertical height and become less extensible, due in large part to reduced water content and degradation of the disk substance. Disk degeneration is accompanied by osteophyte (bony outgrowth) formation and increased stresses on articular cartilage. These structural alterations increase the risk of spinal stenosis (narrowed canal), impingement on neural tissue, and impaired blood perfusion of the spinal cord. Symptoms associated with cervical spondylosis include paresthesia, neck and arm pain, weakness, and sensory loss. Recent advances in imaging technologies (e.g., magnetic resonance imaging) have improved diagnostic accuracy. Considerable debate continues, however, on the advisability of surgical intervention in treating the lesions associated with cervical spondylosis.

Disturbance or disease of the spinal cord (myelopathy) associated with cervical spondylosis is a well-recognized clinical entity. Mechanical factors that may be causal agents in cervical spondylotic myelopathy include a narrowing of the spinal canal, kyphotic conditions causing cervical flexion, spinal cord compression and related ischemia, and ligamentous ossification. Despite the often insidious onset of cervical spondylosis, its sequelae have significant potential for causing severe neuromuscular dysfunction.

Trunk Injuries

The trunk (also called truncus or torso) extends from the base of the neck down to the pelvic girdle. As the largest body region, the trunk accounts for 45% to 50% of the body's mass and contains such vital organs as the heart (and its major vessels), spinal cord, lungs, stomach and intestines, kidneys, liver, and spleen. The sternum, ribs, and vertebrae of the axial skeleton protect these important organs.

Trunk musculature serves both movement and protective functions. The principal muscles of the anterior trunk are the pectoralis major, serratus anterior, rectus abdominis, external obliques, internal obliques, and transversus abdominis (figure 8.22b). Important posterior trunk muscles include the trapezius, latissimus dorsi, rhomboids (major and minor), and erector spinae (figure 8.22, a and c).

Vertebral Fracture

Spinal fractures are a major health concern, with more than 80,000 cases in the United States each

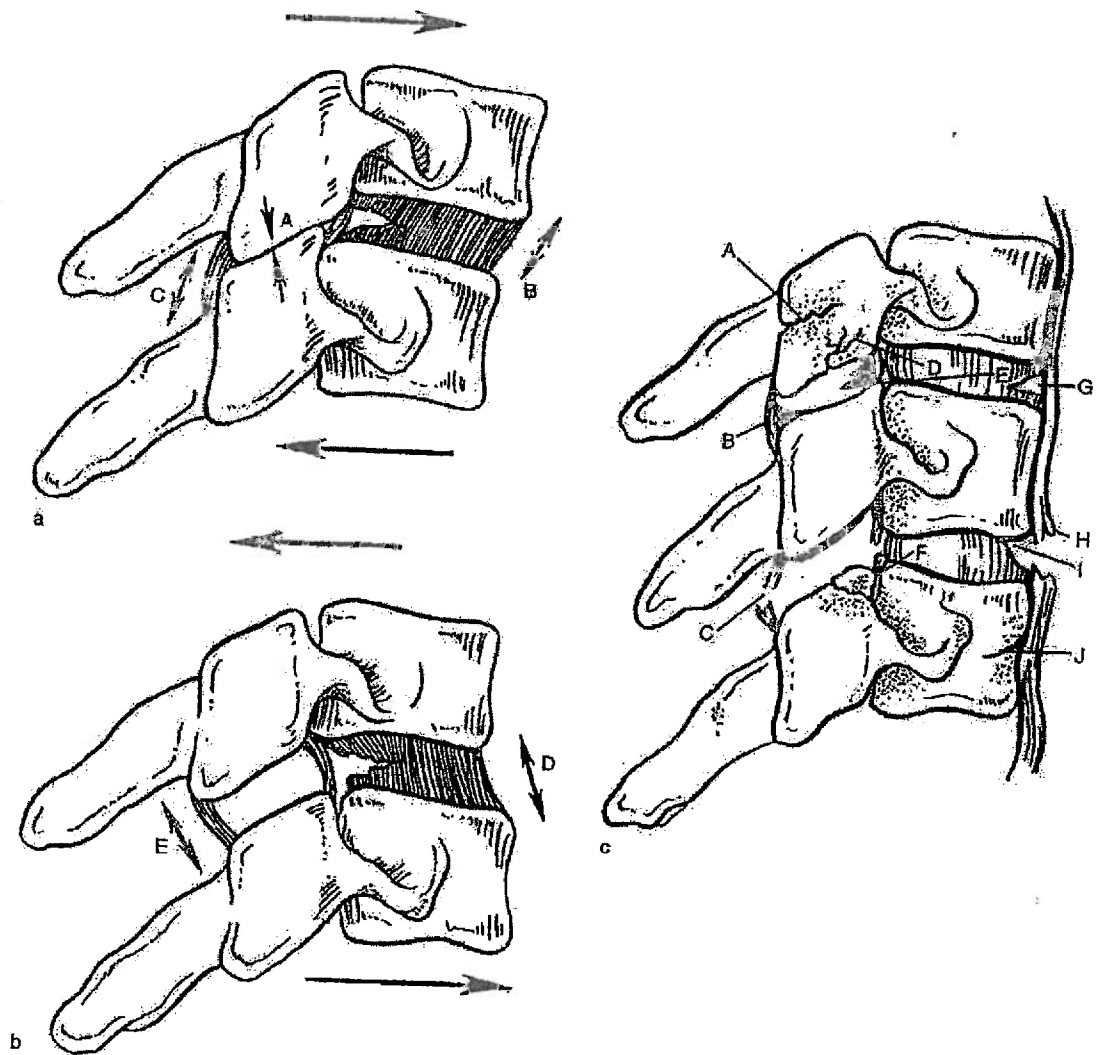


Figure 8.21 Shear forces affecting a spinal motion segment. (a) Translation of the superior vertebral body anteriorly relative to the inferior body. This movement stresses the articular surfaces of the zygapophyseal joints (A), the anterior annulus fibrosus (B), and the zygapophyseal joint capsule (C). (b) Translation of the superior vertebral body posteriorly relative to the inferior body, which stresses the intervertebral disk (D) and the zygapophyseal joint capsules (E). (c) Common lesions affecting the cervical spine following whiplash injury. A, articular pillar fracture; B, hemarthrosis (hemorrhage into a joint) of the zygapophyseal joint; C, rupture or tear of the zygapophyseal joint capsule; D, fracture of the subchondral plate; E, contusion of the intraarticular meniscus of the zygapophyseal joint; F, fracture involving the articular surface; G, tear of the annulus fibrosus; H, tear of the anterior longitudinal ligament; I, end-plate avulsion fracture; J, vertebral body fracture.

year (Praemer, Furner, & Rice 1992). Fractures of the vertebrae are of particular concern because of their close proximity to the spinal cord. In displaced

spinal fractures, bone fragments may be forced into the spinal canal and impinge on the cord. This impingement can cause severe neural damage and

attendant paralysis or even death. Vertebral fractures usually are caused by axial compressive loads and occur most commonly in the cervical and thoracolumbar regions. Vertebrae in the thoracolumbar region (variably defined to include vertebrae between T11 and L3) are especially susceptible to fracture because of the spine's relatively neutral alignment (minimal curvature) in this region, and because this region is a transition zone between the relatively rigid thoracic region and the more flexible lumbar region.

Roaf (1960) and Holdsworth (1963, 1970) provided early descriptions of the mechanism of compressive vertebral fracture. Holdsworth (1963) postulated a two-column model of the spine, consisting

of an anterior column (region between the anterior longitudinal ligament and the posterior longitudinal ligament) and a posterior column (posterior bony complex bounded by the posterior longitudinal ligament and the posterior ligamentous complex that includes the supraspinous ligament, interspinous ligament, capsule, and ligamentum flavum). Holdsworth's two-column model was modified by Denis (1983), who proposed a three-column model (figure 8.23) to explain the pattern of thoracolumbar injuries (table 8.5).

In describing the mechanism of compressive vertebral fracture, Holdsworth (1970) coined the term *burst fracture*, noting that when a severe compression force is applied to either cervical or

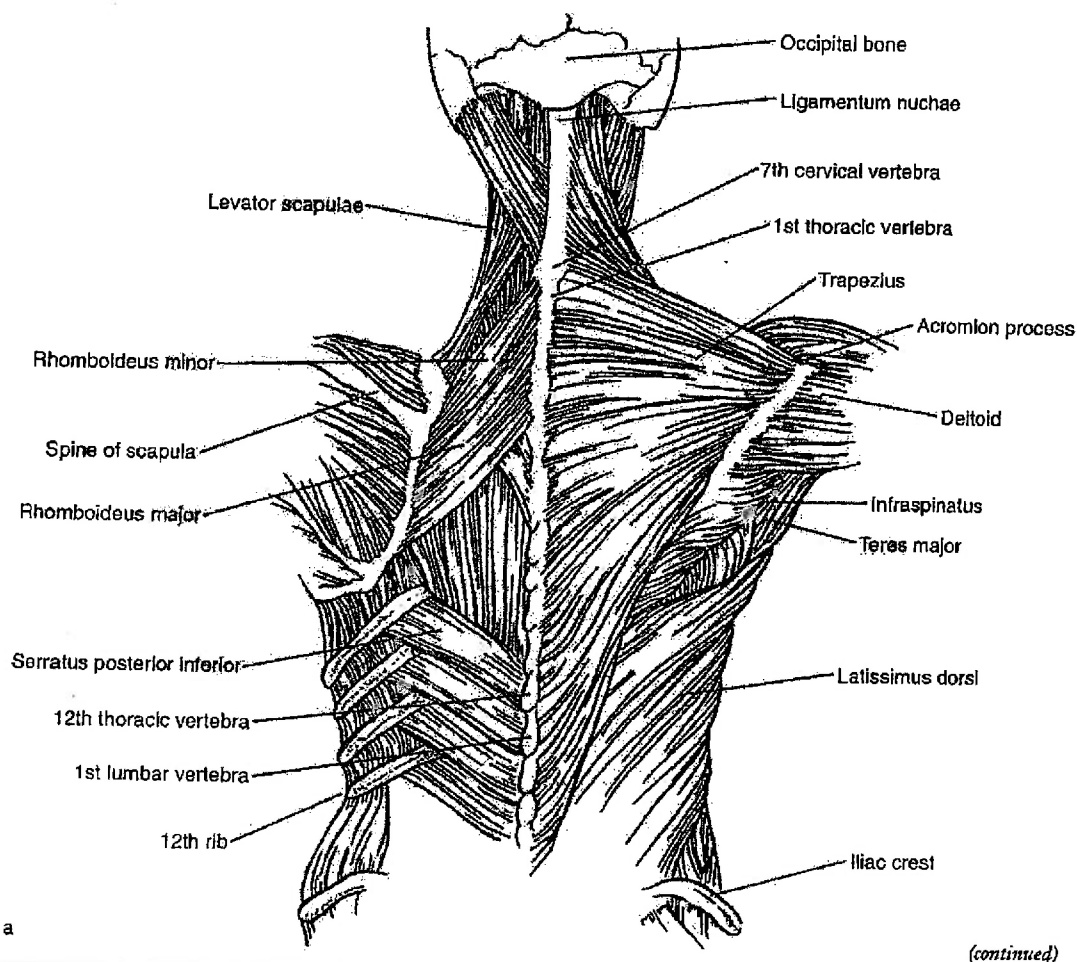


Figure 8.22 Musculature of the trunk. (a) Posterior view.

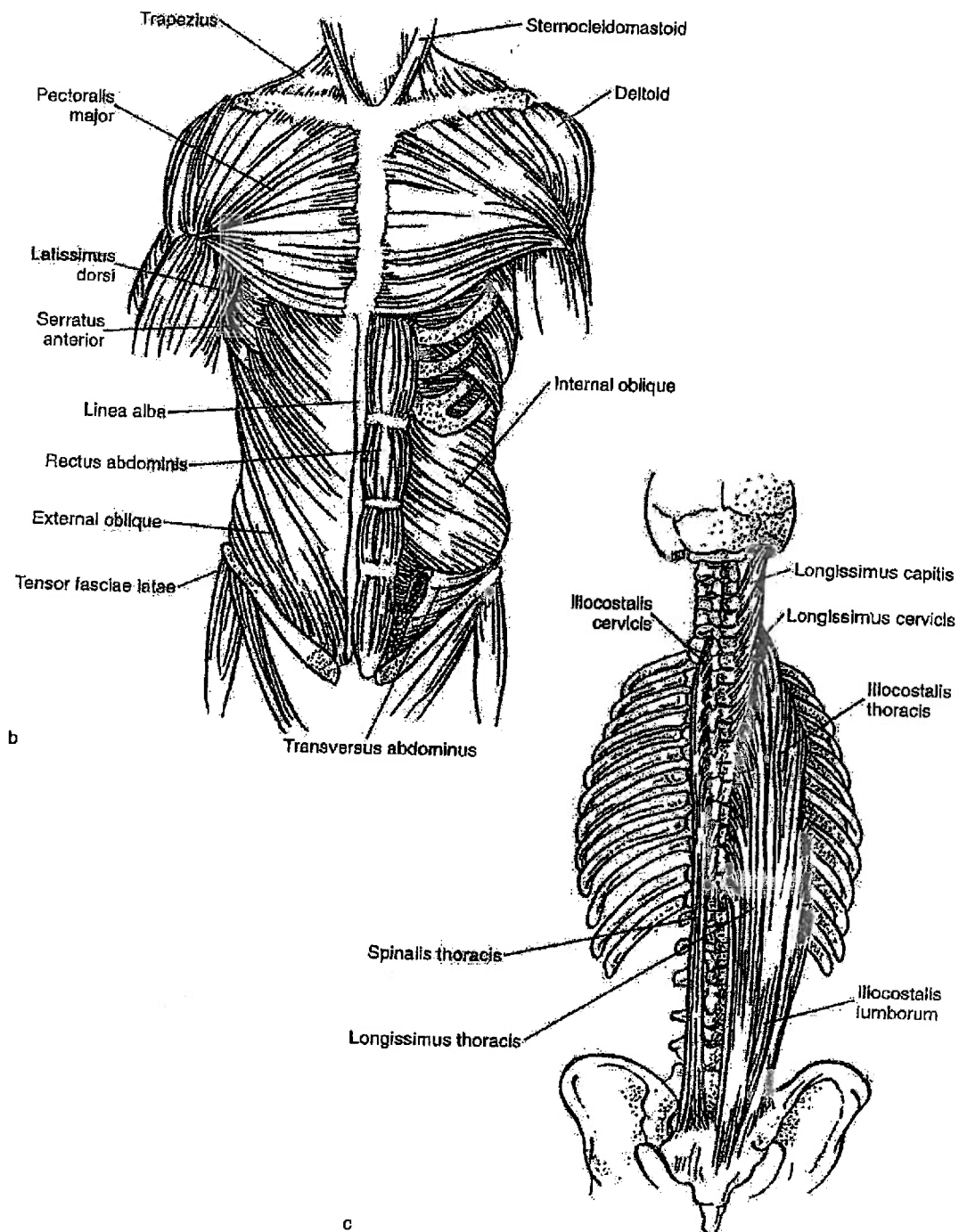


Figure 8.22 (continued) Musculature of the trunk. (b) Anterior view. (c) Deep muscles of the back, including the three subdivisions of the erector spinae group (iliocostalis, spinalis, longissimus).

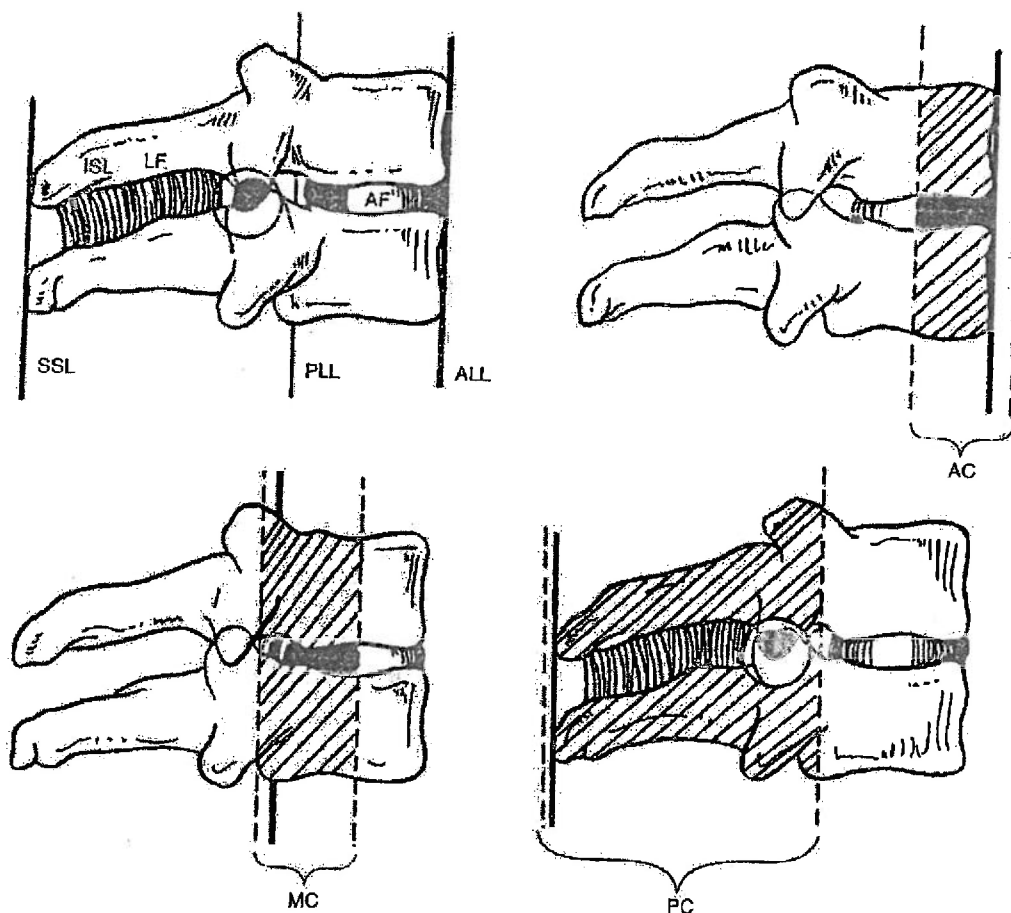


Figure 8.23 Three-column model of the spine: AC, anterior column (*upper right*); MC, middle column (*lower left*); PC, posterior column (*lower right*). Vertebral structures: SSL, supraspinous ligament; PLL, posterior longitudinal ligament; ALL, anterior longitudinal ligament; AF, annulus fibrosus; LF, ligamentum flavum; ISL, interspinous ligament. From "The three column spine and its significance in the classification of acute thoracolumbar spinal injuries" by F. Denis, 1983, *Spine*, 8(2), (Fig. 1, p. 818). Copyright 1983 by J.B. Lippincott Company. Reprinted by permission.

Table 8.5 Failure Mechanisms Using a Three-Column Model of the Spine

Type of fracture	Column		
	Anterior	Middle	Posterior
Compression	Compression	None	None or distraction (severe)
Burst	Compression	Compression	None
Seat-belt type	None or compression	Distraction	Distraction
Fracture dislocation	Compression rotation shear	Distraction rotation shear	Distraction rotation shear

From "The three column spine and its significance in the classification of acute thoracolumbar spinal injuries" by F. Denis, 1983, *Spine*, 8(2) (Table 1, p. 818). Copyright 1993 by Lippincott-Raven. Adapted by permission.

lumbar vertebrae when they are aligned in a straight (noncurved) row, or column, the body of the vertebra can shatter from within (i.e., explode or burst).

The danger of spinal cord lesion due to fragment displacement depends on the rate of loading. In controlled conditions, with constant energy input and force direction, spine motion segments impacted at high loading rates fracture with significant encroachment into the spinal canal. Low loading rates, in contrast, produce minimal intrusion (Tran et al. 1995).

The level of instability created by burst fractures has been the subject of some controversy, especially in cases where there is an absence of neurological deficit associated with the fracture. A study by Panjabi and colleagues (1994) found multiaxial instabilities, especially in response to axial rotation and lateral bending. Their results suggest that treatment of burst fractures requires caution and that their fixation and stabilization should be approached conservatively.

The degree of disk degeneration confounds the mechanism of burst fracture. A finite-element computer model (figure 8.24; Shirado et al. 1992) showed that in motion segments with normal disks, the highest stresses were found under the nucleus and at the superoposterior portions of the trabecular body. In a severely degenerated disk, no stresses were seen under the nucleus and little stress at the middle of the end plate. Based on the computer model of thoracolumbar loading, the researchers concluded that with healthy disks, rapid axial compressive loading induces a burst fracture with bone fragments retropulsed into the spinal canal. In people with severely degenerated disks (e.g., elderly with osteoporosis), burst fractures would be much less likely and, should they occur, would involve the anterior column and thus not have associated neurological deficits (Shirado et al. 1992).

Spinal Deformities

Injury, disease, and congenital predisposition all can cause deformities of the spinal column that take the form of abnormal structural alignment or alteration of spinal curvatures. These deformities are not injuries, per se, but since they often result in abnormal force distribution patterns and pathological tissue adaptations, they may indirectly lead to or exacerbate other musculoskeletal injuries and thus deserve mention in our discussion.

There are three primary types of spinal deformity: scoliosis, kyphosis, and lordosis. These deformities are classified by their magnitude, location, direction, and cause and can occur in isolation or in combination. Spinal deformities have long been associated with cardiopulmonary dysfunction. Hippocrates, for example, noted that hunchbacks (those with kyphosis) had difficulty breathing, and that patients afflicted with scoliosis commonly exhibited dyspnea, or shortness of breath (Padman 1995).

Scoliosis is defined as a lateral (frontal plane) curvature of the spine, which is also usually associated with a twisting of the spine (figure 8.25a). Mild spinal deviations are well tolerated and usually are asymptomatic. Severe deformities, in contrast, can markedly compromise cardiopulmonary processes. Scoliotic curvatures exceeding 90° greatly increase the risk of cardiorespiratory failure through the cumulative effect of decreased lung and chest wall compliance, poor blood oxygenation (hypoxemia), increased work of breathing, reduced respiratory drive, enlarged heart (cardiomegaly), and pulmonary arterial hypertension (Padman 1995).

Treatment options for scoliosis are either non-operative or operative. Nonoperative interventions include electrical stimulation, biofeedback, manipulation, and bracing. Of these, bracing has proved most successful (figure 8.25b). For severe scoliotic curvatures, the preferred treatment is operative vertebral fusion in which adjacent vertebrae are fused to forestall further progression of the deformity (figure 8.26).

The importance of early diagnosis and intervention should not be understated, since in many cases scoliotic deformity is progressive. Lack of early intervention can result in severe, even life-threatening, deformities later in life. While the causal mechanisms of scoliosis are often unknown, the mechanics of treatment in the form of braces or implanted spinal rods are well established and proven to be effective.

Kyphosis is a sagittal-plane spinal deformity characterized by excessive flexion and usually is seen in the thoracic region, where it produces a hunchback posture. Kyphosis is more severe in women than in men and is more prevalent with advancing age in both genders. Elderly, postmenopausal women are at particular risk, largely because of the strong association between kyphosis and osteoporosis (Bradford 1995). Kyphosis in these women is readily evident by the presence of a characteristic hump.

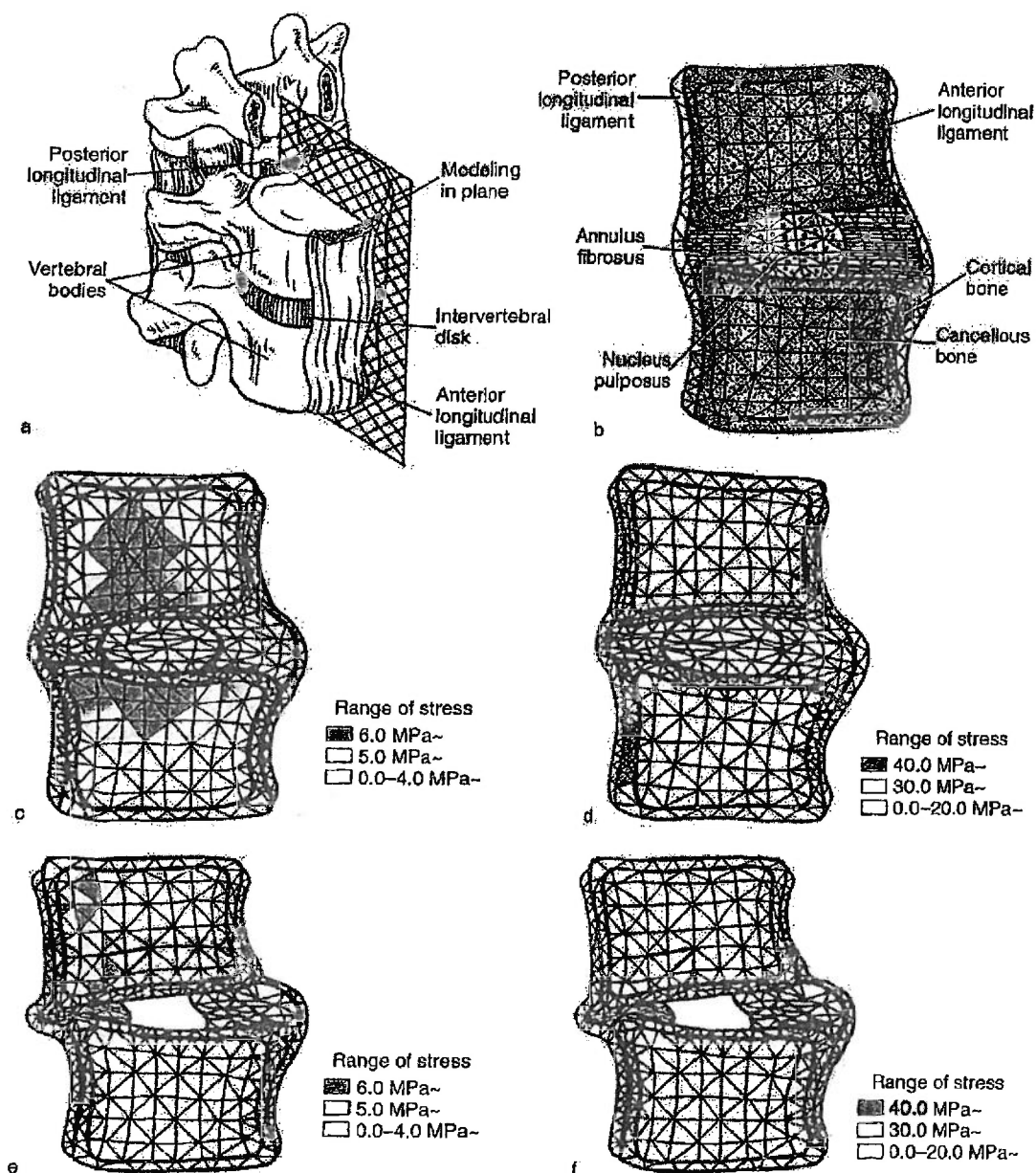


Figure 8.24 (a) Median (midsagittal) plane of modeling. (b) Finite-element plane model. (c) Stress distribution of one motion segment with a healthy disk under axial compression showing highest trabecular bone stresses under the nucleus pulposus and at the superoposterior regions, and (d) highest cortical shell stresses at the middle of the end plate and posterior wall cortex. (e) Stress distribution in a model of a severely degenerated disk shows no stresses in the trabecular bone under the nucleus, and (f) highest stresses in the cortical bone of posterior wall.

From "Influence of disc degeneration on mechanism of thoracolumbar burst fractures" by O. Shirado, K. Kaneda, S. Tadano, H. Ishikawa, P.C. McAfee, & K.E. Warden, 1992, *Spine*, 17(3) (Fig. 1, p. 287; Figs. 5 & 6, p. 291). Copyright 1992 by Lippincott-Raven. Adapted by permission.

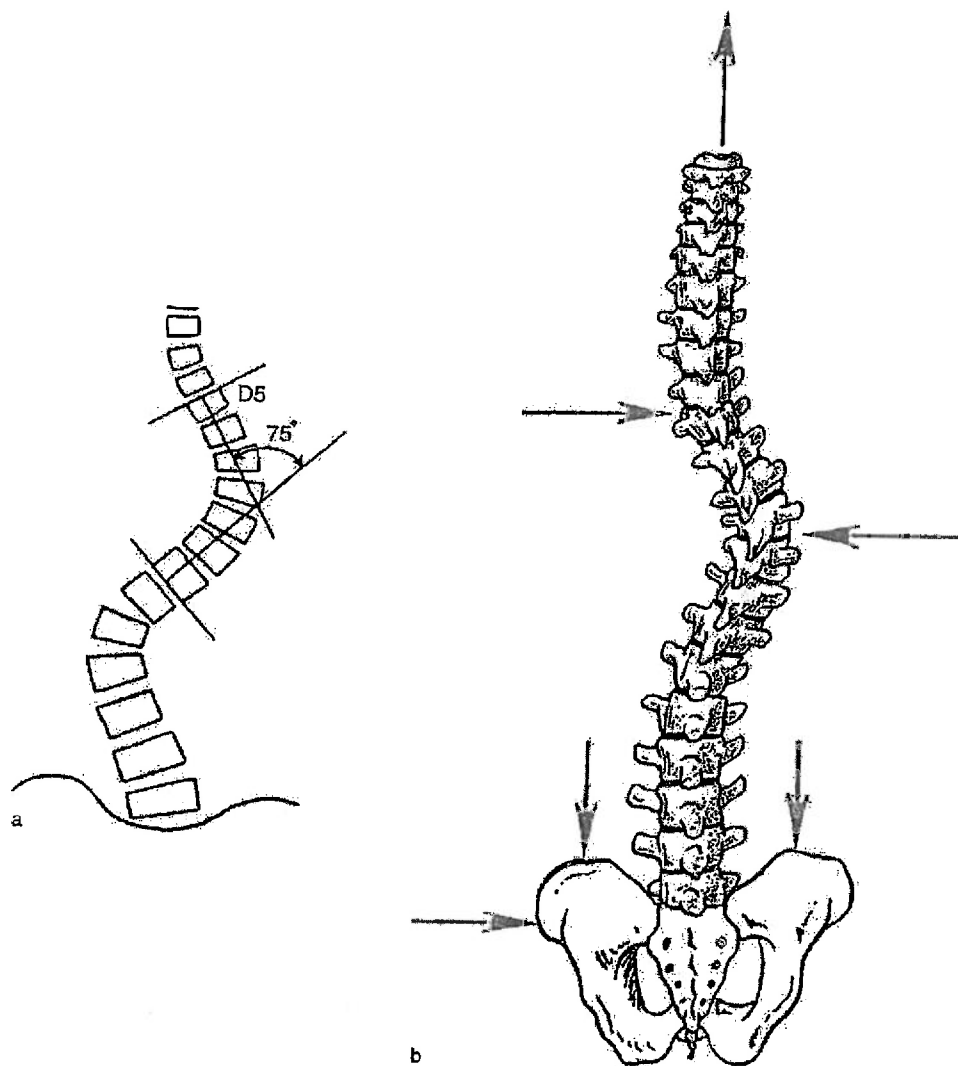


Figure 8.25 (a) Cobb's angle, defined as the angle (75° in the example shown here from Cobb's work) between the two lines that perpendicularly bisect the lines through the surfaces of the vertebrae at each end of the curvature. (b) Free-body diagram of the forces exerted on the spine by a brace to correct scoliosis deformity.

The degree of kyphosis is measured by the curvature of the spine in the sagittal plane (using a method similar to Cobb's angle, described in figure 8.25) or alternatively by the sum of the wedge angles between adjacent vertebrae (figure 8.27). The wedge angles of thoracic vertebrae T4-T12 increase exponentially as a function of age, up to 70 years (Puche

et al. 1995). This vertebral wedging and its attendant kyphosis affect rib mobility and pulmonary function. Specifically, the thoracic angle in kyphosis has a significant negative correlation with inspiratory capacity, vital capacity, and lateral expansion of the thorax (Culham, Jimenez, & King 1994). The best treatment for kyphosis may lie in prevention.

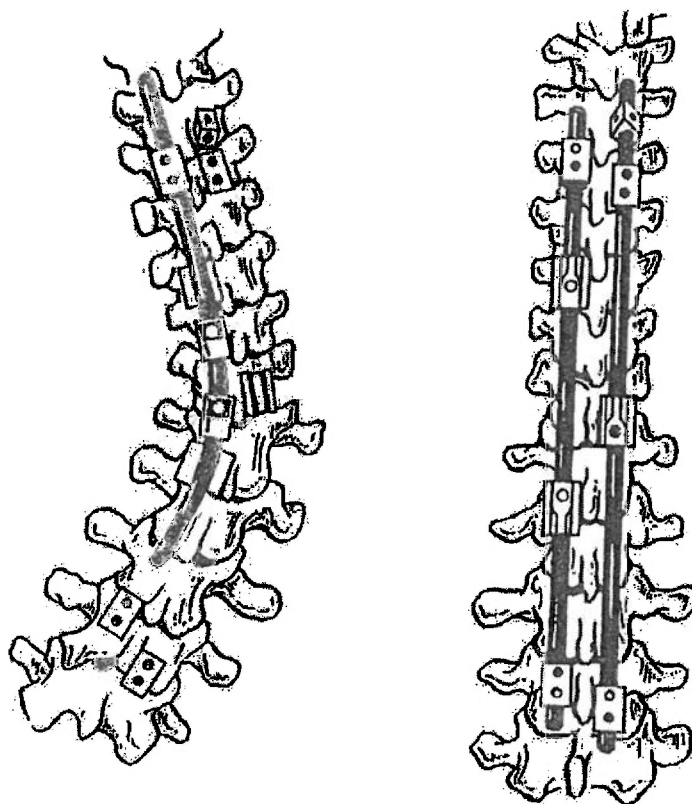


Figure 8.26 Variations of Harrington instrumentation used to correct spinal deformities.

Women with satisfactory exercise habits have a significantly lower index of kyphosis, suggesting that physical conditioning programs aimed at proper postural maintenance may delay or prevent the onset of kyphosis associated with aging (Cutler, Friedmann, & Genovese-Stone 1993).

Children may exhibit a special type of kyphosis, known as *Scheuermann's kyphosis*, in which structural changes are seen in the end plates of the growing vertebral bodies. Scheuermann's kyphosis is idiopathic, and mild cases are readily controlled by appropriate back extension exercises, with symptoms subsiding on completion of bone growth. More severe cases may require bracing or surgery as described earlier.

Lordosis is an abnormal extension deformity, usually seen in the lumbar region, that produces a hollow or swayback condition. Forward tilting of

the pelvis accentuates the lumbar lordosis. This tilting increases the lumbosacral (L5-S1) angle above its normal 30° orientation (figure 8.28) and accentuates the shear loading on the intervertebral disks and surrounding structures.

Spondylolysis and Spondylolisthesis

Low-back pain arises from myriad causes, including structural abnormalities, chronic overuse, and trauma. Two specific conditions that especially afflict young and athletic populations are spondylolysis and spondylolisthesis. These conditions affect the bony structure of the vertebrae, especially at the L4-L5 and L5-S1 levels. Spondylolysis is defined as a defect in the area of the lamina between the superior and inferior articular facets known as the

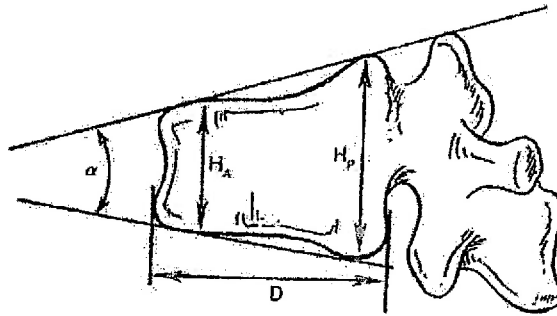


Figure 8.27 Vertebral wedging as measured by the angle α . The amount of wedging can also be measured by calculating the body height ratio (H_A/H_P).

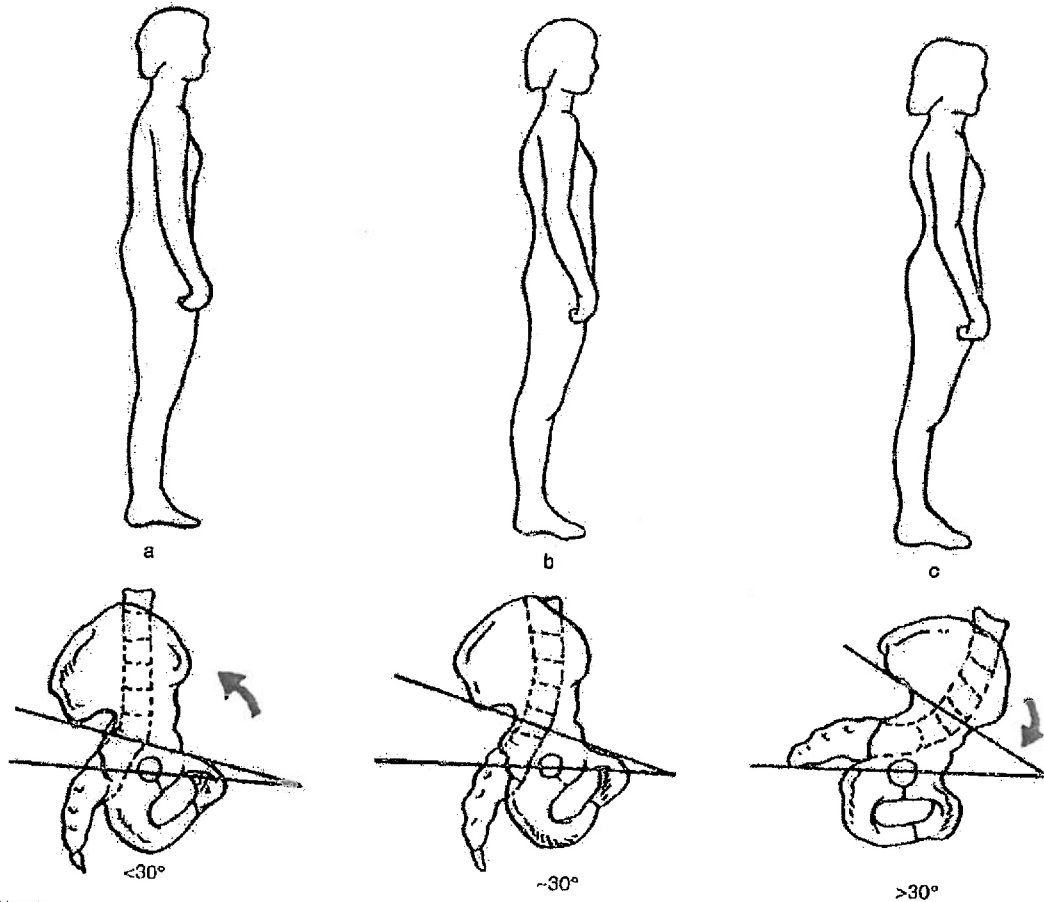


Figure 8.28 Effect of pelvic tilting on the lumbosacral (L5-S1) angle. (b) Normal standing creates a lumbosacral angle of approximately 30° . (a) Tilting the pelvis backward decreases the lumbosacral angle ($< 30^\circ$) and flattens the lumbar spine. (c) Tilting the pelvis forward increases the lumbosacral angle ($> 30^\circ$) and exaggerates the lumbar lordosis. Reprinted from Lindh 1989.

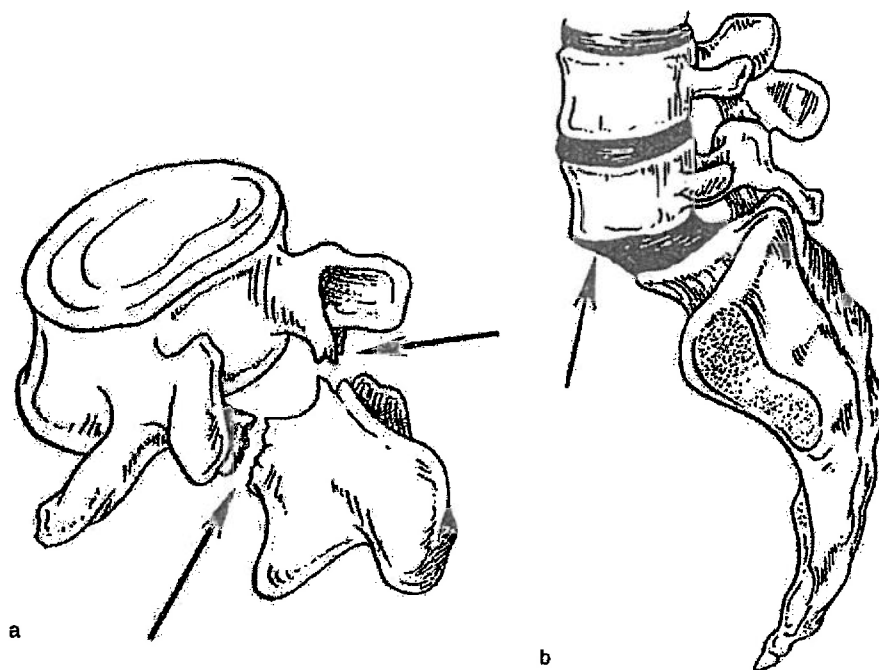


Figure 8.29 (a) Spondylolysis showing bilateral fracture of the pars interarticularis (arrows). (b) Spondylolisthesis exhibiting slippage (arrow) between the L5 and S1 vertebrae.

pars interarticularis (figure 8.29). Spondylolisthesis is translational motion, or slippage, between adjacent vertebral bodies. Most individuals with either condition remain asymptomatic.

Despite having been described in the literature for many years, spondylolysis and spondylolisthesis have remained a source of controversy. Recent advances in imaging techniques have permitted a better understanding of the pathogenesis of both conditions.

Classification of spondylolysis and spondylolisthesis according to their etiological and anatomical characteristics commonly identifies five types: dysplastic, isthmic, degenerative, traumatic, and pathological (Newman & Stone 1963; Wiltse, Newman, & MacNab 1976). The involved anatomic structures and pathogenesis for each type are presented in table 8.6. Of greatest concern to young athletes is the isthmic type; in which repeated loading of the pars region causes microfractures and eventual bone failure. Among the mechanisms responsible for these pars defect failures are repetitive spinal flexion, combined flexion and extension, forcible hyperextension, and lumbar spine rotation. Not sur-

prisingly, the populations most at risk are those whose training exposes them to repeated, high, compressive spinal loading, especially in combination with flexion-extension and rotational positions and movements. These include gymnasts, weight lifters, wrestlers, and divers. Spondylolysis is exacerbated by the stresses imposed on the vertebral laminae by the body's lumbar lordosis.

In spondylolisthesis, slippage occurs between adjacent vertebrae. The process involved in slippage differs between younger and older individuals (typically in women over 50 years old). In older populations, spondylolisthesis occurs most frequently at L4-L5, due in part to degenerative lesions associated with arthritis of the facet joints and to relative instability at this level compared to L5-S1. This instability may be due to a developmental predisposition to more sagittally oriented facet joints at the L4-L5 level (Grobler et al. 1993).

In young athletes the mechanism allowing spondylolisthesis differs from that observed in adults. In patients between 9 and 18 years old, Ikata and co-workers (1996) found end-plate lesions in all cases of vertebral slip between L5-S1 exceeding 5%. The

Table 8.6 Classification of Spondylolysis and Spondylolisthesis

Type	Name	Anatomic involvement	Etiology
I	Dysplastic	Neural arch dysplasia	Hereditary or congenital facet orientation anomalies, particularly L5-S1 facets and supporting structure
II	Isthmic	Pars interarticularis abnormality	Succession of microfractures; mechanical, hormonal, hereditary causes
III	Degenerative	Degenerative disk, facet, and ligamentous disease	Advanced pan-column degenerative changes
IV	Traumatic	Traumatic column instability with delayed translational changes	Trauma
V	Pathological	Pars and other components	Noncongenital or acquired (e.g., infection or neoplasm)

Adapted from Stillerman, Schneider, & Gruen 1993.

implicated mechanism was slippage between the osseous and cartilaginous end plates secondary to spondylolysis. The likelihood of progression (continuing slippage) depends on the type, stability, and degree of slippage, and slip angle (Bradford 1995; figure 8.30).

Lumbosacral Pathologies

Lumbosacral injuries can involve any of the many structures comprising the spinal column and in general involve three basic mechanisms: (1) spinal compression or weight bearing, (2) torsional loading, which results in various patterns of shearing in the transverse (horizontal) plane, and (3) tensile stresses resulting from excessive spinal motion (Watkins & Dillin 1994b). We present one class of lumbosacral injury (intervertebral disk pathologies) whose injury mechanisms are typical of other lumbosacral injuries.

Normal activities load the intervertebral disks in complex ways. The combined effects of spinal flexion-extension, lateral bending, and rotation exert considerable forces on the disks and their supporting structures. These forces are highest in the lumbar region, largely due to the compressive forces imposed by the weight of superior body segments.

Since disk morphology dictates mechanical response, it is important to understand some details of disk anatomy. The intervertebral disk is a viscoelastic structure consisting of two distinct structural elements, the *annulus fibrosus* and *nucleus pulposus*. The disk is separated from the vertebra by a thin

layer of hyaline cartilage (*cartilaginous end plate*). The nucleus pulposus is a gelatinous mass consisting of fine fibers embedded in a mucoprotein gel, with water content ranging from 70% to 90%. Water and proteoglycan contents are highest in the young and decrease with age. The mechanical consequences of these losses include decreases in disk height, elasticity, energy storage ability, and load-carrying capacity. The lumbar nucleus pulposus occupies 30% to 50% of the total disk area in cross section and is located slightly posteriorly (rather than centrally) between adjacent vertebral bodies.

The annulus fibrosus is composed of fibrocartilage and consists of concentric bands of annular fibers that surround the nucleus pulposus and form the outer boundary of the disk. The collagen fibers of adjacent annular bands run in opposite directions (figure 8.31). This criss-crossed fiber orientation allows the annulus to accommodate multidirectional torsional and bending loads.

When subjected to compressive loading, the disk components respond differently. In an unloaded state, the nucleus pulposus exhibits an intrinsic pressure of $10 \text{ N}\cdot\text{cm}^{-2}$ due to preloading provided by the longitudinal ligaments and the ligamenta flava. In a loaded state, the nucleus pulposus accepts 1.5 times the externally applied load, while the annulus experiences only 0.5 times the compressive load (figure 8.32). Due to the relative incompressibility of the nucleus pulposus, the load is transmitted (see Poisson's effect, chapter 3) as a tensile load to the fibers of the annulus fibrosus. These forces radiate circumferentially in what is described as a *hoop effect*.

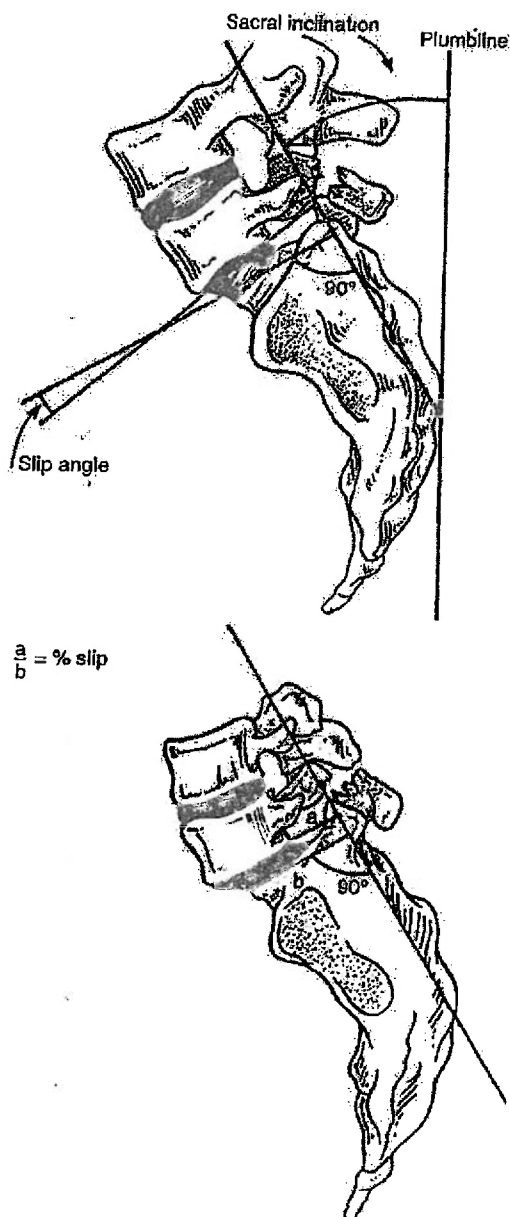


Figure 8.30 Schematic of sacral inclination and slip angle (*top*) and percentage slip (*bottom*). Adapted from Stinson 1993.

The resulting tensile stresses are four to five times greater than the externally applied compressive load (Nachemson 1975).

Many mechanisms have been suggested as being

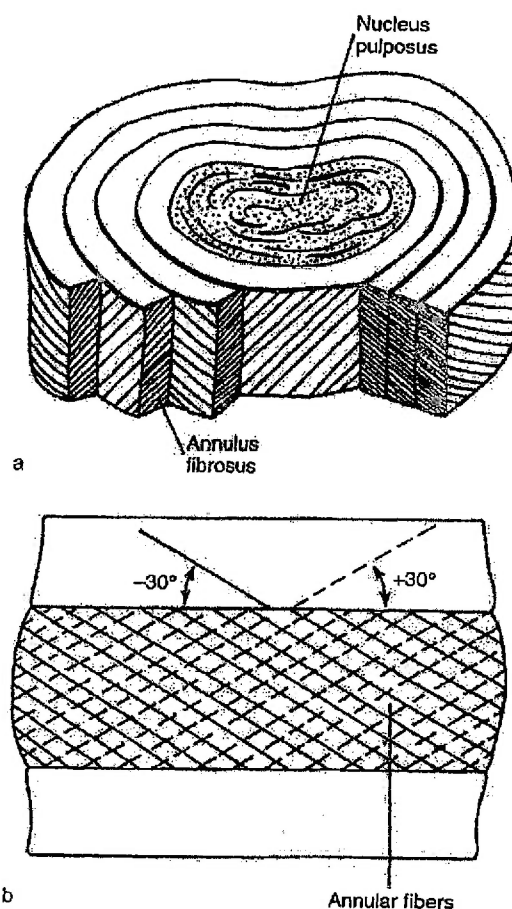


Figure 8.31 (a) Concentric rings of the annulus fibrosus surrounding the centrally located nucleus pulposus. (b) Alternating 30° angulation of annular fibers. This structural orientation enhances the ability of the annulus fibrosus to accommodate multidirectional loading.

responsible for lumbar disk pathologies. In a classic work, Charnley (1955) presented a theoretical framework of potential pathoanatomic mechanisms responsible for intervertebral disk pathologies. These are summarized in table 8.7.

We will examine one of these factors (type IV, bulging disk) in detail here. In this mechanism the nucleus pulposus is displaced from its normal position within the annulus fibrosus. Rotational body movements produce shearing stress in the annular fibers and can lead to circumferential and radial tears. The resulting weakness in the annular layers reduces the ability of the annulus to contain the

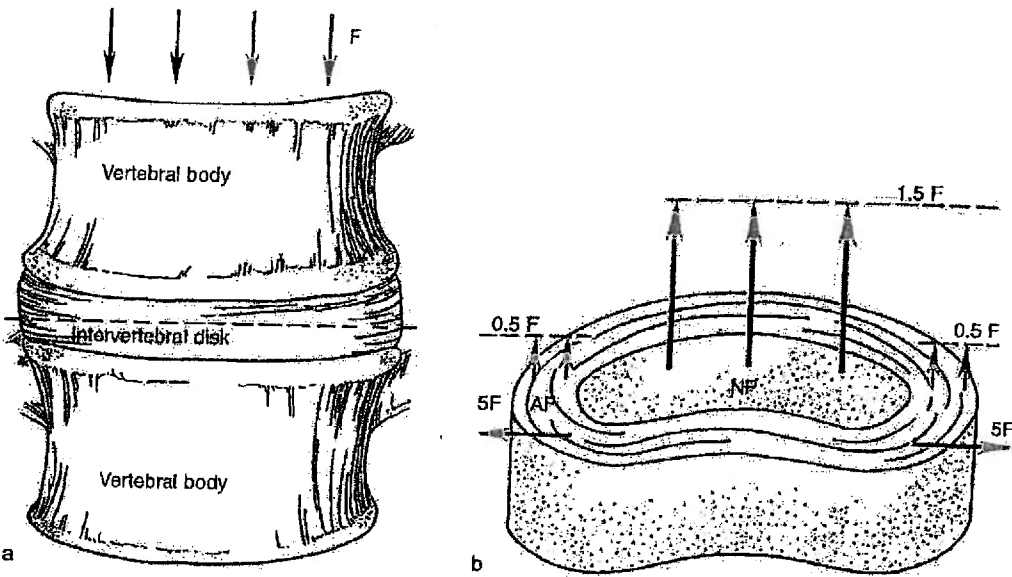


Figure 8.32 Uneven stress distribution across the lumbar intervertebral disk. A uniform compressive load (F) applied through the vertebral body (a) creates an axial stress of $1.5 F$ (per unit area) in the nucleus pulposus (NP) (b). The annulus fibrosus (AF), in contrast, generates an axial stress of only $0.5 F$. The orthogonal stress in the annulus (perpendicular to the applied load) can reach levels up to five times the applied force ($5F$). Reprinted from Nachemson 1975.

Table 8.7 Causal Factors in Intervertebral Disk Pathologies

Type	Name (description)
I	Acute back sprain (injury to annular fibers, other posterior ligaments, or musculotendinous structures)
II	Fluid ingestion (increased fluid uptake in the nucleus pulposus)
III	Posterolateral annulus disruption (annular disruption with consequent stimulation of sensory innervation by mechanical, chemical, or inflammatory irritants)
IV	Bulging disk (protrusion of the nucleus pulposus with impingement on neural structures)
V	Sequestered fragment (separated piece of tissue, or <i>sequestrum</i> , from the annulus fibrosus or nucleus pulposus that wanders within the joint space and causes irritation)
VI	Displaced sequestered fragment (displacement of sequestrum into the spinal canal or intervertebral foramen)
VII	Degenerating disk (progressive degeneration of the annulus fibrosus)

From *Clinical Biomechanics of the Spine* (2nd ed.) (p. 391-395) by A.A. White, III, & M.M. Panjabi, 1990, Philadelphia: J.B. Lippincott Company. Copyright 1990 by Lippincott-Raven. Adapted by permission.

nucleus pulposus. Compressive loads then squeeze the nucleus pulposus (disk prolapse) into the area of annular weakness. Sudden disk prolapse occurs acutely and typically is precipitated by a hyperflexion mechanism, often in conjunction with lateral bend-

ing. This mechanism creates tensile stresses on the posterolateral aspect of the annulus fibrosus (figure 8.33), which, when combined with a compressive load, results in disk prolapse. Adams and Hutton (1982) suggested that sudden disk prolapse occurs

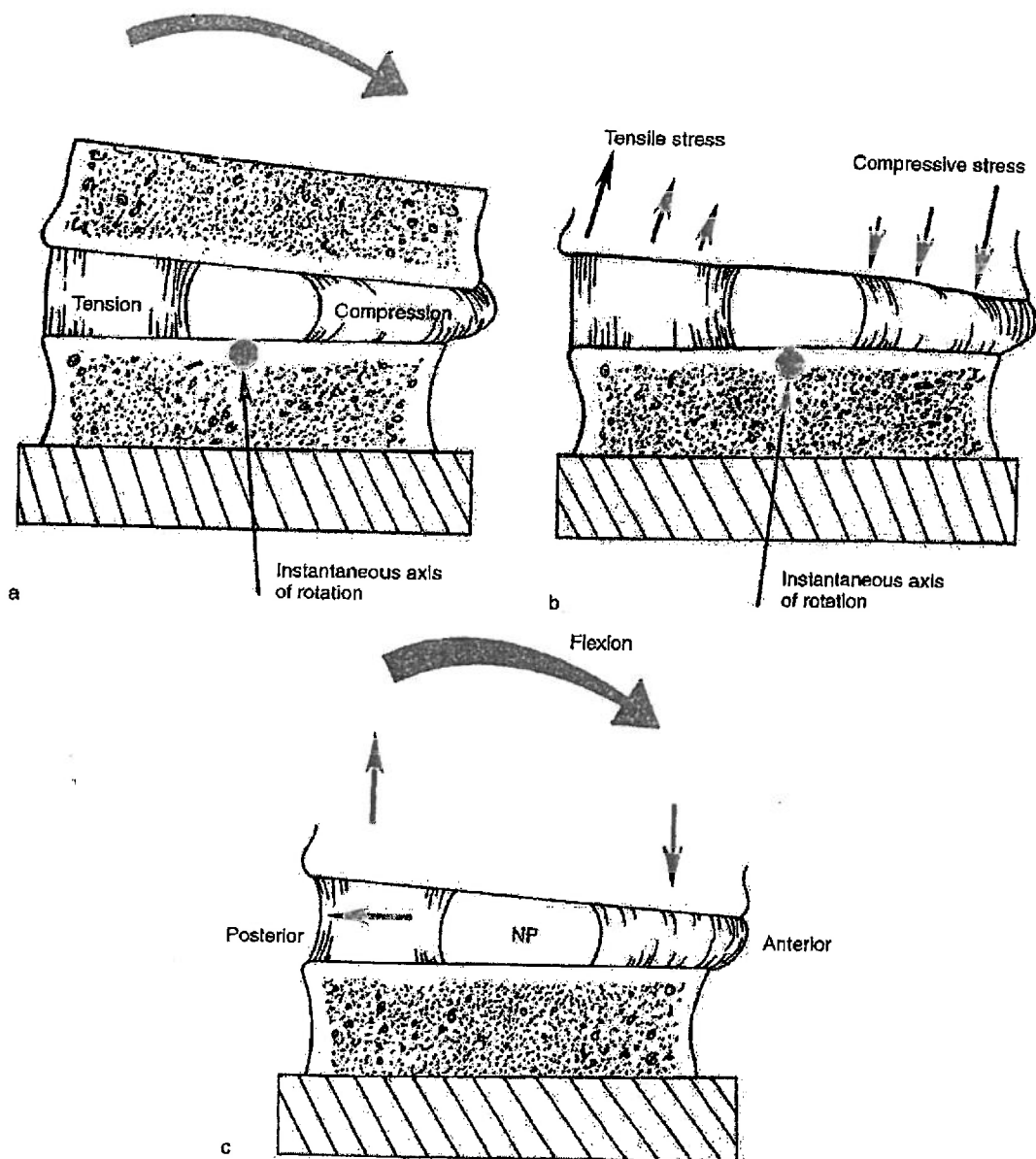


Figure 8.33 Intervertebral disk stress in response to bending. (a) In bending, one side of the disk experiences compression while the other side undergoes tension. (b) The compressive and tensile stresses are at a maximum at the outer borders of the disk and decrease toward the center of the disk. (c) Forward flexion of the spine tends to squeeze the nucleus pulposus (NP) posteriorly.

Parts (a, b) from *Clinical Biomechanics of the Spine* (2nd ed.) (Fig. 1-10, p. 15) by A.A. White & M.M. Panjabi, 1996, Philadelphia: J.B. Lippincott Company. Copyright 1990 by Lippincott-Raven. Adapted by permission.

most often in the lower lumbar region (L4-L5 or L5-S1) and is associated with disk degeneration.

The hyperflexion mechanism is not implicated in

most cases of gradual disk prolapse (i.e., where there is no identifiable precipitating event). These injuries have been associated with a weakened and

A Real Pain in the (Low) Back

By any measure, lower-back pain is the most costly musculoskeletal disorder in industrial societies. Up to 80% of the population will suffer from low-back pain in their lifetimes. For some people the pain is merely a temporary annoyance. For others, however, the pain associated with low-back pathologies can be completely debilitating.

The pain associated with low-back dysfunction arises from chemical or mechanical irritation of pain-sensitive nerve endings in structures of the lumbar spine. Chemical irritation is associated with the biochemical events of inflammatory diseases or subsequent to tissue damage. Mechanical irritation, in contrast, can result from stretching of connective tissues such as ligaments, periosteum, tendons, or the joint capsule. Compression of spinal nerves by a herniated intervertebral disk, damage to the disk itself, local muscle spasms, and zygapophyseal joint pathology can also result in low-back pain. Whatever its source, low-back pain either can be felt locally in the lumbar region or may be referred to the buttocks, lower extremities, or less commonly to the abdominal wall or groin.

The efficacy of various treatment strategies remains controversial, largely due to the fact that an estimated 85% of low-back pain cases remain unspecifically diagnosed. Conservative treatment (e.g., ice, rest, gentle activity), manipulative therapies, and therapeutic exercise interventions all have their proponents. Only rarely is surgical intervention indicated. The limited number of well-controlled, randomized studies addressing the issues of low-back pain treatment leave this area open to continuing debate and controversy.

degenerative annulus and other loading mechanisms (e.g., bending and twisting).

Whatever the causal mechanism, the bulging, or protruding, disk impinges on adjacent structures. Since many disk prolapse injuries occur in the posterolateral direction, the affected structure often is a nerve root. This results in mechanical, and possibly chemical and/or inflammatory, irritation of the nerve root with resultant pain in the back, buttocks, thigh, lower leg, and possibly even the foot. Lower-back pain, whether from disk pathology or other causes, will afflict about 80% of individuals at some time during their lives and is the most common occupationally related disability. Given the serious and pervasive nature of this musculoskeletal condition, knowledge of its causal mechanisms is essential in prescribing treatment programs and designing injury prevention strategies.

Concluding Comments

Of all the body's regions, the head, neck, and trunk have the greatest potential for catastrophic injury. As highlighted by the many examples in this chapter, the risks are real and considerable. Injuries to

vital structures in these regions can readily compromise essential body functions and, in all too many cases, result in paralysis or death.

An understanding of injury mechanisms in all body regions can assist health professionals in effectively diagnosing and treating patients who suffer these unfortunate injuries and can facilitate the efforts of researchers and medical professionals to reduce the risk of injury and develop effective injury prevention programs. While our understanding of musculoskeletal injury has increased considerably in recent decades, much remains to be discovered. Among the challenges requiring further investigation are those related to the in vivo responses of biological tissues to mechanical loading, the relations between load volume (i.e., intensity, duration, frequency) and tissue response in real-world situations (e.g., ergonomic, sport), computer modeling of injury dynamics, and effective education programs across all strata of society. Our continuing efforts to understand the biomechanics of musculoskeletal injury are well worth the effort and resources expended. Injury prevention holds the key. After all, the best injury is the one that never happens.

Suggested Readings

Head, Neck, and Trunk

- Becker, D.P., & Gudeman, S.K. (Eds.). (1989). *Textbook of Head Injury*. Philadelphia: Saunders.
- Cooper, P.R. (Ed.). (1993). *Head Injury* (3rd ed.). Baltimore: Williams & Wilkins.
- Hoerner, E.F. (Ed.). (1993). *Head and Neck Injuries in Sports*. Philadelphia: American Society for Testing and Materials.
- Levine, R.S. (Ed.). (1994). *Head and Neck Injury*. Warrendale, PA: Society of Automotive Engineers.
- Lonstein, J.E., Bradford, D.S., Winter, R.B., & Ogilvie, J.W. (Eds.). (1995). *Moe's Textbook of Scoliosis and Other Spinal Deformities* (3rd ed.). Philadelphia: Saunders.
- Rizzo, M., & Tranel, D. (Eds.). (1996). *Head Injury and Postconcussive Syndrome*. New York: Churchill Livingstone.

Torg, J.S. (Ed.). (1991). *Athletic Injuries to the Head, Neck, and Face* (2nd ed.). St. Louis: Mosby-Year Book.

Vinken, P.J., Bruyn, G.W., & Klawans, H.L. (Eds.). (1990). *Head Injury*. New York: Elsevier.

General Sources

- Browner, B.D., Jupiter, J.B., Levine, A.M., & Levine, P.G. (1992). *Skeletal Trauma*. Philadelphia: Saunders.
- Feliciano, D.V., Moore, E.E., & Mattox, K.L. (Eds.). (1996). *Trauma* (3rd ed.). Stamford, CT: Appleton & Lange.
- Fu, R.H., & Stone, D.A. (1994). *Sports Injuries: Mechanisms, Prevention, Treatment*. Baltimore: Williams & Wilkins.
- Nicholas, J.A., & Hershman, E.B. (Eds.). (1995). *The Lower Extremity and Spine in Sports Medicine*. St. Louis: Mosby-Year Book.

**SAE TECHNICAL
PAPER SERIES**

2001-01-0900

Vehicle and Occupant Response in Heavy Truck to Passenger Car Sideswipe Impacts

C. Brian Tanner and John F. Wiechel
S.E.A., Inc.

Dennis A. Guenther
The Ohio State University

Reprinted From: **Accident Reconstruction-Crash Analysis**
(SP-1572)

SAE *The Engineering Society*
For Advancing Mobility
Land Sea Air and Space®
INTERNATIONAL

SAE 2001 World Congress
Detroit, Michigan
March 5-8, 2001

The appearance of this ISSN code at the bottom of this page indicates SAE's consent that copies of the paper may be made for personal or internal use of specific clients. This consent is given on the condition, however, that the copier pay a \$7.00 per article copy fee through the Copyright Clearance Center, Inc. Operations Center, 222 Rosewood Drive, Danvers, MA 01923 for copying beyond that permitted by Sections 107 or 108 of the U.S. Copyright Law. This consent does not extend to other kinds of copying such as copying for general distribution, for advertising or promotional purposes, for creating new collective works, or for resale.

SAE routinely stocks printed papers for a period of three years following date of publication. Direct your orders to SAE Customer Sales and Satisfaction Department.

Quantity reprint rates can be obtained from the Customer Sales and Satisfaction Department.

To request permission to reprint a technical paper or permission to use copyrighted SAE publications in other works, contact the SAE Publications Group.



GLOBAL MOBILITY DATABASE

All SAE papers, standards, and selected books are abstracted and indexed in the Global Mobility Database

No part of this publication may be reproduced in any form, in an electronic retrieval system or otherwise, without the prior written permission of the publisher.

ISSN 0148-7191

Copyright 2001 Society of Automotive Engineers, Inc.

Positions and opinions advanced in this paper are those of the author(s) and not necessarily those of SAE. The author is solely responsible for the content of the paper. A process is available by which discussions will be printed with the paper if it is published in SAE Transactions. For permission to publish this paper in full or in part, contact the SAE Publications Group.

Persons wishing to submit papers to be considered for presentation or publication through SAE should send the manuscript or a 300 word abstract of a proposed manuscript to: Secretary, Engineering Meetings Board, SAE.

Printed in USA

2001-01-0900

Vehicle and Occupant Response in Heavy Truck to Passenger Car Sideswipe Impacts

C. Brian Tanner and John F. Wiechel
S.E.A., Inc.

Dennis A. Guenther
The Ohio State Univ.

Copyright © 2001 Society of Automotive Engineers, Inc.

ABSTRACT

There have been a number of papers written about the dynamic effects of low speed front to rear impacts between motor vehicles during the last several years. This has been an important issue in the field of accident analysis and reconstruction because of the frequency with which the accidents occur and the costs of injuries allegedly associated with them. Sideswipe impacts are another, often minor, type of motor vehicle impact that generate a significant number of injury claims. These impacts are difficult to analyze for a number of reasons. First, there have been very few studies in the literature describing the specific dynamic effects of minor sideswipe impacts on the struck vehicles and their occupants. Those that have been performed have focused on the impact of two passenger cars. Second, typical accident reconstruction programs are not well suited to accurately determine the vehicle speed changes and accelerations resulting from impacts where the line of the impact force lies far from the vehicle center of gravity, and is influenced by specific features of vehicle geometry.

This paper will present the results of two controlled low speed sideswipe impact tests between a crane truck and a passenger car. The tests were performed to duplicate a real world accident that resulted in litigation. The acceleration near the car's center of gravity is measured, as is the acceleration of the head of an adult male human volunteer. In addition, the relationship between vehicle damage and speed change is addressed for the subject impacts, and the occupant kinematics are described. Finally, the effect of full and partial vehicle braking by the passenger car in the impacts is discussed. The data presented will give some reference for comparison in other heavy truck to car sideswipe accidents.

INTRODUCTION

Although much testing has been done during the last 10 years on the subject of low speed impact and associated testing, very little of this had focused on sideswipe impacts. In 1995, Bailey, Wong and Lawrence published a paper that described a large number of minor impact tests, including two series of sideswipe impacts with passenger cars. They found that the acceleration and speed changes of vehicles involved in minor sideswipe impact are quite low, and that the production of injury is unlikely.¹

Because rules for commercial vehicles in the United States require their operators to carry large liability insurance policies, the potential for large damage claims is greater when a minor impact occurs between a truck and a car as opposed to two cars. Despite this fact, there is little or no information in the literature regarding the relationship between vehicle damage and impact severity or injury potential when a heavy truck sideswipes a passenger car. Hopefully, the information presented in this paper will provide a useful first step toward providing that information.

METHODOLOGY

VEHICLES - For this testing, the same two vehicles were used for a pair of tests. The striking vehicle was a 1982 American Model 5470 Truck Crane. The crane had two front and two rear axles, and its chassis supported an operator house and the first section of crane boom. Near the middle of the crane and at its rear were extendable hydraulic support legs for stabilizing it during operation. At the front left of the crane truck chassis was the driver's compartment. Both front axles of the crane truck were steerable, and its unloaded vehicle weight was about 21,000 kilograms.



Figure 1 - The truck crane or striking vehicle

The struck vehicle in the testing was a 1983 Chevrolet Monte Carlo. The car weighed only about 1500 kilograms, or about a fifteenth the weight of the truck, and its roof barely rose above the truck crane chassis' platform. It was intended that normal braking would be applied for the Chevrolet in each test. However, with the engine off there was insufficient vacuum boost to the power brakes to achieve this in the first test. This was remedied in the second test by having the engine running. The vehicles are shown in Figures 1 through 3.

TEST CONTROL AND DOCUMENTATION - During the testing, both of the vehicles contained drivers. In the case of the driver of the Chevrolet, he was simply a test subject who also controlled the degree of braking of the Chevrolet during the impact. In contrast, the driver of the crane truck was not a test subject but rather simply drove the truck throughout the test. He controlled the speed, direction of travel and stopping of the truck throughout the impact sequence. To aid the truck driver, the crane was fitted with a fifth wheel measurement device that drove a large digital readout installed in the driver's cab. This accurately measured and displayed the speed of



Figure 2 - Alternate view, the left side of the truck crane

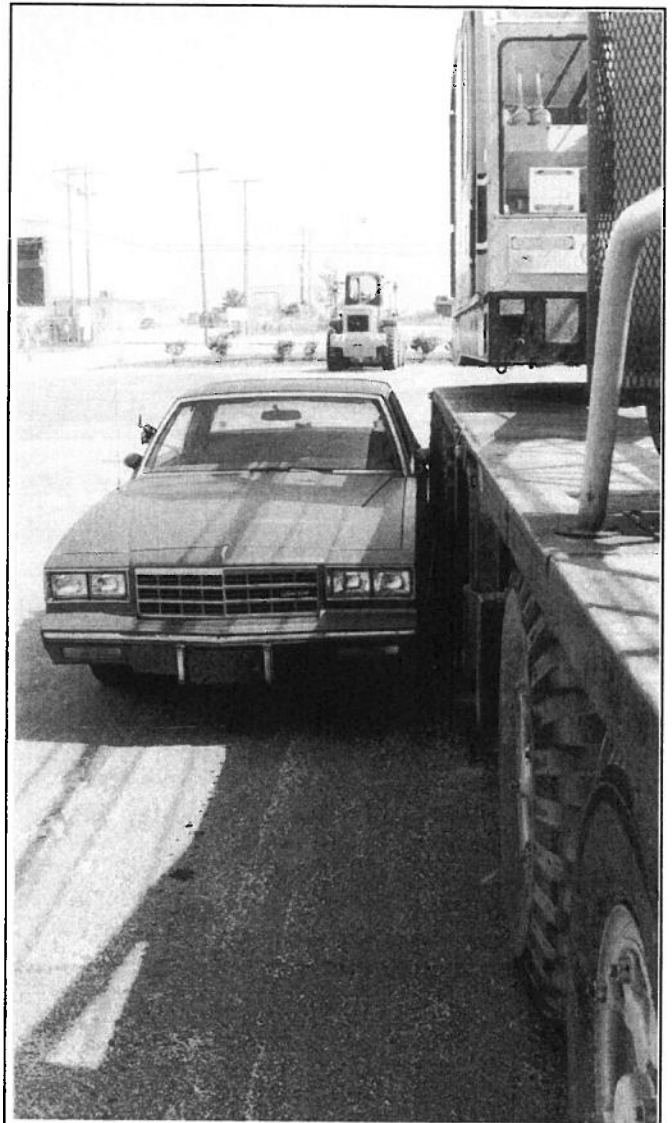


Figure 3 - The 1983 Monte Carlo next to the truck

the truck to the nearest tenth of a mile per hour. The only other aid provided to the truck driver was visual reference points describing the path he should steer throughout the impact. Because of the large weight difference between the vehicles, the effect of the impact on the kinematics of the truck and driver would be negligible, thus no instrumentation was used on the truck or its driver.

The same was not true for the Chevrolet. Both the car and its driver were fitted with triaxial accelerometers. In the case of the car these were rigidly mounted to the floor near the vehicle's center of gravity. The accelerometers were fitted to the driver by use of a biteplate that could be rigidly clenched between his teeth. Thus, the biteplate would undergo the same general motion as the skull. The instrumentation in the car is shown in Figure 4. The triaxial accelerometer block was mounted in the vehicle so that the x-direction was in the positive forward direction, the y-direction was positive to



Figure 4 - The instrumentation of the car and driver

the left and the z-direction was positive upward. This would generally also be true for the vehicle driver when he was seated with his neck straight and was looking forward. To each block was mounted three Sensotech piezoresistive low profile accelerometers having a full scale range of ± 50 g's.

TEST PROCEDURE - The tests were conducted by having the driver of the crane truck begin moving well behind and just to the left of the car. The truck driver accelerated until he reached a speed of eight kilometers per hour, which he was instructed to maintain. He then followed a line on the pavement that directed the vehicle immediately along the driver's side of the car. After the truck made it about half way past the car, the driver was instructed to steer right toward a cone placed on the pavement. This caused the side of the truck to strike the side of the car. Figure 5 shows the approximate position of the truck when the driver was to begin steering right.

Accelerometer data was collected for each channel at 1000 Hz. Processing of the data included eliminating any pre-event offset from the signals. Next, the vehicle acceleration data was digitally filtered using the algorithm detailed in SAE J211-1 to achieve a four pole anti-aliasing Butterworth low pass filter. The cutoff frequency of the filter was 100 Hz, making the data channel frequency class (CFC) 60. There was no filtering of the driver data. Finally, vehicle longitudinal and lateral acceleration data were integrated in an attempt to determine the speed change of the car during the impacts.

TEST RESULTS - Two tests were performed. In the first, there was minimal braking by the car occupant, while in the second, maximum braking was employed. In each of the tests, the overall impact was recorded with videotape, as was the motion of the occupant's body. Because the driver of the truck was a little early and tentative in performing his steering maneuver, there was relatively minimal impact between the car and the truck. This was made even more apparent by the light braking by the car driver. As a result of the contact between the

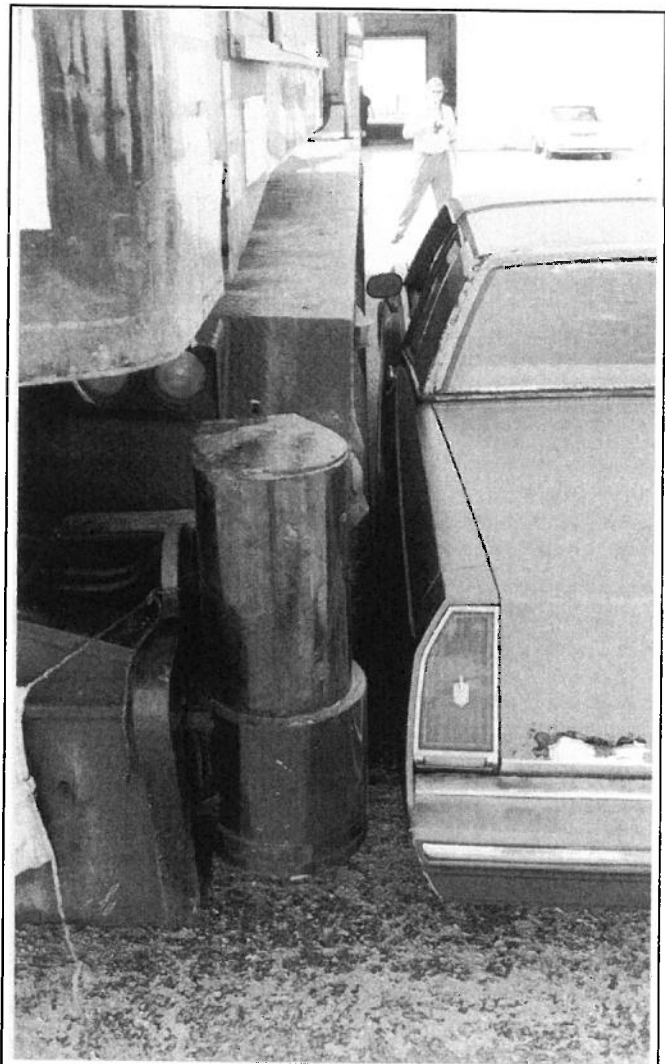
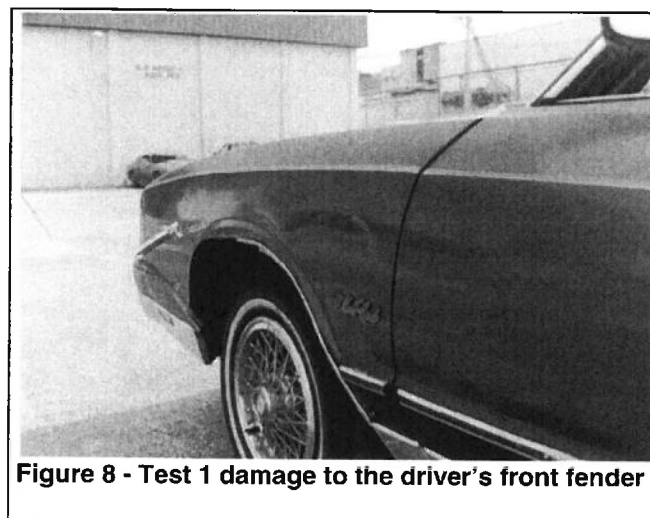
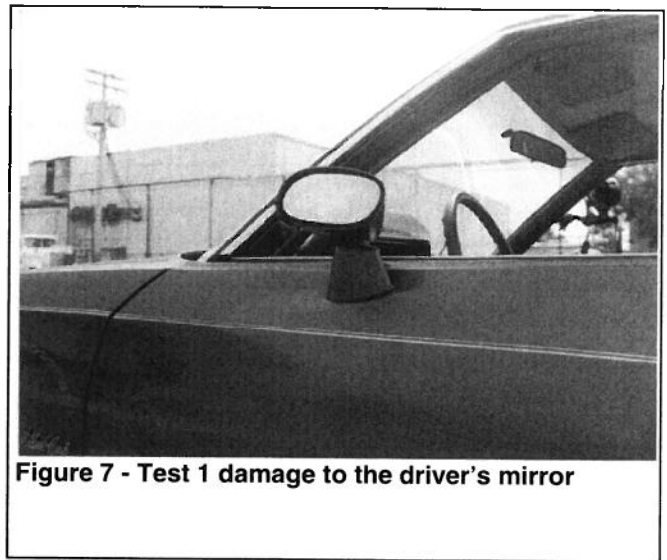
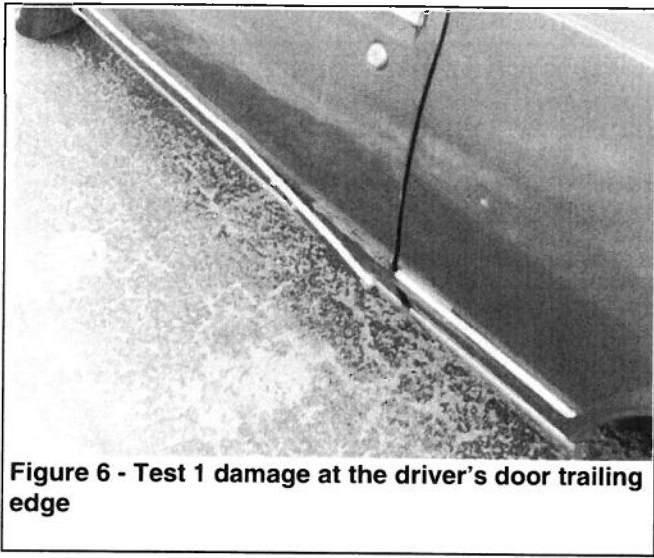


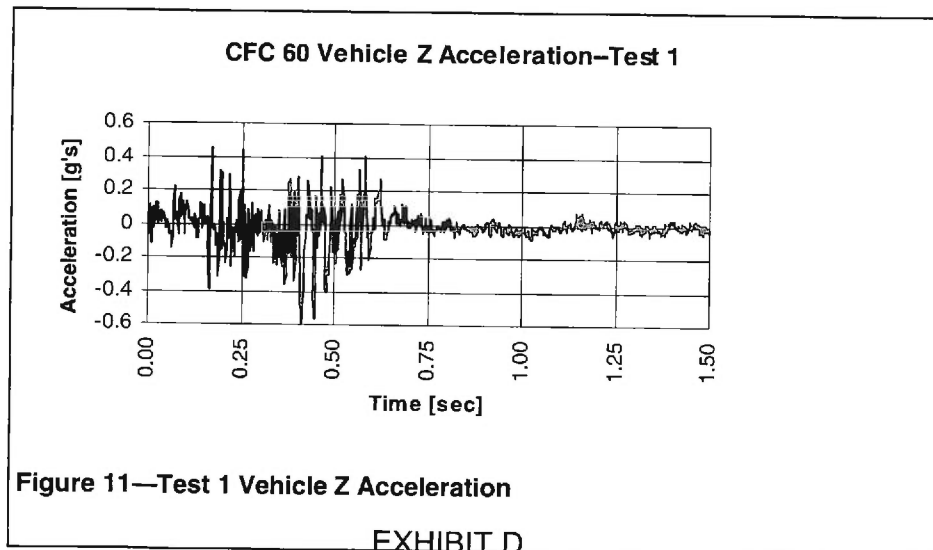
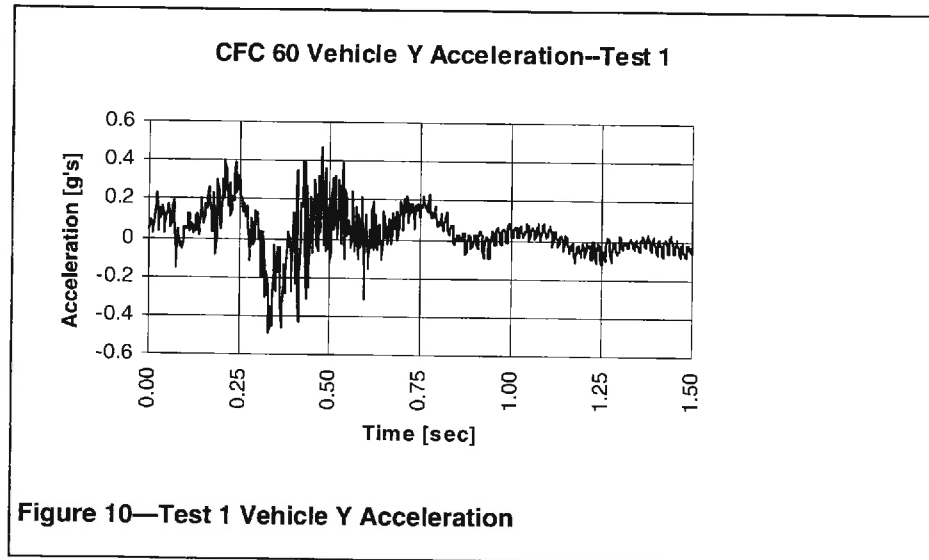
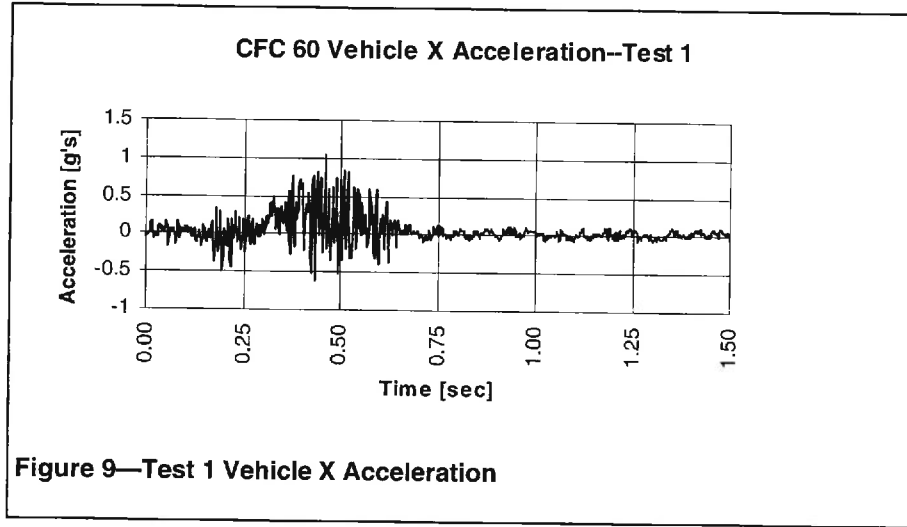
Figure 5 - The target position for the truck driver to begin steering right

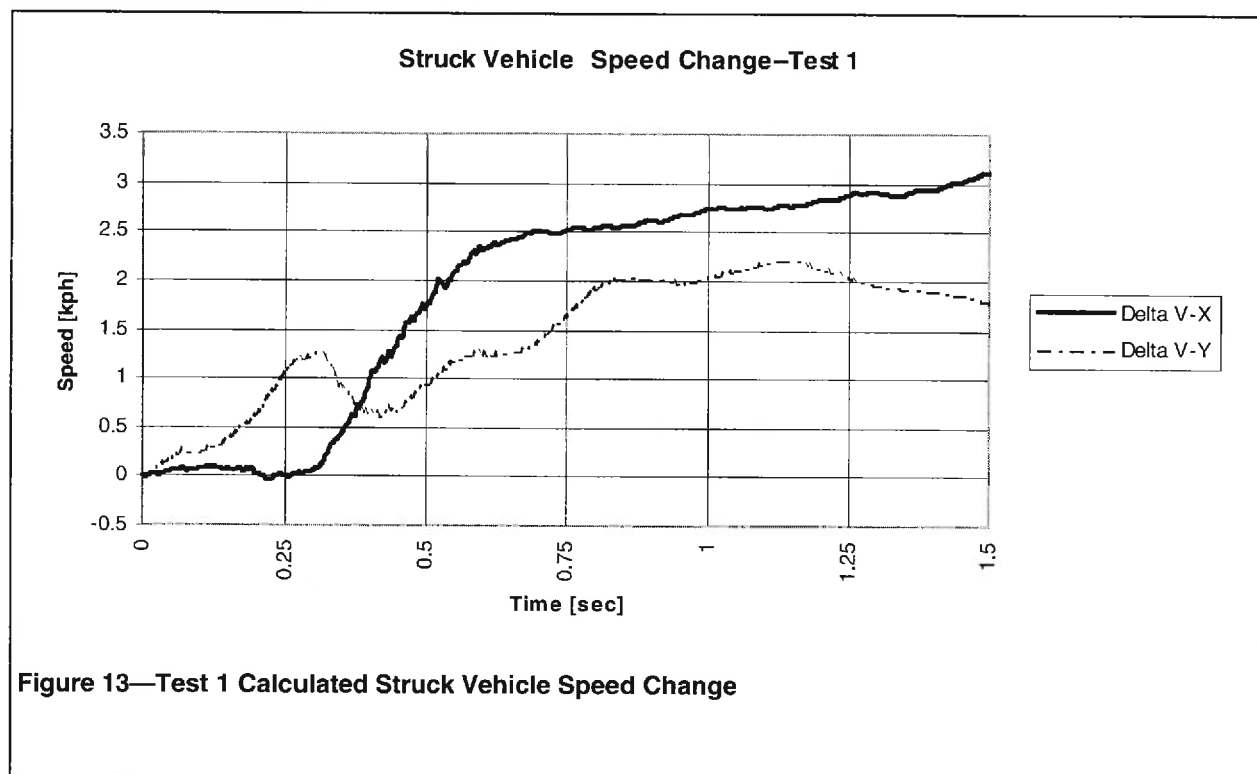
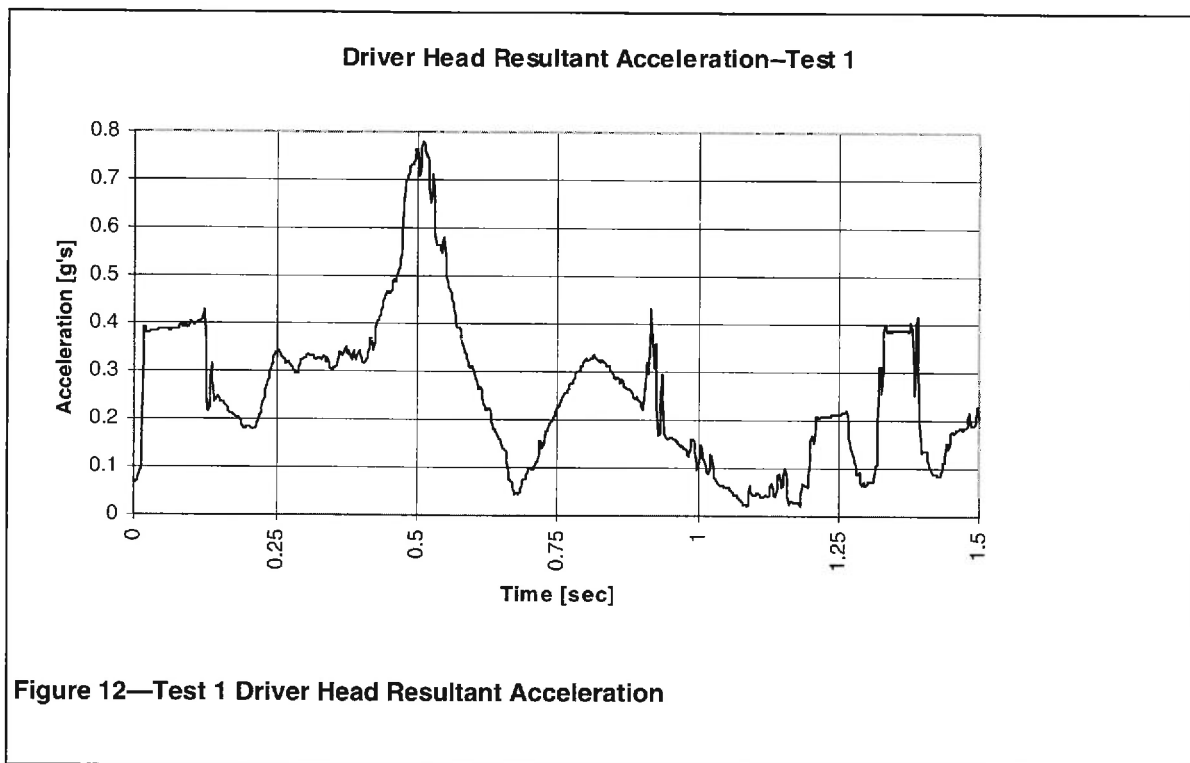
truck and the car, the car was almost immediately shifted to be parallel to the truck. Shortly after that, the front wheel well area of the car was snagged by the side of the truck and the car was dragged up to about 3.2 kph. When each driver began braking, and the truck driver steered back to the left, the vehicles separated.

The damage to the car in this first test was minimal, and consisted only of some scuffing and torn trim at the trailing edge of the driver's door, a torn and rotated driver's mirror housing, and a minor dent and scuff with torn trim on the driver's front fender. This damage is shown in Figures 6 through 8.

The acceleration data for the car and driver during the first test is shown in Figures 9 through 12. In Figure 13, the vehicle acceleration data is integrated to give vehicle speed change. Interestingly, the magnitude of the vehicle acceleration is about 0.5 g's in all directions. The y and z axis accelerations correspond primarily to the rocking of the vehicle as the crane scrapes by, and occurs in both directions. This rocking is similar to the







acceleration experienced by the car occupant, who is gently moved along with the vehicle at maximum accelerations less than 0.8 g's. The x axis acceleration primarily served to accelerate the entire vehicle in the forward direction. This occurred despite the driver/subject's attempt at braking because there was no vacuum available in the power brake booster of the vehicle. The speed change of the vehicle shown in figure 13 in the x direction is consistent with the post-impact motion observed for the vehicle, however, the speed change indicated for the y direction did not occur. There was some minimal initial rotation of the car to bring it parallel with the crane truck, however, following this the car basically rolled in a straight direction.

In the second test, the crane driver followed a better path, and the car driver was able to keep the brakes on the vehicle locked, to prevent significant rolling of the car from the impact. In order to do this, the engine in the car was running during the test, resulting in some vehicle vibration. The damage to the car in the second test was significantly greater than in the first, with clear dents in each of the body panels on the left side of the vehicle, probably 2.5 to 5 centimeters in depth, and with sufficient deformation around the door opening to cause partial jamming that required three people to overcome. Figures 14 and 15 show the damage. For a newer vehicle such damage would be quite costly to repair, and might be used to justify significant injury claims by the driver of the car.

Figures 16 through 19 show the vehicle and driver acceleration data for the second test. The pattern of accelerations of the vehicle and the driver was very similar to the first test, except the magnitudes were slightly higher with maximum accelerations just over 1 g. Again, most of these accelerations are due to the vehicle chassis rolling and pitching on its suspension. In fact, in this case, since the brakes on the vehicle remained locked throughout the test, the pitching of the vehicle was at least visible. The car speed change calculated from integration of the acceleration data collected during the impact is shown in Figure 20. During the impact, the car moved at most a couple of inches, thus the short duration shift to 1.6 kilometer per hour and less in both the x and y data is difficult to explain. Based on the shape of the curves it would be logical that this represents only a temporary offset in the output of the accelerometer.

With this in mind upon review of the test videos, it is clear that just such offsets occur as the vehicles are in contact. The videotape clearly showed that when the contact between the vehicles occurred, very significant roll angle quickly developed for the car and was maintained throughout the impact. This occurred because the contact between the truck and the side of the car took place above ground level. However, the friction force between the tires and the pavement resisted any lateral slipping. These forces cause a roll moment to act upon



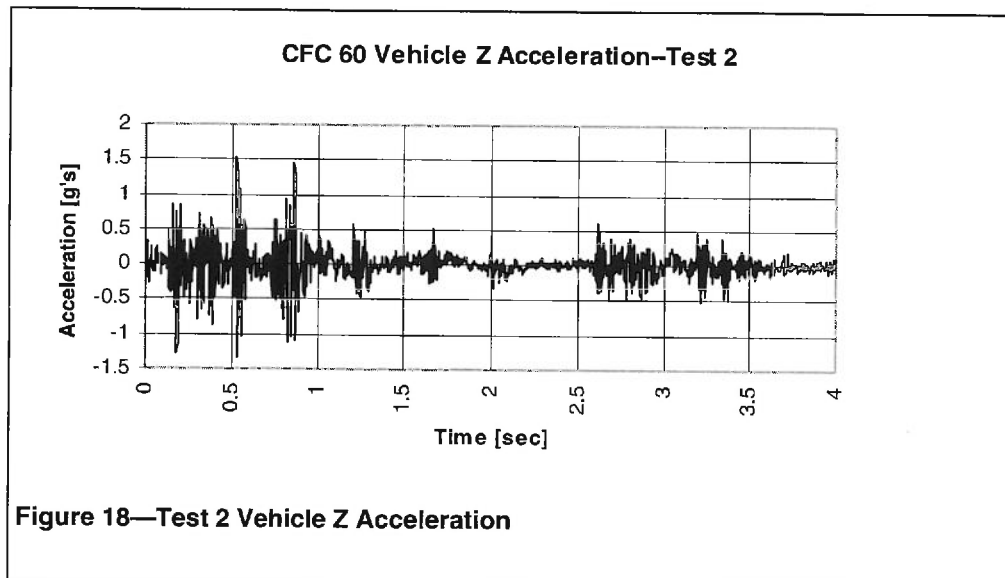
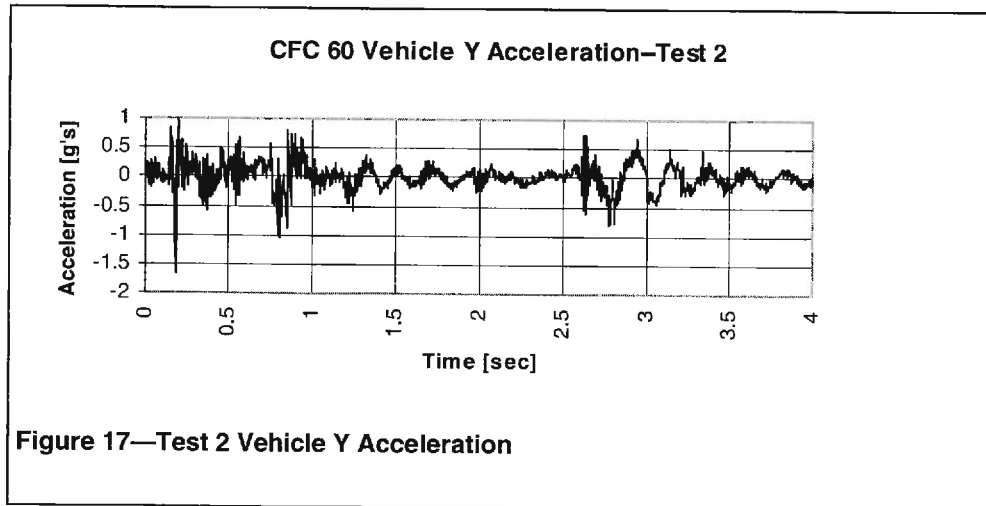
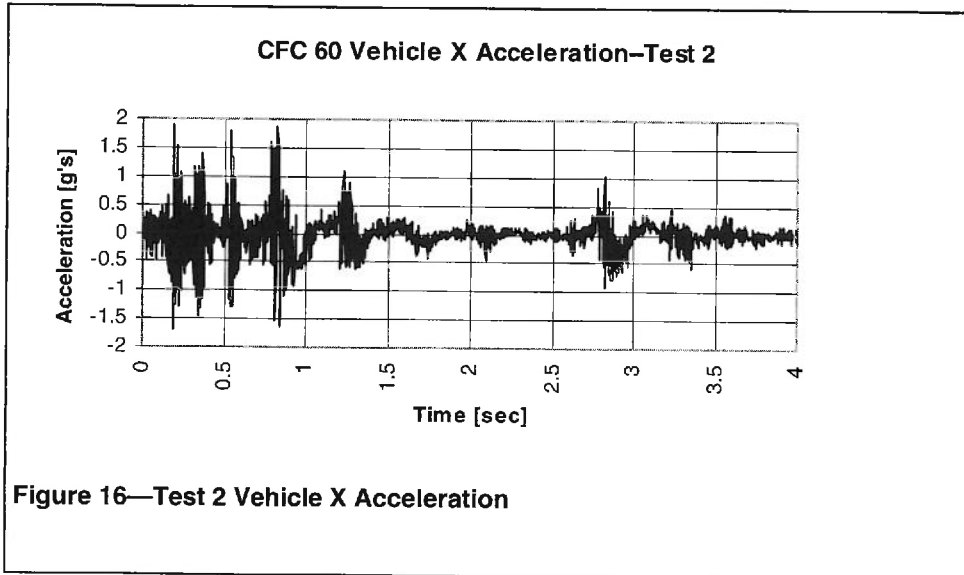
Figure 14 - Test 2 damage to the driver's side of the car

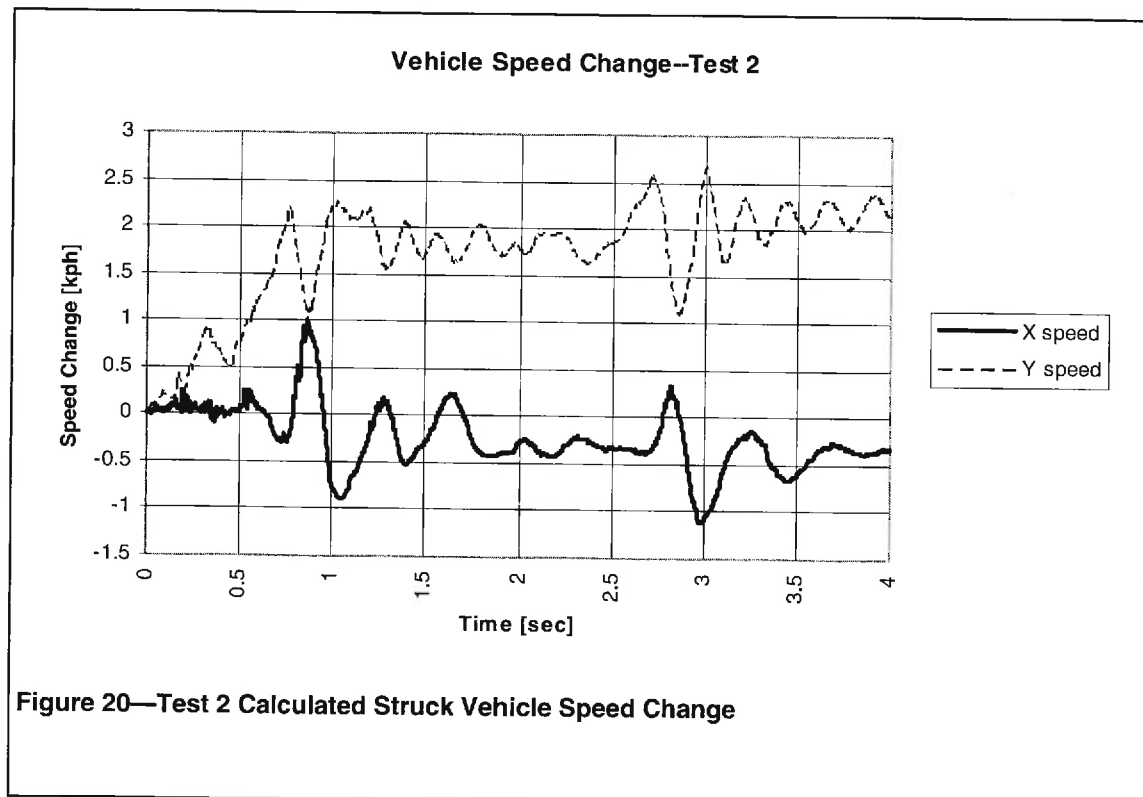
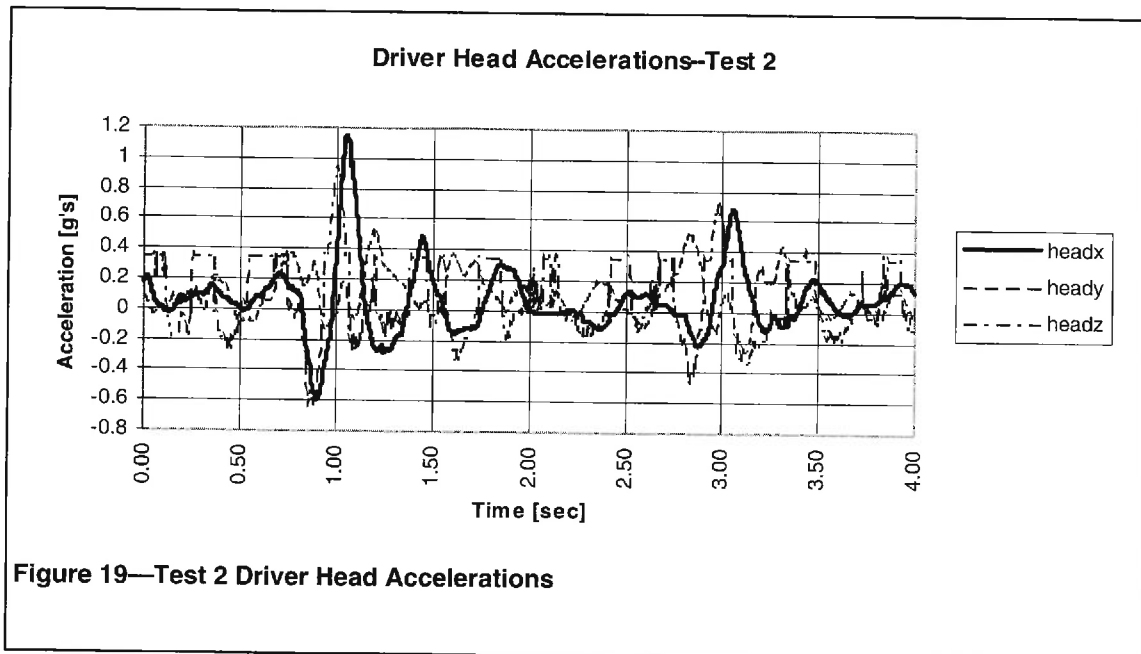
the vehicle chassis. Similarly, in the second test, when the car's wheels were locked throughout the impact, the combination of the contact forces between the vehicle and the friction of the tires with the pavement caused a pitch moment to act on the vehicle. As a result of the pitch and yaw of the car, the orientation of the vehicle mounted accelerometers within the gravitational field was changed slightly, by a couple of degrees in both directions. While this caused only a small shift in the sensitive axis of the accelerometers, the contact between the vehicles lasted long enough so that the integration of the data with this shift caused resulted in small, but erroneous velocity measurements. Because the accelerometer offsets only lasted as long as the pitch and roll displacements of the vehicle during the contact, the result was not continuously increasing velocity curves, but rather signals that only increased during the contact, but then remained approximately constant following the contact.

While no instrumentation was included in the test vehicle for measuring the dynamic pitch and roll angles during the impact, the velocity curves could be used to determine at least what the average pitch and roll were during the impact, and then to correct the acceleration



Figure 15 - Another view of the damage from test 2





and velocity curves. This is done by identifying the portion of the acceleration curves that correspond to contact between the vehicles. Once the time window of the contact is determined, the necessary average offset in the acceleration to cause the indicated speed change can be estimated. This value is then subtracted from the acceleration signal and the signal is integrated. This process is repeated until the known velocity condition of the vehicle at the end of the signal (in this case, zero) is reached. The corrected curves for the y axis vehicle accelerations are given in Figures 21 and 24 for tests one and two, while the corrected curve for the x axis acceleration in the second test is given in Figure 23. Because of the minimal vehicle pitching in the first test, it was felt no correction was necessary for the x axis data in that test. In addition, the vehicle was rolling with some unknown speed when the data signal stopped, so application of the method would not have been feasible. The corrected vehicle speed change curves are given in Figures 22 and 25.

It is interesting to note that the average correction factor applied to the y axis data suggested an average roll angle in the vehicle of 2.7 degrees for both tests. This is logical, since the contact geometry of the vehicles would tend to determine the amount of roll in the type of impact performed for this study, and there was no major change in the contact geometry between the tests. The corresponding relative change in the height of the vehicle from one side to the other would be around three inches. In contrast, the amount of average pitch during the impact suggested by the correction factor for the x axis data in the second test was about 0.4 degrees. This pitch would result in a relative height change at the front and rear suspension of the car of about 2 centimeters. While the pitch would be visibly observable, the roll would be quite obvious, and this corresponds with observations during the tests.

OCCUPANT KINEMATICS

In the actual accident that these tests were meant to duplicate as closely as possible, the driver of the involved passenger car alleged after the accident that he had been severely thrown about inside the vehicle, and that as a result of the collision, he had suffered disabling injuries to his left leg and lower back. Thus, video cameras were focused on the test subject in the driver's seat of the Chevrolet.

The test subject was in his early fifties, and was about 1.8 meters tall with a mass of 90 kilograms. He had no significant reported history of neck, back or lower extremity injury. When the test impacts occurred, the motion of the occupant was, for the most part, the same general motion of the driver's seat. Thus, when the driver's seat rose because of the rolling nature of the vehicle loading, the test subject also moved upward. In addition, the loading rates were generally mild, so there

was no bouncing of the subject on the seat. Similarly when the vehicle was pushed forward, the effect was gradual, and there was no whiplash type loading of the subjects back or neck.

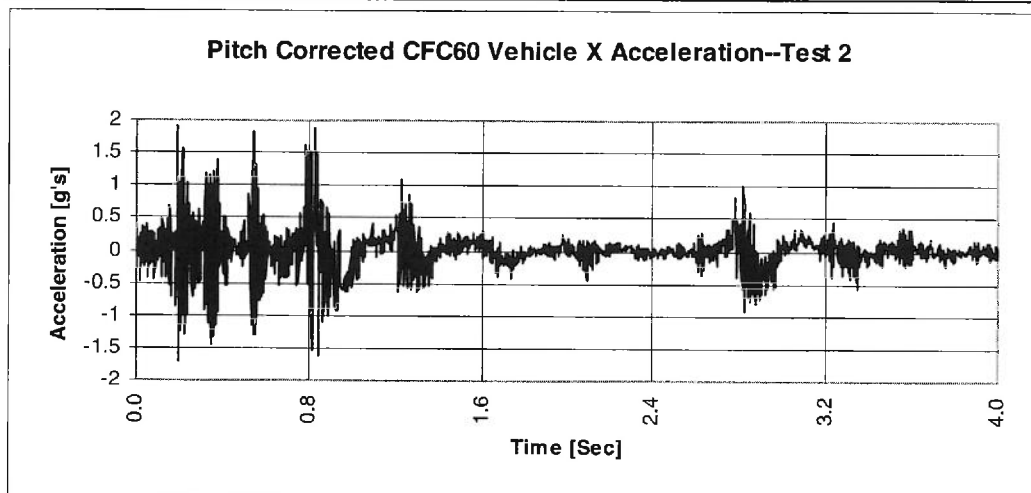
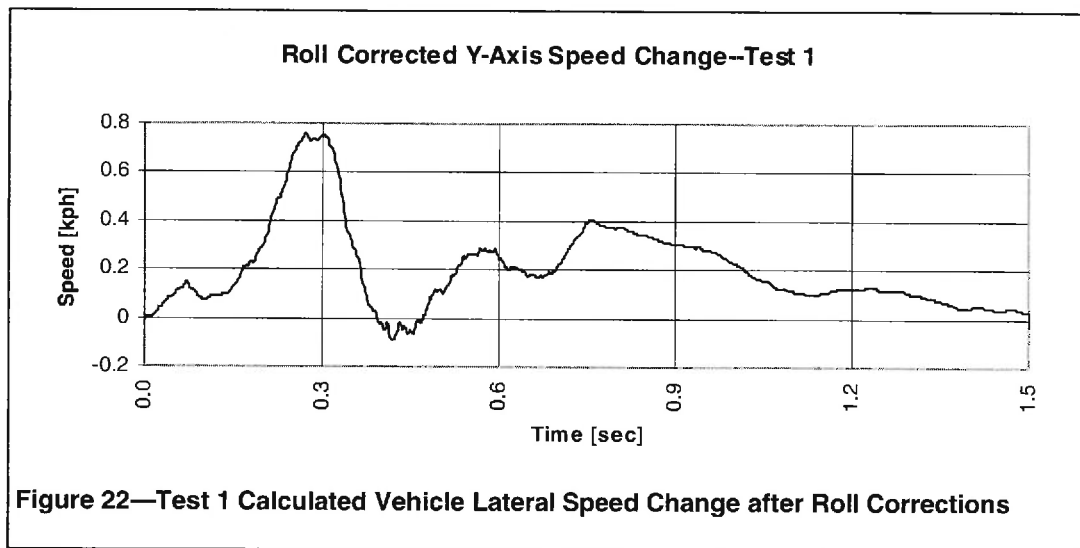
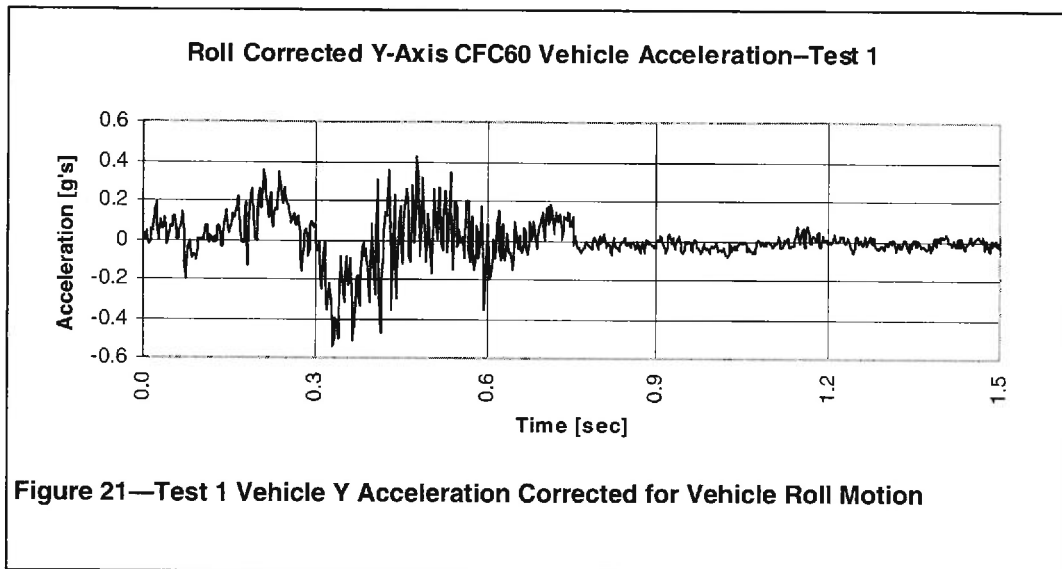
From this it was clear that there was no great relative motion of the test subject in the car, and he was not thrown about in the vehicle. Apart from normal contact between the test subject, the seat, the steering wheel and the vehicle floor and pedals. There was no significant impact or contact between any portion of the subject's body and the interior of the vehicle. In fact, the accelerations measured at the driver's head through the biteplate were not significantly greater or more rapid than he would experience during a brisk walk.

CONCLUSIONS

This paper describes the results of two low speed, heavy truck to car sideswipe impacts. These results indicate that there can be significant damage to the passenger car with only minor accelerations and speed changes being experienced by the car and its occupants. In fact, the forces necessary to cause measurable crush along a significant portion of the side of the vehicle only caused a braked vehicle to rock on its suspension. There would be practically no potential for the occupants of the car to be injured in such an impact unless they were directly contacted by some protruding object from the truck, or part of their body was caught between the vehicles during the impact.

REFERENCES

1. Bailey, M.N., Wong, B.C., and Lawrence, J.M., Data and Methods for Estimating the Severity of Minor Impacts, S.A.E. Paper No. 950352, 1995.



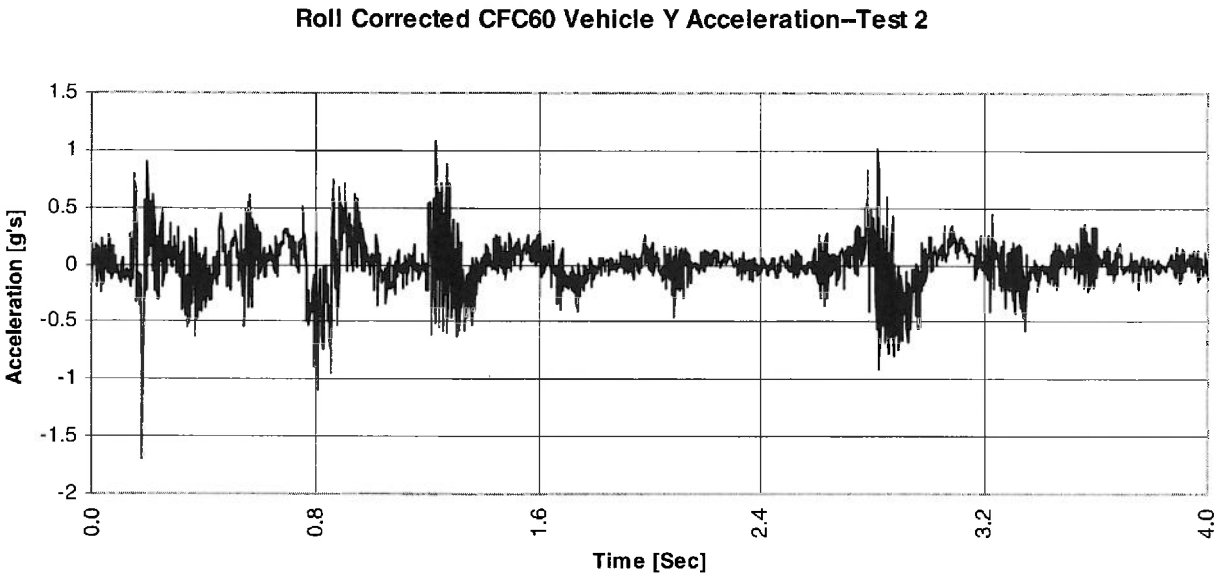


Figure 24—Test 2 Vehicle Y Acceleration after Vehicle Roll Correction

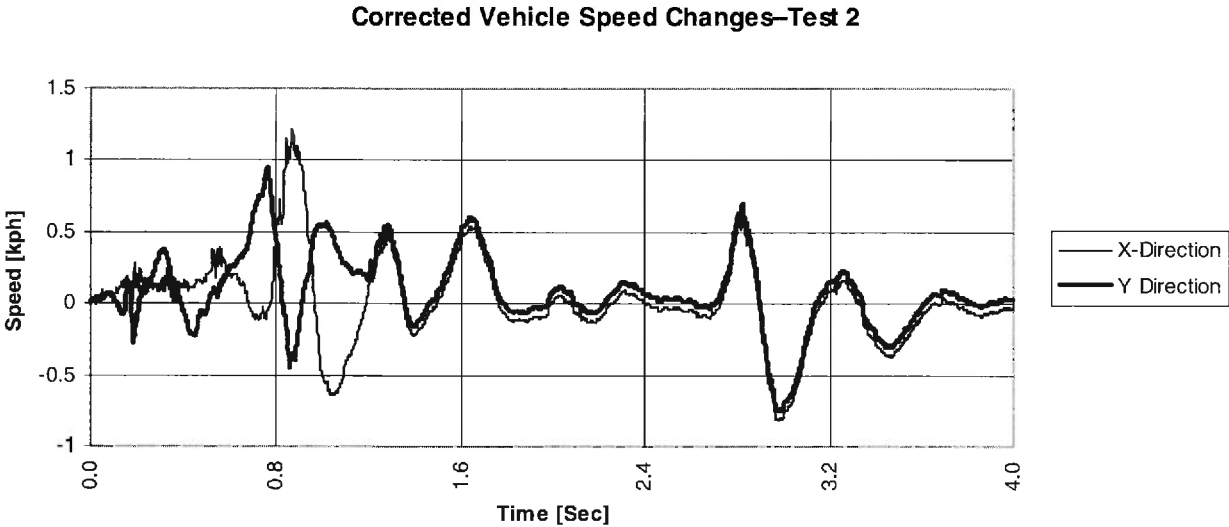


Figure 25—Test 2 Vehicle Speed Change after Vehicle Pitch and Roll Corrections

**SAE TECHNICAL
PAPER SERIES**

2002-01-0020

Human Occupant Kinematics in Low Speed Side Impacts

**Thomas F. Fugger, Jr., Bryan C. Randles
and Jesse L. Wobrock**

Accident Research and Biomechanics, Inc.

Judson B. Weicher and Daniel P. Voss

Biomechanical Research and Testing, LLC

Jerry J. Eubanks

Automobile Collision Cause Analysis

**Reprinted From: Impact Biomechanics
(SP-1665)**

SAE *The Engineering Society
For Advancing Mobility
Land Sea Air and Space®*
INTERNATIONAL

**SAE 2002 World Congress
Detroit, Michigan
March 4-7, 2002**

400 Commonwealth Drive, Warrendale, PA 15096-0001 U.S.A. Tel: (724) 776-4841 Fax: (724) 776-5760

EXHIBIT E

The appearance of this ISSN code at the bottom of this page indicates SAE's consent that copies of the paper may be made for personal or internal use of specific clients. This consent is given on the condition, however, that the copier pay a per article copy fee through the Copyright Clearance Center, Inc. Operations Center, 222 Rosewood Drive, Danvers, MA 01923 for copying beyond that permitted by Sections 107 or 108 of the U.S. Copyright Law. This consent does not extend to other kinds of copying such as copying for general distribution, for advertising or promotional purposes, for creating new collective works, or for resale.

Quantity reprint rates can be obtained from the Customer Sales and Satisfaction Department.

To request permission to reprint a technical paper or permission to use copyrighted SAE publications in other works, contact the SAE Publications Group.



GLOBAL MOBILITY DATABASE

All SAE papers, standards, and selected books are abstracted and indexed in the Global Mobility Database

No part of this publication may be reproduced in any form, in an electronic retrieval system or otherwise, without the prior written permission of the publisher.

ISSN 0148-7191

Copyright © 2002 Society of Automotive Engineers, Inc.

Positions and opinions advanced in this paper are those of the author(s) and not necessarily those of SAE. The author is solely responsible for the content of the paper. A process is available by which discussions will be printed with the paper if it is published in SAE Transactions. For permission to publish this paper in full or in part, contact the SAE Publications Group.

Persons wishing to submit papers to be considered for presentation or publication through SAE should send the manuscript or a 300 word abstract of a proposed manuscript to: Secretary, Engineering Meetings Board, SAE.

Printed in USA

2002-01-0020

Human Occupant Kinematics in Low Speed Side Impacts

Thomas F. Fugger, Jr., Bryan C. Randies and Jesse L. Wobrock
Accident Research and Biomechanics, Inc.

Judson B. Welcher and Daniel P. Voss
Biomechanical Research and Testing, LLC

Jerry J. Eubanks
Automobile Collision Cause Analysis

Copyright © 2002 Society of Automotive Engineers, Inc.

ABSTRACT

A search of the automotive collision trauma literature reveals that over the last 35 years shows that there have been less than ten published Society of Automotive Engineers (SAE) articles describing the collision effects and resulting human occupant kinematics in low speed side impact collisions. The aim of this study was to quantify the occupant response for both male and female occupants for a battery of low-speed side impacts with various impact speeds and configurations.

Eight volunteers were used in a series of twenty-five staged side impact collisions with impact speeds ranging from approximately 2 km/h to 10 km/h and impact configurations to the front, middle and rear side portions of the vehicle. A NHTSA FMVSS 301 moving barrier was used as the impacting vehicle. A stiff bumper was constructed to fit the front of the barrier and was attached at a normal passenger vehicle bumper height. Occupant and vehicle responses were monitored by accelerometers and high-speed video. Occupant kinematic severity was found to have a positive correlation with increasing lateral Delta V.

INTRODUCTION

Lateral impact studies have traditionally concentrated on higher speed impacts that generally result in severe or fatal injuries [1,2,3]. Many of these studies assess the crashworthiness of vehicle side structures and occupant survivability using crash data from various reporting sources, such as the National Accident Sampling System (NASS), Fatal Accident Reporting System (FARS), Transport Canada and others [4-11]. Early research regarding side impacts utilized cadavers and primates in an effort to determine injury threshold values for the development of anthropomorphic test dummies suitable for side impacts [12-13]. The use of biomechanically based mathematical models and anthropomorphic test devices (ATD's) have become

prominent in side impact research [14-15]. Increased implementation of side impact airbags and supplemental inflatable restraints for the occupant head have spawned the development of improved side impact ATD's and protocols for side impact testing that are more representative of real world crashes. However, government compliance testing and independent agency testing is almost exclusively performed at relatively high closing speeds of 50 km/h or greater.

Approximately 50% of side impacts reported in the National Automotive Sampling System (NASS) and Crashworthiness Database System (CDS) for both vehicle-to-vehicle and narrow object near side collisions occurred at delta-V's less than 24 km/h (15 mph). Of these near side impacts, 11% of the vehicle-to-vehicle impacts resulted in an MAIS 3+ compared to 25% in narrow object crashes [11]. Side impacts have been shown to result in more severe injuries for near side occupants compared to far side occupants for the same impact speeds and relative configurations [9]. Recent years have seen a rise in injury claims resulting from low-speed lateral impacts. A review of the current literature yielded only a handful of published studies that address the severity and occupant kinematics of human subjects in low-speed side impacts [16-22]. This study was undertaken to quantify the occupant kinematics of both near side and far side occupants in lateral impacts with differing resulting speed changes.

LITERATURE REVIEW

SEVERITY OF IMPACT – A search of the accident reconstruction literature found two papers that concentrated on the quantification of low-speed side impacts. Bailey *et al* used a momentum-energy-restitution model to predict the change in linear and angular velocity for the target vehicle [16]. This model also predicted the linear velocity change for the bullet vehicle and the energy absorbed during the impact. Toor *et al* proposed a methodology for quantifying

sideswipe collisions that is also applicable to low-speed side impacts [17]. This model utilizes the principles of the CRASH 3 algorithm along with several other calculated parameters, including: contact forces, longitudinal acceleration rates, relative sliding distance and contact duration. Users of these models, as well as users of the CRASH 3 and SMAC algorithms, must apply these models with appropriate care given to the evaluation of the input parameters. Side impact crush coefficient data from government testing is not available for many vehicle makes and models. Additionally, side impacts that include involvement of the axle add an increased stiffness component that is not accounted for in most FMVSS 214 testing.

HUMAN SUBJECT TESTING – In the mid-1960s, a series of lateral impact tests on human subjects was performed by the United States Air Force [18,19]. The first series of tests used a controllable lateral deceleration device with lap belted subjects [18]. The occupant kinematic data, physiologic data and associated symptoms were reported for the subjects for each of the impacts. Subjects experienced average impact decelerations of 3.25 to 9.02 G and impact durations of 0.3 to 0.1 seconds. This study found that no permanent physiological changes were found at exposure to an average deceleration of 9.02 G with a 0.1 second duration for this population. Minor physical complaints were noted for approximately 50% of the subjects at an average deceleration of 6.25 G or above. Physical complaints generally consisted of minor to moderate headache lasting a few minutes and up to a couple of hours and cervical pain lasting a few minutes with possible stiffness up to a couple of days. In a follow-up study, the same controllable deceleration device was used in conjunction with a lap belt and a shoulder harness consisting of two over the shoulder harness straps [19]. In this battery of tests, subjects were exposed to average decelerations of 4.47 to 11.59 G and durations of 0.22 to 0.09 seconds, respectively. Individual physical complaints were not reported; however, it was reported that no permanent physiological changes occurred in this population of young, healthy males. Minor complaints, such as neck muscle soreness, were reported in 60% of the exposures at an average deceleration of 8.8 G and above.

The Naval Aerospace Medical Research Laboratory studied a quantification of the dynamic response of the head and neck to lateral accelerations in the late 1970s [20]. Five volunteers were exposed to sled acceleration profiles ranging from 2 to 11 G, in 1 G increments. Various rates of onset and duration of acceleration were tested. It was determined that increased peak accelerations at the first thoracic vertebrae (T_1) resulted in increased head angular acceleration. Peak T_1 acceleration was the major determinant of peak head angular acceleration and velocity. Time profiles for the acceleration duration was found to be significantly related to T_1 and head linear accelerations and to head angular accelerations. Additional work looked at the

effects of initial positioning of the head using the same basic sled test setup [21]. Peak accelerations ranged from 2 to 7 G, with the rate of onset increasing with the peak acceleration. Different time durations were not tested in this study. Four different seating positions were tested as the initial condition and were defined as follows: neck up/chin up, head tilted left, head tilted right and head down. A peak acceleration of 5 G was the highest acceleration at which all conditions were analyzed. The conclusions of the study determined that, for this population, the initial lateral bending of the head in the direction of the induced acceleration reduces the peak angular acceleration and velocity of the head but increases the head linear acceleration. The effects of initial lateral flexion in the direction of the induced acceleration were found to be greater than in the direction contrary to the induced acceleration. It was also determined that lateral bending of the head in general significantly reduced the peak head angular acceleration and velocity. Forward flexion of the cervical spine increases the angular acceleration and velocity of the head put this after lateral bending discussion. No physical symptoms were reported in these studies, however, it was indicated in the head down (flexed) condition that subjects who had struck their chin against the right shoulder or right shoulder restraint at 5 G were not run at 6 G and no head down conditions were run at 7 G.

Matsushita *et al* studied human neck motion using cineradiographic techniques and accelerometry in low-speed rear-end, frontal and lateral impacts [22]. Only three tests were performed laterally at delta V's of 3.4, 3.4, and 4.2 km/h. The use of electromyography (EMG) permitted the reporting of relaxed or tensed muscle activity in the neck prior to and immediately after impact. All three subjects were reported as relaxed at the time of impact. One male subject was unbelted and the other male subject and female subject were both lap-shoulder belted at the time of impact. No physical complaints were documented and it was noted that severe cervical lateral flexion did not occur because of the lack of a side structure to restrict the movement of the torso.

Low speed vehicle-to-vehicle lateral impact testing with human volunteers was performed by Bailey *et al* [16]. The five tests had a delta V range of 0.7 to 6.8 km/h with a peak vehicle acceleration of 4.8 G. The vehicle motion was described as lateral with no significant rotational displacement. Occupant kinematic data were not reported. The male occupants were seated as far side passengers and the volunteers did not strike anything in the vehicle interior. No physical symptoms were reported by any of the volunteers.

METHODS

COORDINATE SYSTEM - All acceleration axis systems were in accordance with SAE J211/1 Recommended Practice and SAE J1733 Information Report with the positive X, Y and Z axes forward, rightward and downward, respectively [23,24]. The SAE sign

convention dictated that lateral flexion of the spine was positive going from left to right (+Y axis directed mediolaterally from L to R).

HUMAN SUBJECTS – Four male (28.8 ± 7.5 years, 179 ± 1.5 cm, 83 ± 2.9 kg) and four female (22.3 ± 3.5 years, 167.6 ± 3.7 cm, 61.1 ± 4.1 kg) volunteers were subjected to six impacts. Basic anthropometric data for each subject can be found in Table 1. Each of the male subjects were directly involved in the research and the female subjects were previously known to the researchers. For each of the impacts, the male subject was seated as the near side front passenger and the female subject as the far side front passenger. The volunteers were adequately informed of the aims, methods, anticipated benefits and potential hazards of the study. Each participant was informed that they were at liberty to abstain from participation at any time. The subjects submitted informed consent in writing according to the Declaration of Helsinki [25].

Subject	Seating Position	Age	Height (cm)	Weight (kg)
F1	far side	26	163.8	61.4
M1	near side	24	177.8	86.4
F2	far side	24	165.1	55.9
M2	near side	25	180.3	81.8
F3	far side	18	171.5	65.9
M3	near side	26	180.3	79.5
F4	far side	21	170.2	61.4
M4	near side	40	177.8	84.1

Table 1 – Anthropometric data and seating position for vehicle occupants

Head accelerations for both the near side and far side occupants were obtained via a single triaxial block of IC Sensors 3031-050 (50 g) accelerometers affixed to the center of the forehead via a lightweight headband. The headband was made of rubber which, when tightly fastened to the subject's head, formed a secure bond.

Thorax and lumbar accelerations were also obtained for the far side (female) occupants. A specially developed low profile (<1 cm) triaxial block of accelerometers was constructed using two Entran EGAXT-50 accelerometers and one IC Sensors 3031-050 accelerometer. This was affixed to the occupant with medical adhesive at the approximate level of C7-T1 on the anterior torso. A lightweight uniaxial IC Sensors 3031-050 accelerometer was affixed with medical adhesive to the base of the subject's lumbar spine at the approximate location of L5-S1.

VEHICLES – A Federal Motor Vehicle Safety Standard (FMVSS) 301 rigid moving barrier was used as the bullet vehicle. Photographs of the FMVSS 301 barrier used can be found in Appendix A. A rigid bumper was attached to the face of the barrier at a normal bumper

height. The target vehicles were two 1989 Ford Escort GT's. Neither of the vehicles were modified other than removal of the center console and carpeting for sensor placement. Vehicle and barrier data for the tests can be found in Table 2.

Year	Make	Model	VIN	Wf (kg)	Wr (kg)	Wt (kg)
1989	Ford	Escort GT	1FAPP93J1KWxxxxxx	663.2	404.5	1067.7
1989	Ford	Escort GT	1FAPP93J0KWxxxxxx	664.1	404.1	1068.2
N/A	FMVSS	301 Barrier	N/A	1250	627.3	1877.3

Table 2 – Vehicle and barrier information



Figure 1 - Barrier/vehicle exemplar orientation

The barrier was accelerated down an inclined roadway and was assisted by the researchers for the higher speed impacts. The barrier was perpendicular to the target vehicle for all impacts. Figure 1 shows the impact configuration for the tests to the front side portion of the vehicle. Each portion of the vehicle's side (front, door/middle, rear) were impacted twice; once at an approximate damage onset threshold (approximately 2 to 4½ km/h) and a second time at a damage producing speed (approximately 6 to 10 km/h). A time trap (DTS Timer Interval Meter) triggered by pressure sensitive tape switches (Tape Switch Corporation Type 102A) and an optical time trap (Farmtek, Inc.) recorded the bullet vehicle's velocity immediately prior to impact. A triaxial array of accelerometers (IC Sensors 3031-050) was affixed to the target vehicle's approximate static center of gravity. The accelerometer placement was approximately equal to the longitudinal (X-axis) position of the normal seating position of the occupants. The acceleration data were used to determine the kinematic response of the center of gravity of the target vehicle. The target vehicle was in neutral with the driver's foot on the brake pedal prior to impact.

TEST PROTOCOL – Six impacts were performed to each side of the vehicles. The first three impacts were at the damage onset threshold speed and the second series at the higher damage producing speed. Each series of three side impacts started with an impact to the front, followed by an impact to the door structure and then an impact to the rear section of the vehicle.

The volunteers were given no specific instruction regarding seating position, and were simply told to adopt a normal driving or seating position. The volunteers adjusted the seat fore-aft position and seat back angle to whatever position they determined was comfortable. Standard lap and shoulder belt were worn for all tests. The only instruction given to the occupants was to maintain their normal seating position and to look forward prior to impact. Figure 2 represents a basic schematic of the test impact configurations relating the barrier position to the vehicle.

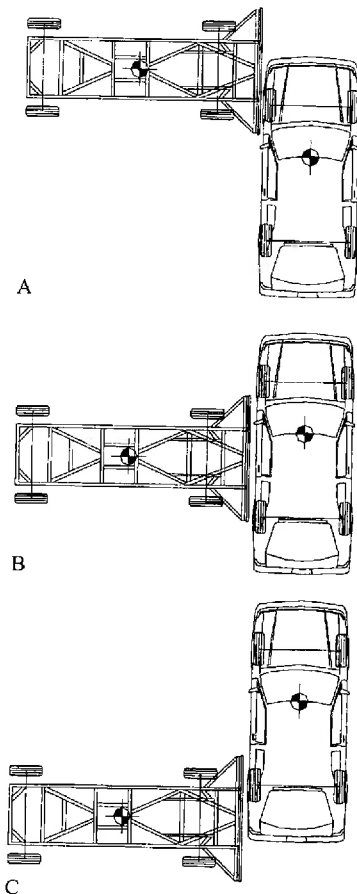


Figure 2 - Barrier/vehicle impact orientation to (A) front, (B) door area/middle and (C) rear

DATA ACQUISITION AND POST PROCESSING - All data were collected following the general theory of SAE Recommended Practice: Instrumentation for Impact Test - J211/1 Mar95 [23]. All accelerometer data were collected at 1000 Hz. Vehicle changes in velocity were calculated from vehicle acceleration data filtered with an SAE Class 180 filter. Occupant acceleration data were filtered with an SAE Class 60 filter in accordance with previous research [26].

RESULTS

The lateral acceleration were collected from the target vehicle and used to determine the Delta V (change in

velocity of the struck vehicle). In addition, the lateral displacement of the front and rear tires of the target vehicle were measured immediately post impact. The relevant peak values are shown in Table 3.

Test	Area of target contact	Peak Y-Axis Accel.	Lateral Delta V (km/h)	Front wheel Y disp. (mm)	Rear wheel Y disp. (mm)
Right Sided Impacts					
8	front	-3.9	-2.5	-102	0
9	door	-2.5	-2.0	-102	-32
10	rear	-1.6	-1.3	-76	-279
11	front	-9.7	-5.4	-356	-25
12	door	-17.0	-6.4	-366	-343
13	rear	-5.0	-3.6	-152	-579
14	front	-4.4	-3.2	203	0
15	door	-5.2	-3.9	-83	-127
16	rear	-1.2	-2.2	-254	-533
17	front	-18.3	-5.8	-991	-203
18	door	-14.8	-9.8	-686	-673
19	rear	-7.0	-4.0	-2083	-1727
Left Sided Impacts					
1	front	3.2	1.7	133	13
3	door	5.1	3.7	76	146
4	rear	2.7	2.0	0	292
5	front	8.8	5.3	57	140
6	door	4.8	5.8	273	413
7	rear	6.0	3.5	203	129
20	front	12.6	3.0	216	0
21	door	5.4	4.3	114	152
22	rear	1.6	1.8	91	699
23	front	22.0	6.7	1308	451
24	door	18.6	7.5	508	762
25	rear	6.8	4.0	1378	2870

Table 3 - Peak Y-axis vehicle parameters

Lateral occupant accelerations were recorded for both near and far side occupants. More acceleration measures were collected from the female occupant in all tests due to their under representation in the human subject testing literature. Relative acceleration between the thorax and lumbar region was also considered as an indicator of possibly deleterious occupant motion. Table 4 shows the peak values of the selected quantities. Note that, as with the vehicle parameters, the occupant parameters are reported in accordance with the SAE J211 sign convention. Thus, the peak value of interest is typically of opposite sign for left vs. right-sided impacts.

Minor physical complaints were noted immediately after five of the twenty-five impacts. The complaints were generally a transient complaint of pain in the back or a slight headache that lasted only a few minutes. All of these came after the higher velocity impacts. Physical complaints were noted/experienced within the one to three days following testing in four of the eight subjects. They consisted of minor neck or shoulder soreness that lasted a day in three of the subjects and a maximum of three days in one of the subjects. All symptoms resolved without treatment and no permanent physiological changes were noted. Occupant information including answers to the post-impact questionnaire for each test and a follow-up regarding any physical symptoms are reported in Appendices B and C.

Test	Near Side	Far Side			
	Head (Y) G	Head (Y) G	Thorax (Y) G	Lumbar (Y) G	Thorax relative to Lumbar (Y) G
Right Side Impacts					
8	-1.0	dl	dl	dl	dl
9	-1.4	-0.9	-0.6	-1.6	-1.6
10	-1.2	-1.4	-1.3	-2.1	-2.1
11	-2.2	-1.7	-1.6	-3.6	-3.6
12	-2.2	-1.9	-2.7	-1.5	-1.5
13	-2.4	-2.6	-5.6	-5.7	-5.7
14	-1.4	-1.0	-1.2	-1.8	-1.8
15	-1.5	-1.3	-2.1	-3.0	-2.5
16	-1.3	-1.3	-1.7	-2.1	-1.9
17	-2.4	-2.8	-2.2	-2.6	-2.8
18	-7.1	-3.8	-6.4	-5.3	-6.7
19	-6.1	-2.5	-4.3	-4.9	-6.2
Left Side Impacts					
1	1.5	0.7	0.7	1.3	1.4
3	2.5	2.4	2.2	3.4	3.4
4	1.7	1.4	1.6	2.2	2.0
5	2.5	0.8	2.0	2.3	1.9
6	4.3	3.4	5.2	4.5	6.2
7	4.5	dl	dl	dl	dl
20	2.1	0.7	0.7	1.6	1.5
21	1.7	1.3	1.4	0.5	1.1
22	1.4	1.4	1.6	2.0	1.9
23	2.7	1.5	3.0	2.4	2.4
24	8.8	4.1	7.7	6.5	5.8
25	8.4	4.9	5.9	6.2	6.5

Table 4 - Peak Y-axis occupant parameters

DISCUSSION

The results indicate that there was a clear difference between near and far sided occupants with respect to peak head lateral acceleration. Near sided occupants typically had higher peak accelerations and shorter duration acceleration curves. This was most pronounced in impacts where the near side occupant reported body contact (i.e. arm, shoulder, head) with the interior structure of the door; however, the condition still persisted where no contact was reported. A representative comparison is shown in Figure 3. This result would appear to be similar to what Matsushita [22] found in that the far side occupant's lateral motion is not restricted by occupant interior contact. There may also be effects from the stature differences between the near and far sided occupants (typically the far side occupant was 8-15 cm shorter).

In addition, a time shift of acceleration onset for different portions of the occupant was clearly represented for both near and far side occupants. The lumbar region acceleration was most tightly coupled with the vehicle acceleration. The thorax acceleration lagged behind the lumbar acceleration and almost always had a lower peak. Likewise, the onset of significant head acceleration did not occur until after the vehicle acceleration pulse had already subsided and was generally lower than both the lumbar and thorax accelerations. This is similar to the trend seen in antero-posterior (X-axis) direction acceleration pulses seen in rear end collisions with the exception that the head accelerations in rear end impacts tend to be higher due

to head-to-head restraint contact. An example of this phenomenon is shown in Figure 4.

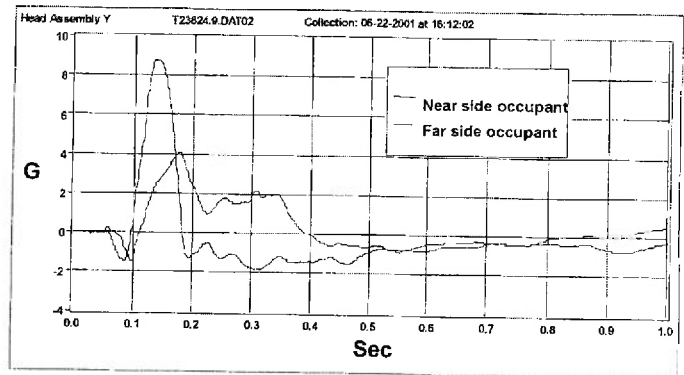


Figure 3 - Head acceleration comparison of near side to far side occupant for a driver's side impact

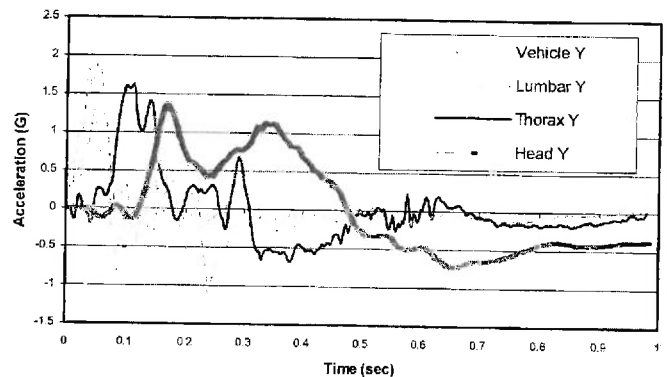


Figure 4 - Comparison of acceleration profiles for the lumbar, thoracic and head mounted accelerometers

Finally, there was weak but significant ($p < 0.05$) correlation between the measured target vehicle lateral Delta V and the relevant lateral occupant acceleration measures.

Physical complaints immediately after impact were noted in only five out of the 50 exposures (10%). Of these complaints, 60% were reported by the far side (female) occupant and all were transient in nature. Care should be used when attempting to extend this result to an occupant involved in a single impact as each human subject in this test series was exposed to a total of six impacts. Multiple exposures in the subject study may have resulted in an increased prevalence of complaints. Post-test interviews with the subjects revealed that three of the subjects that had experienced physical complaints immediately following a test, experienced symptoms consisting of minor muscle soreness in the back or neck region of not more than 24 hours in duration. One of the female subjects who did not experience any symptoms the day of or day after testing had minor muscle soreness two days after the series of tests. This soreness lasted only one day and was similar to the phenomenon of delayed onset muscle soreness (DOMS).

CONCLUSION

A series of 24 lateral impact tests were performed resulting Delta V's of the struck vehicle of 1.3-9.8 km/h. Acceleration measurements were recorded from eight human occupants (4 female, 4 male) with particular emphasis on the far side, or female, occupant. Each occupant underwent six impacts. The data indicated a tight coupling between the lumbar region of the occupant and the vehicle (likely due to lap belt use and frictional effects of the seat). In addition, statistical analysis showed an increase in occupant kinematic severity with increasing lateral Delta V measured at the center of gravity of the target vehicle.

ACKNOWLEDGMENTS

The authors would like to thank the volunteers for their participation in this study.

REFERENCES

1. Severy, D., Mathewson, J. and Siegel, A. Automobile side-impact collisions. Society of Automotive Engineers 600470, Warrendale, PA, 1960.
2. Severy, D., Mathewson, J. and Siegel, A. Automobile side-impact collisions – Series II. Society of Automotive Engineers 620149, Warrendale, PA, 1962.
3. Shaw, L. and Clark, C. Side impact restraint development and evaluation techniques. Society of Automotive Engineers 806052, Warrendale, PA, 1980.
4. O'Day, J. and Kaplan, R. The FARS data and side-impact collisions. Society of Automotive Engineers 790736, Warrendale, PA, 1979.
5. Melvin, J., O'Day, J., Campbell, K., Robbins, D. and Huelke, D. Side impacts: a comparison of laboratory experiments and NCSS crashes. Society of Automotive Engineers 800176, Warrendale, PA, 1980.
6. Partyka, S. and Rezabek, S. Occupant injury patterns in side impacts – a coordinated industry/government accident data analysis. Society of Automotive Engineers 830459, Warrendale, PA, 1983.
7. Dalmotas, D. Injury mechanisms to occupants restrained by three-point seat belts in side impacts. Society of Automotive Engineers 830462, Warrendale, PA, 1983.
8. Hobbs, C. and Mills, P. Injury probability for car occupants in frontal and side impacts. Transport and Road Research Laboratory Report 1124. 1984.
9. Miltner, E. and Salwender, H. J. Injury severity of restrained front seat occupants in car-to-car side impacts. *Accid. Anal. and Prev.* 27(1), 105-110, 1995.
10. Augenstein, J., Bowen, J., Perdeck, E., Singer, M., Stratton, J., Horton, T., Rao, A., Digges, K., Malliaris, A. and Steps, J. Injury patterns in near-side collisions. Society of Automotive Engineers 2000-01-0634, Warrendale, PA, 2000.
11. Zaouk, A., Eigen, A. and Diggs, K. Occupant injury patterns in side crashes. Society of Automotive Engineers 2001-01-0723, Warrendale, PA, 2001.
12. Stalnaker, R., Roberts, V. and McElhaney, J. Side impact tolerance to blunt trauma. Society of Automotive Engineers 730979, Warrendale, PA, 1973.
13. Morgan, R., Marcus, J. and Eppinger, R. Correlation of side impact dummy/cadaver tests. Society of Automotive Engineers 811008, Warrendale, PA, 1981.
14. Payne, A. and Hopton, J. Comparison study of EuroSID, USSID, and BioSID performance using MIRA's new M-SIS side impact simulation technique. Society of Automotive Engineers 960103, Warrendale, PA, 1996.
15. Ahn, C. and Bae, H. Development of finite element US-SID and Euro-SID model. Society of Automotive Engineers 2000-01-0160, Warrendale, PA, 2000.
16. Bailey, M., Wong, B. and Lawrence, J. Data and methods for estimating the severity of minor impacts. Society of Automotive Engineers 950352, Warrendale, PA, 1995.
17. Toor, A., Roenitz, E., Johal, R., Overgaard, R., Happer, A. and Araszewski, M. Practical analysis technique for quantifying sideswipe collisions. Society of Automotive Engineers 1999-01-0094, Warrendale, PA, 1999.
18. Zaborowski, A. Human tolerance to lateral impact with lap belt only. Proceedings of the 8th Stapp Car Crash Conference, 1964.
19. Zaborowski, A. Lateral impact studies: lap belt shoulder harness investigations. Proceedings of the 9th Stapp Car Crash Conference, 1965.
20. Ewing, C., Thomas, D., Lustik, L., Muzzy, W., Willems, G. and Majewski, P. Dynamic response of the human head and neck to +Gy impact acceleration. SAE 770928. Proceedings of the 21st Stapp Car Crash Conference, 1977.
21. Ewing, C., Thomas, D., Lustik, L., Muzzy, W., Willems, G. and Majewski, P. Effect of initial position on the human head and neck to +Y impact acceleration. SAE 780888. Proceedings of the 22nd Stapp Car Crash Conference, 1978.
22. Matsushita, T., Sato, T., Hirabayashi, K., Fujimura, S., Asazuma, T. and Takatori, T. X-ray study of the human neck motion due to head inertia loading. SAE 942208. Proceedings of the 38th Stapp Car Crash Conference, 1994.
23. SAE: "Surface Vehicle Recommended Practice: (R) Instrumentation for impact test – Part 1 – Electronic instrumentation – SAE J211-1", Society of Automotive Engineers, J211-1, 1995.
24. SAE: "Surface Vehicle Information Report: Sign Convention for Crash Testing - SAE J1733", Society of Automotive Engineers, J1733, 1994.

25. "Recommendations Guiding Medical Doctors in Biomedical Research Involving Human Subjects", 41st World Medical Assembly, World Medical Assembly Declaration of Helsinki, September, 1989.
26. Szabo, T.J. and Welcher, J.B.: "Human Subject Responses to Various Acceleration Fields", in Low Speed Collision TOPTEC, Society of Automotive Engineers, Richmond, BC, 1996.

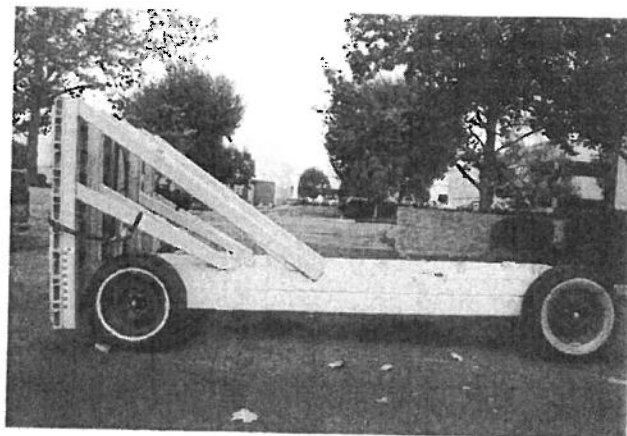
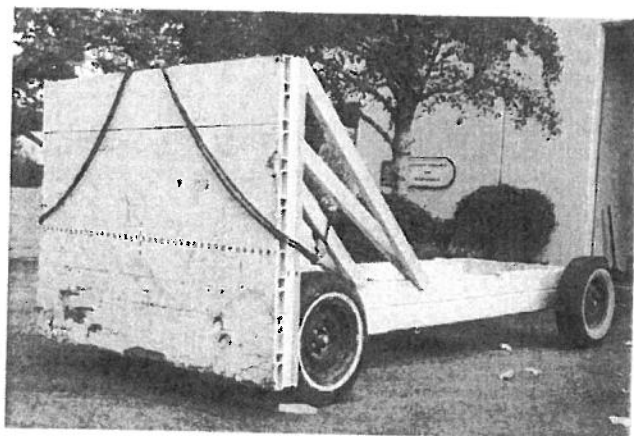
CONTACT

Thomas F. Fugger, Jr., P.E.
Accident Research and Biomechanics, Inc.
27811 Avenue Hopkins, Suite 1
Valencia, CA 91354
arb@accidentresearch.com

Judson B. Welcher
Biomechanical Research and Testing, LLC
1827 Ximeno Avenue, #2
Long Beach, CA 90815
welcher@scf.usc.edu

APPENDIX

Appendix A - NHTSA FMVSS 301 rigid moving barrier photos



Appendix B – Post-test follow-up interview summary

Subject	Day of test	1 day post	1 week post	2 weeks post	3 weeks post	1 month post	2 months post	3 months post	4 months post	5 months post	6 months post
F1	reduced movement of neck and slight headache after test 4	left subscapular, subclavicular neck stiffness 1 day duration	none	none	none	none	none	none	none	none	none
M1	slightly light-headed after test 7	none	none	none	none	none	none	none	none	none	none
F2	none	none	minor neck stiffness 1 day duration, less than working out, 2 to 3 days post testing	none	none	none	none	none	none	none	none
M2	none	none	none	none	none	none	none	none	none	none	none
F3	slight headache after test 18 and small cut on ankle some upper back stiffness 3 hours post	mid to lower back stiffness only 1 day	rear-ended at approx 20 mph while driving (no additional soreness attributable to testing)	none	none	none	none	none	none	none	none
M3	none	none	none	none	none	none	none	none	none	none	none
F4	slight pain in thoracic (T7) area following test 24	none	none	none	none	none	none	none	none	none	none
M4	slight dizziness after last impact test 25	exacerbation of previous soft-tissue complaints in left shoulder	none	none	none	none	none	none	none	none	none

Appendix C – Post-impact questionnaire responses.

Responses following right-sided impacts

Test #	Subject	Perceived body motion	Impact vehicle interior	Hands remain on steering wheel	Foot remain on brake	Vehicle pushed lateral	Relaxed/not anticipating	Rate impact to 1st	Seatbelt engage	Physical Complaints
8	M2	Right	Yes - upper arm hit door	N/A	N/A	No	Yes	Normal	No	No
	F2	Left	No	Yes	Yes	Yes - couple of inches	Yes	Very light	No	No
9	M2	Right	Yes - upper arm hit door	N/A	N/A	No	Yes	Less Severe	No	No
	F2	Jostelled	No	Yes	Yes	No	Yes	Less Severe	No	No
10	M2	Right	No	N/A	N/A	Yes - 10" at rear	Yes	About the same	No	No
	F2	Left	No	Yes	Yes	Yes - 5"	No	More Severe, strong	No	No
11	M2	Right	Yes - upper arm hit door, head hit edge of roof	N/A	N/A	Yes - 20" at front, 4" at rear	Yes	More severe	No	No
	F2	Left	No	No	Yes	Yes - 2'	Yes	Much more severe	No	No
12	M2	Right	Yes - upper arm hit door	N/A	N/A	Yes - 6" total	Yes	More severe	No	No
	F2	Left	Yes - right ankle hit center console mount	Yes	No	Yes - 2'	Yes	More severe	Yes	No
13	M2	Right	Yes - upper arm hit door, head hit edge of roof, knee hit window crank	N/A	N/A	Yes - 5' at rear, 1.5' at front	Yes	More severe	No	No
	F2	Left	Yes - left shoulder hit side door	Yes	Yes	Yes - 4' at the rear	Yes	More severe	Yes	No
14	M3	Left	No	N/A	N/A	Yes - 6"	Yes	Minor impact	Yes	No
	F3	Right	No	Yes	Yes	Yes - 3"	Yes	N/A	No	No
15	M3	Right	No	N/A	N/A	Yes - 1'	Yes	Less Rotation	No	No
	F3	Left	No	Yes	Yes	Yes - 6"	Yes	About the same	No	No
16	M3	Right	No	N/A	N/A	Yes - 1.5' at rear	Yes	A little worse	No	No
	F3	Right	No	Yes	Yes	Yes - 2'	Yes	More severe	No	No
17	M3	Right	Yes - upper arm hit door, right knee hit door	N/A	N/A	Yes - 2' in the front	Yes - but saw it coming	More severe	No	No
	F3	Left	No	No	Don't know	Yes - 3' at the front	Yes	More severe	No	No
18	M3	Right	Yes - upper arm hit door, right knee hit door	N/A	N/A	Yes - 2'	Yes	More severe	No	No
	F3	Right	Yes - left leg hit door, right ankle hit center console brace	Yes	No	Yes - 2'	Yes	More severe	No	Yes - tension headache, small cut on right ankle
19	M3	Right	Don't know	N/A	N/A	Yes - 5' at rear, 1' at front	Yes	More severe	Yes	No
	F3	Right	No	Yes	Yes	Yes - 6' at rear, 2' at front	Yes	More severe, much worse	No	No

Responses following left-sided impacts

Test #	Subject	Perceived body motion	Impact vehicle interior	Hands remain on steering wheel	Foot remain on brake	Vehicle pushed lateral	Relaxed/not anticipating	Rate impact to 1st	Seatbelt engage	Physical Complaints
1	M1	Right	No	Yes	Yes	Yes - 1'	Yes	Severe/Fo rceful	No	No
	F1	Right	No	N/A	N/A	Yes - 6"	Yes - eyes closed	Harder than expected	No	No
3	M1	Left to Right	No	Yes	No	Yes - 4"	Yes	Not as sharp	N/A	No
	F1	Right	No	N/A	N/A	Yes - < 6"	Yes	Harder	No	No
4	M1	Right	No	Yes	Don't know	Yes - 1'	Yes	Similar	N/A	No
	F1	Right	No	N/A	N/A	Yes - 1' at rear	Yes	More Severe, very hard	No	Yes - Reduced/painful neck movements, headache
5	M1	Right	No	Yes	No	Yes - 1.5'	Yes	Harder	N/A	No
	F1	Slightly to the right	No	N/A	N/A	Yes - 2' at front	Yes	Harder impact, body felt it less	No	No
6	M1	Dramatically to right	No	Yes	No	Yes - 1'	Yes	Stronger	N/A	No
	F1	Right	No	N/A	N/A	Yes - 1.5'	Yes	More Severe/Very hard	No	No
7	M1	Strongly to the right	Yes - shoulder hit door	Yes	No	Yes - it rotated 4'	Yes	Stronger	N/A	Yes - A little lightheaded, not very severe
	F1	Don't know	No	N/A	N/A	Yes - 5'	Yes	More Severe, hardest	No	No
20	M4	Left	No	Yes	Yes	Yes - 1'	Yes	Minor, loud	No	No
	F4	Right then left	No	N/A	N/A	Yes - 1'	Yes	Loud, small jolt	Yes	No
21	M4	Left	No	Yes	Yes	Yes - 1'	Yes	More severe	No	No
	F4	Left	No	N/A	N/A	Yes - 1'	Yes	More severe	No	No
22	M4	Right	No	Yes	Yes	Yes - 1.5' at rear	Yes	Less severe	No	No
	F4	Left	No	N/A	N/A	Yes - 2' at rear	Yes	Less severe	No	No
23	M4	Left	Yes - left knee bumped the door	Yes	Yes	Yes - 3' at the front	Yes	More severe	No	No
	F4	Left	No	N/A	N/A	Yes - 4' at the front	Yes	More severe	No	No
24	M4	Left	Yes - left shoulder hit side door	Yes	Yes	Yes - 4'	Yes	More severe	No	No
	F4	Left then right	Yes - right elbow hit door	N/A	N/A	Yes - 1'	Yes	More severe	Yes	Felt pain immediately after in thoracic, ~ T7
25	M4	Left	Yes - left shoulder hit side door	No	Don't know	Yes - 5' at the rear	Yes	More severe, not as severe as straight broadside	No	Yes - dizziness and unsteadiness
	F4	Forward left	No	N/A	N/A	Yes - 5' at the rear		More severe	Yes	No



Passenger Vehicle Occupant Response to Low-Speed Impacts with a Tractor-Semitrailer

2011-01-1125

Published
04/12/2011

Kathleen Allen Rodowicz, Kenneth Dupont, Janine Smedley, Christine Raasch, Chimba Mkandawire, Daniel Fittanto, Cleve Bare and James Smith
Exponent, Inc.

Copyright © 2011 SAE International

doi:10.4271/2011-01-1125

ABSTRACT

Low-speed sideswipe collisions between tractor-semitrailers and passenger vehicles may result in large areas of visible damage to the passenger vehicle. However, due to the extended contact that occurs during these impacts, it is typical in these incidents for the crash pulse duration to be long and the vehicle accelerations to be correspondingly low. Research regarding the impact environment and resulting injury potential of the occupants during these types of impacts is limited. Five full-scale crash tests utilizing a tractor-semitrailer and a passenger car were conducted to explore the occupant responses during these types of collisions. The test vehicles included a van semitrailer pulled by a tractor and three identical mid-sized sedans. The occupants of the sedans included an instrumented Hybrid III 5th -percentile-male anthropomorphic test device (ATD) in the driver's seat and an un-instrumented Hybrid III 5th -percentile-female ATD in the left rear seat. The ATDs were positioned in the vehicle consistent with Federal Motor Vehicle Safety Standard (FMVSS) Number 208, Occupant Crash Protection. The ATD in the driver's seat was restrained with a lap and shoulder belt, while the rear passenger ATD was unrestrained. Instrumentation on the sedans included accelerometers and rotational rate sensors, and occupant kinematics were recorded using onboard and off-board high-speed video cameras. The tests included four sideswipe impacts, involving extended contact between the semitrailer bottom rail (lower longitudinal structure of the trailer box) and dual wheels and the side of the sedans. A single perpendicular collision involving the semitrailer dual wheels and the right front corner of the sedan was also conducted. The driver ATD's head accelerations, upper and lower neck forces and moments, lumbar spine forces and moments, and left and right femur loads were measured, along with seat belt

webbing loads. Head and spine data were compared to volunteer studies of vigorous activities of daily living, published human tolerance levels, and Injury Assessment Reference Values (IARVs) used in compliance testing of passenger vehicles. It was determined that the biomechanical responses in the head, upper neck, and femur of the ATD were well below the established IARVs, and the biomechanical responses in the head, upper neck, and lower back of the ATD were lower than or comparable to the responses of these body regions to the loads experienced by volunteers during non-injurious activities.

INTRODUCTION

Despite mirror placement and usage, most heavy trucks have blind spots where the driver cannot see other vehicles on the roadway. Warnings and labels are posted on heavy trucks to educate other road users of this visibility hazard, as well as the turning radius and other operating characteristics of such trucks. However, heavy truck-to-passenger vehicle sideswipe crashes do occur, especially during low-speed heavy truck cornering maneuvers, where off-tracking of the trailer tires may be significant. The damage that is produced on the passenger vehicle during such interaction with a tractor-semitrailer often involves damage to the surface of multiple body panels of the passenger vehicle, and is thus costly to repair. However, passenger vehicle accelerations observed during these sideswipe impacts are low with a long duration crash pulse, due to the extended contact and interaction of the passenger vehicle with the tractor-trailer. Review of the literature on heavy truck crashes with passenger vehicles identified a paucity of data on the passenger vehicle occupant response during such impacts. Tanner et al. [1] measured biteplate accelerations in a human driver during two truck-to-car sideswipe impacts, finding peak accelerations below 1.2

g. Although this provided an indication that the occupant loading in such an impact was benign, direct measurement of internal loads and accelerations is desirable in order to more thoroughly quantify injury risk.

Crash testing utilizing anthropomorphic test devices (ATDs) is used by numerous research institutions, government agencies, and private companies as a means of evaluating occupant kinematics and injury potential in a variety of crash modes. As such, a series of crash tests was conducted to further develop objective data regarding the occupant kinematics and injury potential for occupants of passenger vehicles involved in sideswipe collisions with a tractor-semitrailer. The loads acting in the head, upper neck, lower back, and femurs were measured, and these values were compared to their respective injury assessment reference values (IARVs), if applicable, and to the loads experienced by volunteers during non-injurious and vigorous activities (i.e., activities resulting in no documented objective injuries and, at most, complaints of transient subjective symptoms that subsequently resolved after several days). IARVs came into existence approximately 40 years ago, and they are commonly used in academia, industry, and government to evaluate the risk of injury to the body due to a mechanical loading event [2, 3]. Injury tolerance is dependent on a number of variables including gender, age, weight, and height, and therefore IARVs were developed for varying anthropometries [4]. Relating these values to specific injuries often involves use of the Abbreviated Injury Scale (AIS), which codes injuries from minor (AIS 1) to maximum (AIS 6) [5].

As early as 1960, researchers began to establish human tolerance levels to head impacts [3]. This work led to the creation of the head injury criterion (HIC) by Versace in 1971 which was then later modified by the National Highway Traffic and Safety Administration (NHTSA) [3, 6, 7]. HIC is a function of the integral of the resultant linear acceleration of the head with respect to time. The time interval used to compute HIC is either 36 ms (HIC₃₆) or 15 ms (HIC₁₅). Currently, HIC₁₅ is used by the NHTSA to determine the risk of head injury [3]. HIC has been utilized to assess risk for injuries of varying severity, such as skull fracture (AIS 2) and severe brain injury (AIS 4) [4].

Neck injury reference values are utilized to determine the risk of injury to the upper neck during single loading conditions (i.e., tension, compression, extension, and flexion) and combined loading conditions, N_{ij} (i.e., tension or compression combined with extension or flexion). Current neck IARVs are based on a low percentage risk of serious or greater (AIS 3+) upper cervical spine injury [4].

The IARV for femur loading was created to determine the risk of injury due to compressive loading of the femur along

the long axis of the bone. Currently, there are no established IARVs for the lower back. However, the National Institute for Occupational Safety and Health (NIOSH) referenced a lumbar disc compression force limit of 3400 N in deriving a Recommended Weight Limit equation for safe occupational lifting [8].

The Federal Motor Vehicle Safety Standard (FMVSS) Number 208 for frontal impact protection includes the following IARVs, or critical intercepts, for the head, upper neck, and femur of the midsize (50th-percentile) male Hybrid III ATD, shown in Table 1 [9].

Table 1. IARVs and N_{ij} critical intercepts used by FMVSS 208.

	IARV
Head	
HIC ₁₅	700
Upper Neck	
Compression (N)	4000
Tension (N)	4170
N_{ij}	1.0
Femur	
Compression (N)	10000
N_{ij} Critical Intercepts	
Upper Neck	
Compression (N)	6160
Tension (N)	6806
Flexion (Nm)	310
Extension (Nm)	135

Studies have also been conducted to determine the mechanical loading on the body during daily or vigorous activities [10, 11, 12, 13, 14, 15, 16, 17]. By identifying the mechanical loads exerted onto the body during benign loading conditions, one can better distinguish between the types of loads that result in injury and those which the human body can readily withstand. The loads experienced in the head, upper neck, lumbar spine, and femur during the crash testing were compared to the loads experienced by volunteers during non-injurious activities. The peak neck loads were also compared to non-injurious, static neck tolerance levels reported in studies where volunteers resisted various applied loads with their neck musculature.

METHODS

TEST DESCRIPTION

A series of full-scale tests involving a loaded tractor-semitrailer and three (3) identical sedans were conducted. Five (5) tests were run, including sideswipe impacts along both sides of Vehicles 1 and 2 (Tests 1A, 1B, 2A, 2B) and a single 90-degree collision between the semitrailer left front dual wheels and the right front corner of Vehicle 3 (Test 3). The test configuration for Test 1A and Test 3 are shown below in [Figure 1](#) and [Figure 2](#), respectively. The sedans were instrumented, and the vehicle and occupants movements were captured using onboard and remote-positioned real-time and high-speed video cameras. A detailed description and analysis of the test vehicles, test setup, the resulting vehicle kinematics and discussion of the resulting damage can be found in the companion paper by Fittanto et al. [18].

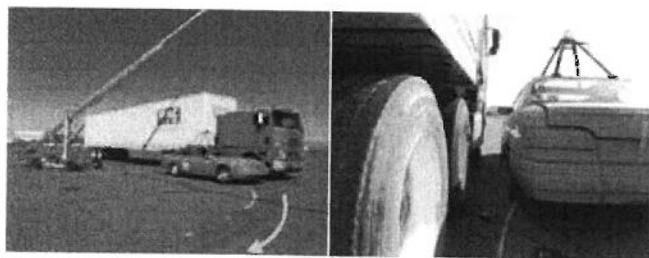


Figure 1. Sideswipe pre-test configuration (Test 1A). Orange arrow shows direction of sedan movement as it is pulled forward/laterally by turning semitrailer.

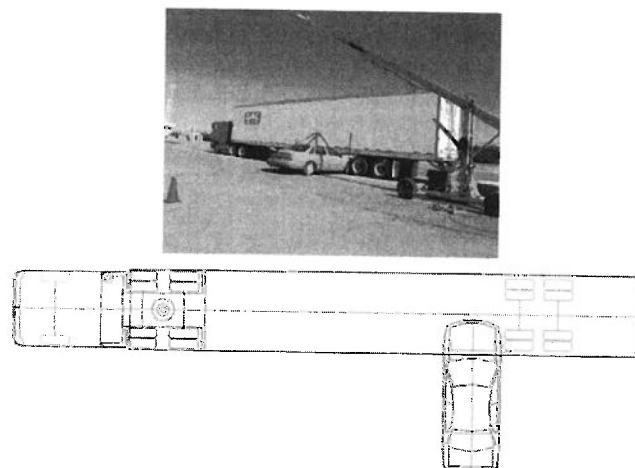


Figure 2. 90-degree collision pre-test configuration (Test 3). The speed of the tractor-semitrailer was 12 mph, and the speed of the sedan was 6 mph.

For the sideswipe tests (1A thru 2B), the tractor-semitrailer was accelerated by the driver to its maximum speed in 2nd gear, approximately 7 mph, and steered to follow a pre-

determined path that resulted in only the semitrailer contacting the sedan. The sedan was positioned at two different locations along the trailer path, producing different initial contact locations and velocities. Four (4) sideswipe tests were run as described in [Table 2](#).

Table 2. Sideswipe test matrix.

Test	Semitrailer Side	Sedan Side	Trailer Tire First Contact	Sedan Brakes	Sedan Occupants
1A	Right	Left	Rear of LR wheel	Applied	Near Side
1B	Left	Right	Rear of RF wheel	Applied	Far Side
2A	Left	Right	Rear of RR wheel	Applied	Far Side
2B	Right	Left	Rear of LR wheel	Not Applied	Near Side

Tests 1A and 2A were mirror tests, allowing a comparison of near and far side occupant responses. Tests 1B and 2A allowed a comparison of vehicle and occupant responses based upon the initial impact location on the sedan. Tests 1A and 2B allowed a comparison of the vehicle and occupant responses with the sedan brakes applied and not applied. Test 3 was a 90-degree impact, eccentric to the sedan center-of-gravity, with the tractor-semitrailer traveling 12 mph and the sedan traveling 6 mph.

For each test, a midsize (50th -percentile) male Hybrid III ATD was located in the driver's seat of the sedan and a small (5th -percentile) female Hybrid III was located in the left rear seating position. The driver ATD was restrained by the available three-point seat belt, while the rear passenger ATD was unrestrained. Both ATDs had limb joints adjusted to 1 g, wore form-fitting cotton stretch garments, and were placed in a normal seated position consistent with FMVSS 208 (e.g., driver's seat back and steering wheel angles). The driver's seat fore-aft adjustment was set at the mid-position for all tests. The ATDs were positioned with the head level and the torso against the seat back. The driver ATD's hands were positioned at the horizontal centerline of the steering wheel with thumbs lightly taped, legs in the vertical plane with outboard knee clevis distance of 10.6 inches, the right foot resting on the accelerator pedal and the left foot on the floor pan. The rear ATD was positioned with palms against the outer thighs and upper arms in contact with the torso and seatback, legs in the vertical plane with a knee centerline distance of 6.3 to 6.7 inches, and heels on the floor pan. Two colors of chalk were applied to each ATD's head to indicate points of contact. The ATDs were positioned to this standard position and chalk was applied prior to each test.

INSTRUMENTATION & DATA ANALYSIS

The sedans were instrumented with tri-axial accelerometers mounted at the base of the left and right B-pillars, a tri-axial rate sensor at the base of the right B-pillar, and webbing load cells on the torso and lap segments of the driver's seat belt.

The driver ATD was instrumented with tri-axial accelerometers mounted at the head center of gravity. Load cells measured forces and moments in the upper neck, lower neck, and lower lumbar spine, and axial forces in the bilateral femurs. The rear ATD was uninstrumented. SAE sign convention was used, as described in the SAE J1733 and SAE J211-1 standards [19, 20].

Each channel of data was passed through a 2,000 Hz anti-aliasing filter, recorded at 10,000 samples per second and digitally filtered according to impact test standards [20].

IARV and injury risk calculations

HIC was calculated for the driver during each of the crash tests by integrating the maximum time window surrounding the resultant linear acceleration of the center of mass of the head with respect to time [5, 21],

$$HIC = \max \left[\frac{1}{t_2 - t_1} \int_{t_1}^{t_2} a_r dt \right]^{2.5} (t_2 - t_1), \quad (1)$$

where t is time and a_r is the peak resultant head acceleration.

The probability of sustaining a skull fracture ($AIS \geq 2$) was then computed using,

$$p(\text{fracture}) = N\left(\frac{\ln(HIC) - \mu}{\sigma}\right), \quad (2)$$

where $N()$ is the cumulative normal distribution function, $\mu = 6.96352$, and $\sigma = 0.84664$ [3].

The neck injury criterion, N_{ij} , was determined from the sum of the normalized axial load and bending moment,

$$N_{ij} = \frac{F_z}{F_{int}} + \frac{M_y}{M_{int}}, \quad (3)$$

where F_z is the applied axial load, F_{int} is the critical intercept of that load, M_y is the applied bending moment, and M_{int} is the critical intercept of the bending moment.

The probability of sustaining a neck injury during the crash tests and also during non-injurious activities was next determined for various AIS severities using the risk curves from Eppinger et al. [3],

$$p(AIS \geq k) = \left(\frac{1}{1 + e^{\mu - \sigma N_{ij}}} \right), \quad (4)$$

where k is the AIS score and μ and σ are variables, shown in Table 3.

Table 3. Variables used to compute risk of neck injury of varying severity.

k	μ	Σ
2	2.054	1.195
3	3.227	1.969
4	2.693	1.195
5	3.817	1.195

An example of an AIS 2 cervical spine injury is a disc herniation without nerve root damage, and an example of an AIS 5 injury is a spinal cord laceration [5].

The IARV for the femur relates to the compressive load along the long axis of this bone. The probability of sustaining an AIS 2 injury to the femur was determined for the ATD during the crash tests using Eppinger et al. [3],

$$p(AIS \geq 2) = \left(\frac{1}{1 + e^{5.795 - 0.5196 F}} \right) \quad (5)$$

where F is peak femur load in kN. Examples of an AIS 2 lower extremity injury are knee ligament or meniscal tears [5].

Although no IARV or injury risk function for lumbar load exists, the NIOSH recommended maximum vertebral compression load is based on cadaveric studies of vertebral body and/or endplate fracture, and has also been related to incidence of low back pain with repetitive lifting [8].

RESULTS

VEHICLE KINEMATICS AND RESPONSE MEASURES

Vehicle Kinematics

The tractor-semitrailer was successfully driven along the intended path, contacting the sedans with the trailer bottom rail and rear dual tires. As the trailer off-tracked inboard of the tractor's path, the trailer bottom rail contacted the A-pillar

(in three of four tests), causing the sedan to roll. The trailer tires contacted the sedan's side panels, producing black tire transfer marks, accelerating the vehicle laterally and longitudinally. The sedan response to the sideswipe collisions (Tests 1A - 2B) is most accurately described as an extended-duration collision pulse with multiple acceleration peaks. The eccentric 90-degree impact (Test 3) resulted in a traditional short-duration collision pulse.

The highest magnitude vehicle CG acceleration and rotational responses for a sideswipe test occurred in Test 1A. Initial contact occurred between the trailer bottom rail and the left A-pillar on the sedan, causing the car to roll to the right. The outside right tire on the forward trailer axle impacted the sedan's left quarter panel and left rear wheel, displacing the rear of the sedan laterally to the right, and inducing a counterclockwise yaw rotation. The combination of the sedan's lateral displacement and the continued clockwise yaw rotation of the trailer resulted in an increased impact angle for the subsequent impact of the trailer tire with the driver's door of the sedan. This second impact displaced the sedan laterally without substantial associated rotation. Next, the trailer tire continued forward and impacted the fender behind the left front wheel of the sedan, snagging the wheel and inducing a clockwise yaw rotation. The sedan became oriented with the trailer, and was dragged until it was eventually released from the trailer.

In Test 1B, the initial contact occurred between the outside left tire on the forward trailer axle and the sedan's right front door. The impact caused a counter-clockwise yaw rotation on the sedan, and the trailer wheel subsequently snagged the right front wheel of the sedan (which was turned fully to the left). The trailer dragged the sedan a short distance before it was released.

The vehicle kinematics in Test 2A were consistent with, but a mirror image of, the kinematics observed in Test 1A.

In Test 2B, as with Tests 1A and 2A, the initial contact was between the semitrailer bottom rail and the sedan A-pillar. Similar to Test 1A, the outer right tire on the forward trailer axle then contacted the sedan's left quarter panel just rear of the left rear wheel. However, with brakes unapplied, the sedan realigned with and accelerated to the speed of the semitrailer right side wheels shortly after the trailer tire contact. Unlike Tests 1A and 2A, the free rolling sedan's path diverged from the trailer tire's path and additional contacts did not occur to the forward half of the sedan.

In Test 3, the left dual wheels of the semitrailer front axle impacted the sedan in the area of the right front fender and wheel, rotating the sedan counter-clockwise. The impact resulted in a velocity change of 13.1 mph with a principle-direction-of-force (PDOF) of approximately 45 degrees, causing the sedan to rotate counterclockwise and translate to the left.

Vehicle Response

Table 4 and Table 5 contain the peak values for the vehicle response variables and the time at which these peak values occurred for all five tests.

Table 4. Vehicle center of gravity response peak values during sideswipe tests. Left Side and Right Side indicate the impacted side of the sedan. Brakes Applied and Brakes Unapplied indicate the status of the sedan's brakes.

Sideswipe Tests	1A: Left Side, Brakes Applied		1B: Right Side, Brakes Applied	
	Max	Min	Max	Min
Longitudinal Acceleration (g)	1.0 @ 1.90s	-1.1 @ 5.83s	0.7 @ 0.85s	-0.8 @ 1.91s
Lateral Acceleration (g)	1.2 @ 1.29s	-1.0 @ 5.83s	0.9 @ 1.92s	-1.0 @ 1.90s
Vertical Acceleration (g)	0.6 @ 1.28s	-0.9 @ 1.76s	0.4 @ 1.95s	-0.5 @ 0.45s
Resultant Acceleration Max (g)	1.4 @ 1.29s / 5.83s		1.1 @ 1.92s	
Long Velocity Change (mph)	1.9 @ 2.87s		3.0 @ 1.01s	
Lat Velocity Change (mph)	1.5 @ 1.35s		-1.4 @ 1.91s	
Resultant Velocity Change (mph)	2.0 @ 2.12s		3.0 @ 1.01s	
Peak Torso Belt Load (lbf)	28.0 @ 5.94s		2.9 @ 2.12s	
Peak Lap Belt Load (lbf)	13.9 @ 6.11s		2.2 @ 1.99s	

Sideswipe Tests	2A: Right Side, Brakes Applied		2B: Left Side, Brakes Unapplied	
	Max	Min	Max	Min
Longitudinal Acceleration (g)	0.6 @ 0.93s	-0.8 @ 7.18s	0.8 @ 0.58s	-0.3 @ 1.24s
Lateral Acceleration (g)	1.2 @ 1.43s	-1.1 @ 0.92s	0.6 @ 1.15s	-0.7 @ 0.83s
Vertical Acceleration (g)	0.7 @ 0.70s	-0.7 @ 2.10s	0.5 @ 0.64s	-0.5 @ 0.71s
Resultant Acceleration Max (g)	1.2 @ 1.43s		0.9 @ 0.58s	
Long Velocity Change (mph)	2.6 @ 2.21s		5.6 @ 1.20s	
Lat Velocity Change (mph)	-1.8 @ 7.15s		1.8 @ 1.90s	
Resultant Velocity Change (mph)	2.7 @ 6.98s		5.8 @ 1.20s	
Peak Torso Belt Load (lbf)	20.4 @ 7.25s		1.1 @ 0.20s	
Peak Lap Belt Load (lbf)	7.3 @ 0.73s		2.7 @ 0.56s	

Table 5. Vehicle center of gravity response peak values and belt loads during 90-degree collision test.

Two-Moving Vehicles	Test 3: Right Front Corner Impact	
	Max	Min
Longitudinal Acceleration (g)	0.9 @ 246ms	-4.9 @ 104ms
Lateral Acceleration (g)	2.3 @ 157ms	-6.3 @ 91ms
Resultant Acceleration Max (g)	7.8 @ 91ms	
Longitudinal Velocity Change (mph)	-9.1 @ 175ms	
Lateral Velocity Change (mph)	-9.0 @ 141ms	
Resultant Velocity Change (mph)	13.1 @ 151ms	
Roll Rate Max (deg/s)	-68 @ 132ms	
Yaw Rate Max (deg/s)	-112 @ 130ms	
Peak Torso Belt Load (lbf)	654.8 @ 129ms	
Peak Lap Belt Load (lbf)	482.2 @ 130ms	

ATD KINEMATICS AND BIOMECHANICAL MEASURES

Occupant kinematics

In Test 1A, a near-side sideswipe impact with applied brakes on the sedan, both the driver and rear occupant bounced in their seats and moved slightly from side-to-side as the bottom rail of the semitrailer contacted the A-pillar of the sedan, rocking the sedan on its suspension. When the dual wheels of the semitrailer impacted the side of the sedan on the quarter panel and left rear tire, both the driver and rear occupant moved along a path that was primarily leftward relative to the vehicle interior, progressed into a forward motion due to the continued engagement of the semitrailer and resulting clockwise rotation of the sedan, and then moved rearward into their respective seatbacks. There was no contact made between either the driver or the rear occupant and interior vehicle structures forward of their seated positions. As the driver and rear occupant moved rearward and loaded their seat backs, the occipital region of the driver's head contacted the head restraint, and the occipital region of the rear occupant's head contacted the upper portion of the rear seat back. The oscillating (back-and-forth) motion of the ATDs continued, diminishing in velocity and amplitude with each repetition, until the ATDs returned to approximately their original seated position. The driver's head contacted the head restraint during its initial rearward motion, and the rear occupant's head contacted the upper portion of the seat back during its first and second rearward movements. The first contact location of the rear occupant's head was further inboard than the second contact location, which was closer to the final resting position of the head.

The ATDs experienced less movement during Tests 1B and 2A, both far-side sideswipe impacts with applied brakes on the sedan, than resulted from the near-side impact with applied brakes (Test 1A). In Test 1B, the initial contact occurred between the dual wheels and the right front door of the sedan. In Test 2A, the initial contact occurred between the semitrailer bottom rail and the right A-pillar of the sedan, followed by contact between the dual wheels and the right quarter panel and right rear tire of the sedan. In both of the far-side tests, the driver and rear occupant moved minimally relative to the vehicle interior, rocking side-to-side as the semitrailer bottom rail and dual wheels contacted the sedan. Both the driver and rear occupant returned to their approximate original seated positions, and neither occupant contacted their head restraint or any other interior vehicle structure during this far-side impact.

In Test 2B, a near-side sideswipe impact with the brakes unapplied on the sedan, the ATDs rocked slightly from side-to-side as the bottom rails of the semitrailer contacted the left A-pillar area of the sedan, followed by contact between the semitrailer dual wheels and the left quarter panel and left rear wheel of the sedan. As the sedan was pulled along by the semitrailer, the relative movement between the ATDs and the vehicle interior was minimal. Neither the driver nor the rear occupant contacted their head restraint or any other interior vehicle structure during this near-side impact with the brakes unapplied.

In Test 3, the two-moving vehicle perpendicular test, the driver and rear occupant initially moved forward and to the right relative to the vehicle. The driver did not contact any interior vehicle structures forward of its seated position during this motion. However, the left frontal/parietal region of the rear occupant's head impacted the back, left side of the front passenger head restraint. The restrained driver rebounded back and to the left, and the left, parietal region of the driver's head contacted the headliner area above the door. The rear occupant rebounded as well, and the occipital region of the ATD's head contacted the lower portion of the cushioned right, rear seat back. The driver came to rest at approximately its original seated position, and the rear occupant came to rest on its right side, lying across the rear seat.

Occupant biomechanical measures

The maximum and minimum biomechanical measures for the driver ATD during crash Tests 1, 2 and 3 are shown below in [Table 6](#), [Table 7](#), and [Table 8](#), respectively. Additionally, the relationship between occupant kinematics and loading is shown in [Figure 3](#), [Figure 4](#), [Figure 5](#), [Figure 6](#).

Table 6. ATD biomechanical measures during Tests 1A/1B, sideswipe impacts. Near-Side and Far-Side indicate the sideswipe collision experienced by the sedan. Brakes Applied and Brakes Unapplied indicate the status of the sedan's brakes.

Sideswipe 1		1A-Near-Side - Brakes Applied		1B-Far-Side - Brakes Applied	
		Max	Min	Max	Min
HEAD	Longitudinal Acceleration (g)	4.7	-3.8	1.5	-1.3
	Lateral Acceleration (g)	2.5	-2.2	2.4	-2.3
	Vertical Acceleration (g)	1.6	-1.7	0.7	-0.9
	Resultant Acceleration (g)	5.0		2.6	
	HIC 15	0.7		0.1	
	HIC 36	1.3		0.3	
UPPER NECK	Longitudinal Force - Fx (N)	125.5	-155.8	48.1	-50.7
	Lateral Force - Fy (N)	94.3	-82.8	90.8	-92.1
	Vertical Force - Fz (N)	106.8	-79.2	32.9	-33.4
	Lateral Moment - Mx (Nm)	6.8	-5.4	5.8	-6.0
	Fore/Aft Moment - My (Nm)	13.1	-9.8	4.5	-3.8
	Torsional Moment - Mz (Nm)	2.4	-2.0	2.2	-2.2
	Neck Injury Criterion - N _{te}	0.09		0.03	
	Neck Injury Criterion - N _{tr}	0.04		0.01	
	Neck Injury Criterion - N _{te}	0.03		0.01	
	Neck Injury Criterion - N _{tr}	0.04		0.02	
LOWER NECK	Longitudinal Force - Fx (N)	139.7	-112.6	73.9	-59.6
	Lateral Force - Fy (N)	80.1	-90.8	104.6	-98.3
	Vertical Force - Fz (N)	96.6	-122.8	48.1	-48.1
	Lateral Moment - Mx (Nm)	21.9	-20.1	20.8	-22.7
	Fore/Aft Moment - My (Nm)	36.4	-32.8	12.6	-12.2
	Torsional Moment - Mz (Nm)	3.0	-2.2	3.9	-2.8
LUMBAR SPINE	Longitudinal Force - Fx (N)	182.0	-144.2	108.1	-136.6
	Lateral Force - Fy (N)	36.5	-100.6	76.5	-48.1
	Vertical Force - Fz (N)	178.0	-158.9	93.5	-110.4
	Lateral Moment - Mx (Nm)	23.6	-23.6	29.0	-23.1
	Fore/Aft Moment - My (Nm)	43.7	-33.5	24.7	-18.2
	Torsional Moment - Mz (Nm)	28.0	-25.5	37.8	-30.8
FEMUR	Axial Force - Fz, Left (N)	32.5	-77.0	26.3	-47.2
	Axial Force - Fz, Right (N)	9.8	-70.8	51.6	-52.5

Table 7. ATD biomechanical measures during Tests 2A/2B, sideswipe impacts. Near-Side and Far-Side indicate the sideswipe collision experienced by the sedan. Brakes Applied and Brakes Unapplied indicate the status of the sedan's brakes.

Sideswipe 2		2A-Far-Side - Brakes Applied		2B-Near-Side - Brakes Unapplied	
		Max	Min	Max	Min
HEAD	Longitudinal Acceleration (g)	0.9	-1.2	1.2	-1.2
	Lateral Acceleration (g)	2.0	-2.2	1.3	-1.2
	Vertical Acceleration (g)	0.8	-1.3	1.1	-1.4
	Resultant Acceleration (g)	2.2		1.6	
	HIC 15	0.1		0.0	
	HIC 36	0.2		0.1	
UPPER NECK	Longitudinal Force - Fx (N)	37.4	-44.1	39.6	-45.8
	Lateral Force - Fy (N)	71.2	-85.9	46.3	-44.1
	Vertical Force - Fz (N)	39.6	-54.3	47.2	-60.1
	Lateral Moment - Mx (Nm)	4.6	-5.2	4.0	-3.4
	Fore/Aft Moment - My (Nm)	4.0	-2.9	3.8	-2.9
	Torsional Moment - Mz (Nm)	1.9	-1.8	1.2	-1.6
	Neck Injury Criterion - N _{te}	0.02		0.02	
	Neck Injury Criterion - N _{tr}	0.01		0.01	
	Neck Injury Criterion - N _{te}	0.02		0.02	
	Neck Injury Criterion - N _{tr}	0.02		0.02	
LOWER NECK	Longitudinal Force - Fx (N)	58.3	-41.4	54.3	-44.9
	Lateral Force - Fy (N)	84.6	-97.9	41.4	-49.0
	Vertical Force - Fz (N)	71.6	-85.9	72.5	-84.1
	Lateral Moment - Mx (Nm)	16.1	-19.6	10.9	-10.2
	Fore/Aft Moment - My (Nm)	10.4	-8.0	10.4	-9.8
	Torsional Moment - Mz (Nm)	2.8	-3.0	1.3	-1.3
LUMBAR SPINE	Longitudinal Force - Fx (N)	146.9	-126.8	192.7	-106.8
	Lateral Force - Fy (N)	63.2	-55.6	29.8	-57.0
	Vertical Force - Fz (N)	149.5	-193.1	103.2	-89.9
	Lateral Moment - Mx (Nm)	32.2	-21.6	11.6	-11.1
	Fore/Aft Moment - My (Nm)	27.6	-22.0	23.9	-17.3
	Torsional Moment - Mz (Nm)	40.0	-38.8	16.0	-17.4
FEMUR	Axial Force - Fz, Left (N)	40.9	-64.5	19.6	-36.0
	Axial Force - Fz, Right (N)	39.2	-33.4	18.7	-53.8

Table 8. ATD biomechanical measures during Test 3, two-moving vehicles impact.

Two-Moving Vehicles		Max	Min
HEAD	Longitudinal Acceleration (g)	3.3	-6.5
	Lateral Acceleration (g)	10.9	-7.5
	Vertical Acceleration (g)	10.9	-0.7
	Resultant Acceleration (g)	13.1	
	HIC 15	8.3	
	HIC 36	15.8	
UPPER NECK	Longitudinal Force - Fx (N)	78.3	-278.6
	Lateral Force - Fy (N)	277.7	-286.1
	Vertical Force - Fz (N)	517.1	-581.2
	Lateral Moment - Mx (Nm)	16.9	-21.8
	Fore/Aft Moment - My (Nm)	17.6	-6.4
	Torsional Moment - Mz (Nm)	6.0	-5.4
	Neck Injury Criterion - N_{te}	0.07	
	Neck Injury Criterion - N_{tr}	0.09	
	Neck Injury Criterion - N_{co}	0.10	
	Neck Injury Criterion - N_{cf}	0.10	
	Neck Injury Criterion - N_{lv}	0.1	
LOWER NECK	Longitudinal Force - Fx (N)	136.2	-468.6
	Lateral Force - Fy (N)	114.8	-472.1
	Vertical Force - Fz (N)	486.4	-417.0
	Lateral Moment - Mx (Nm)	53.0	-72.8
	Fore/Aft Moment - My (Nm)	61.7	-17.4
	Torsional Moment - Mz (Nm)	39.1	-3.8
LUMBAR SPINE	Longitudinal Force - Fx (N)	355.1	-249.2
	Lateral Force - Fy (N)	144.2	-542.9
	Vertical Force - Fz (N)	537.1	-221.2
	Lateral Moment - Mx (Nm)	24.2	-105.4
	Fore/Aft Moment - My (Nm)	45.1	-43.1
	Torsional Moment - Mz (Nm)	36.9	-71.4
FEMUR	Axial Force - Fz, Left (N)	571.4	-44.5
	Axial Force - Fz, Right (N)	259.0	-174.9

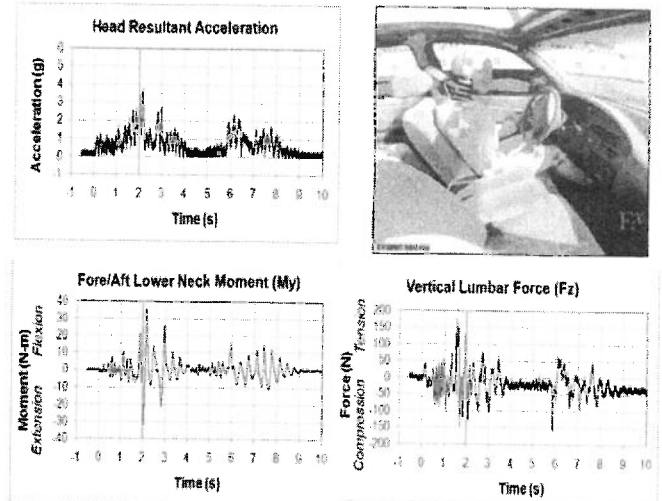


Figure 3. Test 1A - Peak resultant head acceleration of the driver occurred as the head rebounded forward after contact with the head restraint. The peak fore/aft lower neck moment for the ATD occurred immediately after, as the three-point belt arrested the forward ATD motion.

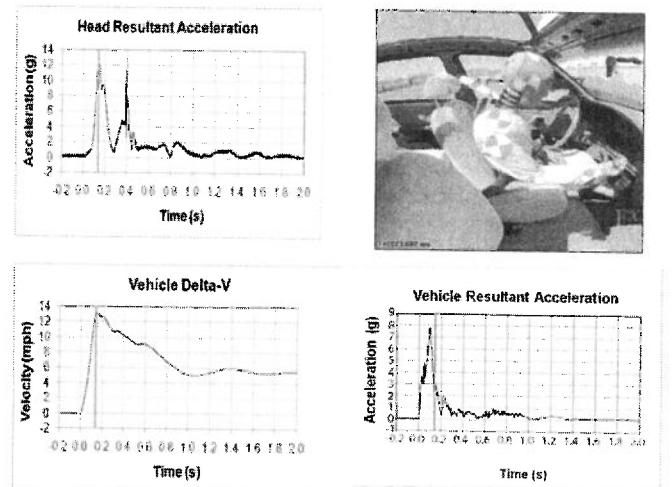


Figure 4. Test 3 - Peak resultant head acceleration occurred for the driver as the head moved forward and to the right as a result of the collision. The peak head acceleration follows closely behind the peak vehicle acceleration and corresponds to the peak in vehicle Delta-V. This time point also corresponds to the peak seat belt loads (data not shown).

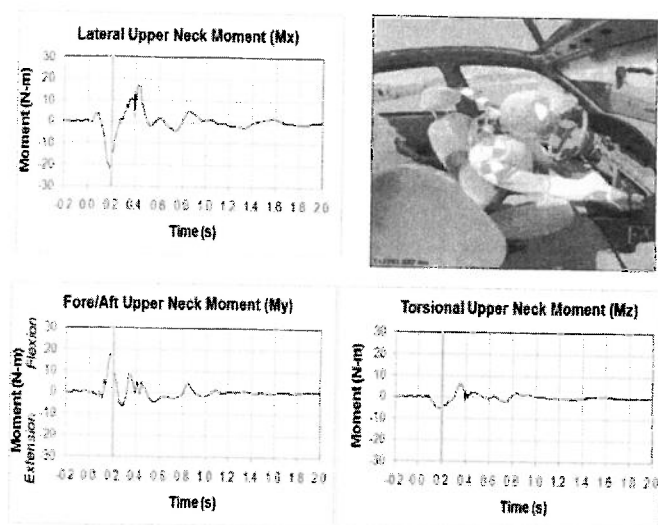


Figure 5. Test 3 - Peak absolute lateral and fore/aft upper neck moments for the driver occurred as the three-point belt arrested the forward motion of the ATD's torso while the head continued forward and to the right. Similar peaks for the lateral and fore/aft lower neck moments occurred at the same time point (data not shown).

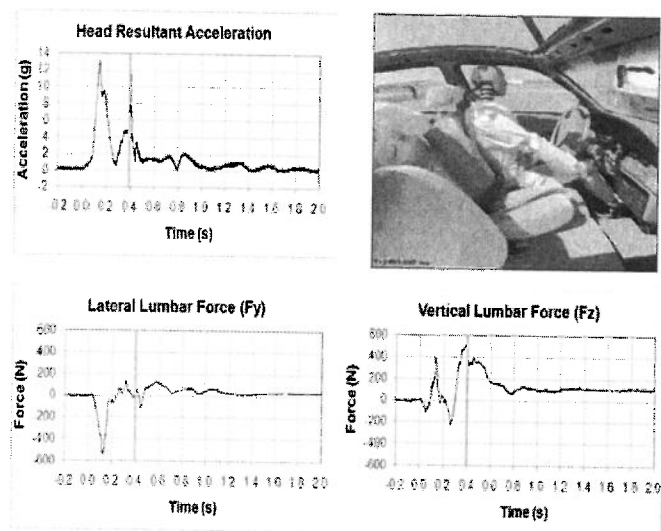


Figure 6. Test 3 - Resultant head acceleration spiked again for the driver as the head contacted the headliner resulting in an impulse load to the head. Vertical lumbar tensile force peaked while the driver's torso extended up and outboard, resulting in the driver's head contacting the headliner.

DISCUSSION

VEHICLE RESPONSE

Vehicle accelerations in these tests were slightly greater in magnitude than those reported by Tanner et al.[1], and considerably longer in duration; i.e., several seconds compared to less than one second for Tanner et al.[1], consistent with more extensive damage observed on the sedan. Test 1A resulted in the largest vehicle CG accelerations of the four sideswipe tests. Peak acceleration of 1.4 g occurred at 1.29 seconds as the trailer tire contacted the driver's side front door and displaced the vehicle laterally. At 1.80 and 1.90 seconds, there were local acceleration peaks of 1.0 g, followed by a yaw rate peak of 45 degrees per second at 1.95 seconds. The vehicle experienced a second acceleration peak of 1.4 g at 5.83 seconds as the sedan was released from the semitrailer wheels.

Test 1B was a shorter and less severe event than Test 1A, with a peak acceleration of 1.2 g. Test 2A, which mirrored Test 1A, resulted in a similar vehicle kinematic response to Test 1A, with a slightly lower peak CG acceleration of 1.2 g.

In Test 2B the sedan was accelerated up to the speed of the semitrailer wheels within 1.15 seconds after the trailer tire made contact in the left rear wheel area. Although this test resulted in the highest change in velocity with a shorter-duration impact than the applied brake sideswipes, the peak acceleration during this test was only 0.9 g. This test demonstrates that due to the extended duration of a sideswipe collisions, the velocity change is not necessarily the best measure of the severity of the impact and injury potential of the impact.

Test 3 resulted in a vehicle CG delta-V of 13.1 mph and a peak acceleration of 7.8 g.

ATD KINEMATICS AND BIOMECHANICAL MEASURES

Occupant kinematics

During contact between the semitrailer and the sedans, the ATDs inside the sedans experienced motion relative to the vehicle interior. In Tests 1A, 1B and 2A, the interactions between the bottom rails of the semitrailer and the A-pillar of the sedans resulted in the ATDs "bouncing" or "rocking" in their seats as the vehicle rolled on its suspension. The greatest movement of the ATDs during these collisions occurred when the dual wheels of the semitrailer impacted the side of the sedan. The movement of the driver in response to the impact of the dual wheels was arrested via interaction with the restraint system and frictional forces between the body of the ATD and the seat cushion. In the case of Test 1A and Test 3, the rebound movement of the driver was also arrested via interaction with interior vehicle structures (i.e., the head

restraint and headliner above the driver's door). The rear occupant's movement continued until it was arrested due to the frictional forces and, in the case of Test 1A and Test 3, due to interaction with interior vehicle structures. After the initial movement of the ATDs, both the driver and rear occupant rebounded at velocities substantially smaller than their forward velocities [22]. During any rearward movement, their lower backs were supported by the padded seat backs and the heads were cushioned and supported by interaction with the padded head restraint or the padded seat back.

In Test 2B, the brakes of the sedan were unapplied. This allowed for the sedan to be pulled along by the semitrailer during the initial contact, resulting in lower occupant accelerations and minimal movement of the ATDs.

Occupant biomechanical measures compared to non-injurious activities

Head accelerations and HIC

The biomechanical literature has reported head accelerations during daily and non-injurious activities. Head accelerations during non-injurious activities performed by volunteers were measured using external head sensors. In contrast, the head accelerations of the ATD during the crash tests were measured by accelerometers at the center-of-gravity (CG) of the ATD's head. A previous study has validated external sensors by comparing measured external accelerations to measured CG accelerations [23]. This study determined that the external sensor "slightly underestimated" linear peak head accelerations. It should be noted that the values reported by Allen et al. [10] do not account for rotation, and therefore may not accurately represent CG acceleration.

Head accelerations during non-injurious activities have been compared to the peak resultant head accelerations experienced by the ATD during the described crash tests, as shown in Figure 7. It was found that the head accelerations experienced by the ATD during the sideswipe tests were slightly higher than those measured by Tanner et al. [1], but comparable to those experienced by volunteers during everyday activities, such as being jostled in a crowd, getting slapped on the back, hopping off a step, plopping into a chair, swinging on a swing, sneezing, and bouncing on a pogo stick [1, 10, 21]. The plotted values from Allen et al. [10] are vector sums of the reported average peak head acceleration components, and those for Funk, Bayly, & Tierney studies [24, 25, 26] are the reported average peak resultant accelerations. Thus some individual subjects had higher peak head accelerations than those shown. The plotted values from Exponent [21] are vector sums of reported maximum peak head acceleration components. The peak resultant head acceleration for Test 2B, near-side sideswipe with the brakes unapplied, produced the lowest head acceleration. This is consistent with the dummy kinematics during this test which demonstrated very little movement of the ATD as the sedan

was pulled along by the semitrailer. The peak head resultant acceleration during the two-moving vehicle test, 13 g, was approximately three times greater than the maximum resultant head acceleration experienced by the ATD during any of the sideswipe tests. Although the ATD peak resultant head acceleration measured during Test 3 was greater than that experienced by volunteers during the benign activities listed above, it was still less than the head accelerations experienced by volunteers during more vigorous activities, such as "heading" a soccer ball, getting struck in the head with a pillow, or falling down onto an exercise mat, without head contact [21, 24].

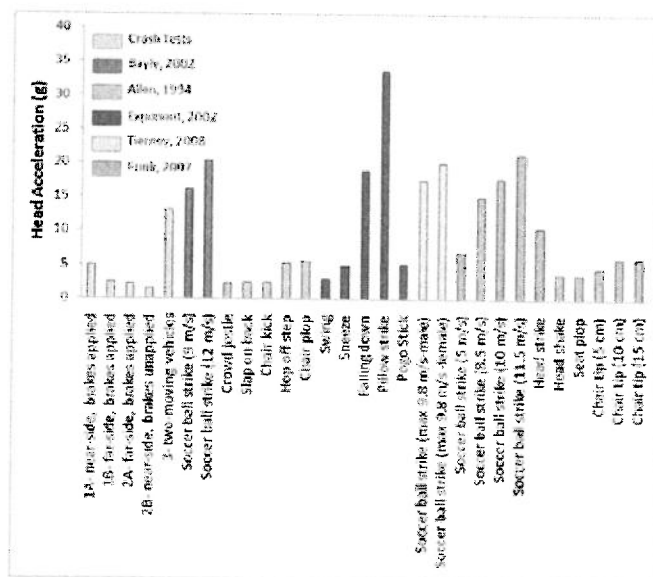


Figure 7. Peak linear head accelerations (g) for crash testing and various non-injurious activities.

In addition to peak head acceleration, the HIC was used to evaluate the risk of head injury during each of the crash tests. The HIC₁₅ computed for the sideswipe tests were all below 1. The HIC value for Test 2B, the near-side impact with the brakes unapplied, was computed as 0.0. These values are less than the maximum HIC value reported while jumping on a pogo stick and less than or comparable to the average HIC values reported for heading a soccer ball [21, 26]. As expected, the HIC value for the two-moving vehicle crash test was greater than those for the sideswipe tests, but it is still well below the established IARV for HIC (700). Further, the maximum HIC values reported for falling down onto an exercise mat or getting struck in the head with a pillow were reported to be approximately twice as great as the HIC values computed for Test 3 [21].

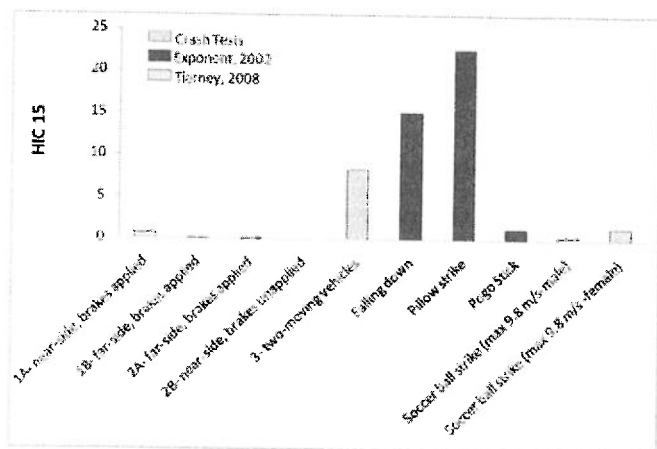


Figure 8. HIC for crash testing and various vigorous activities.

The HIC values were all less than 2% of the IARV for HIC. The risk of sustaining a skull fracture ($AIS \geq 2$) during the crash tests was determined to be less than 0.001% using equation 3.

Head accelerations experienced by the driver ATD in all tests were well below head acceleration levels experienced by high school and college football players that were correlated with concussion risk as reported in the literature, as shown in Figure 9. Schnebel et al. [27] reported that out of 12,000 head impacts producing head accelerations over 30 g, only 6 resulted in a diagnosis of concussion, with the range of associated concussive accelerations between 81.9 g and 145.7 g. Rowson et al. [28] reported that out of 1,712 impacts producing head accelerations over 40 g, none resulted in a diagnosis of concussion. Mihalik et al. [29] reported that out of 1,858 impacts producing head accelerations over 80 g, only 7 resulted in a diagnosis of concussion. Greenwald et al. [30] reported that out of 3,476 impacts producing head accelerations over 99 g, only 11 resulted in a diagnosis of concussion. The percentage of concussive impacts in each of these studies was less than 0.5%. In addition, Funk et al [25] provided risk curves for mild traumatic brain injury (MTBI), and reported a 1% probability of MTBI for head acceleration of 109 g and a HIC value of 232.

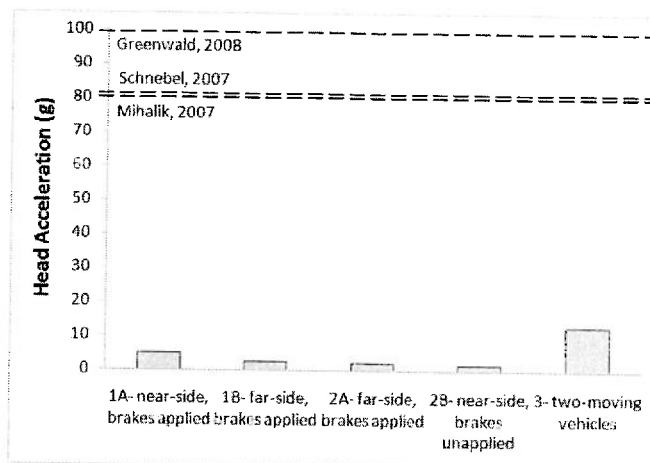


Figure 9. Peak linear head accelerations (g) for crash testing in relation to reported lower limits for concussion.

Upper neck loads

The loads acting on the cervical spine during the near-side and far-side sideswipe collisions were several times less than compressive loads experienced by volunteers during non-injurious activities, such as hopping, falling into a chair, running with an abrupt stop, shaking one's head, or riding a bumper car [12, 13, 14]. The compressive and tensile loads in the upper neck were greatest during Test 3, two-moving vehicles. For all of the crash tests, the compressive and tensile loads in the upper neck were substantially less than the reported non-injurious static neck tolerances [31]. Peak compressive and tensile loads are reported below in Figure 10 and Figure 11, respectively. A bumper car study conducted by Mkandawire et al. [13] reported upper neck loads during lateral impacts, and the bumper car study by Vijayakumar et al. [14] reported upper neck loads for rear-end impacts.

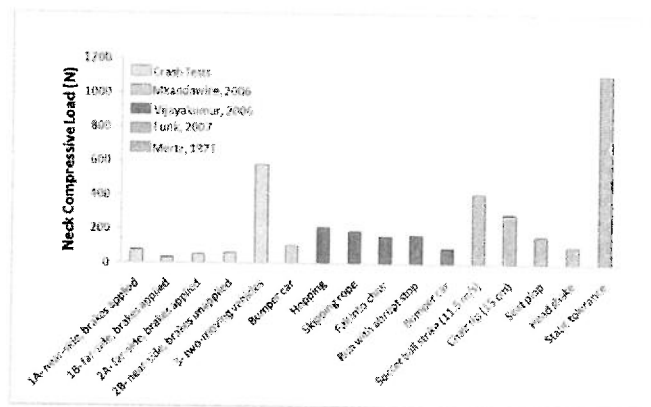


Figure 10. Peak upper neck compressive loads for crash testing and various non-injurious activities.

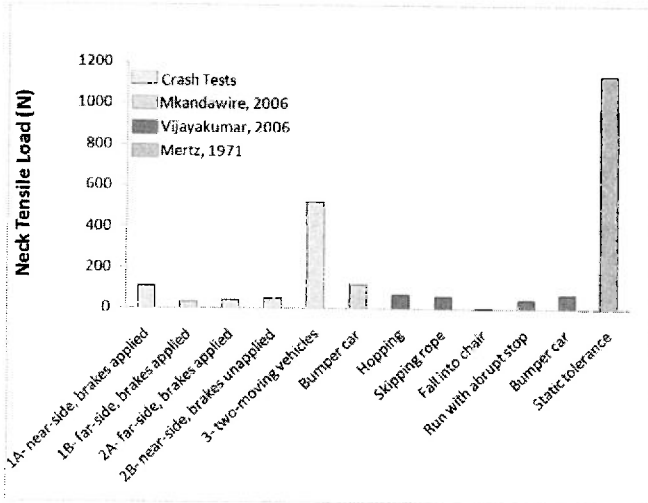


Figure 11. Peak upper neck tensile loads for crash testing and various non-injurious activities.

The peak flexion and extension moments in the sideswipe tests were comparable to the flexion and extension moments experienced by volunteers during non-injurious activities. In Test 3, the peak flexion moment was greater than during non-injurious activities, but the extension moment was smaller than that experienced by volunteers during bumper car riding and hopping. The extension moment in Test 3 was also less than the peak extension moment in Test 1A, the near-side impact with brakes applied. This is consistent with the ATD kinematics during these tests. In Test 1A, the ATD's head experienced flexion and then extension, impacting the occipital region of its head on the head restraint, whereas in Test 3, the driver moved more laterally. The rebound motion of the head in Test 3 was therefore more in the coronal plane of the head, reducing the extension moment. Similar to the single loading conditions, for all of the crash tests, the flexion and extension moments were less than those reported for non-injurious static neck tolerances [31, 32]. Peak flexion and extension moments in the upper neck are reported below in Figure 12 and Figure 13, respectively.

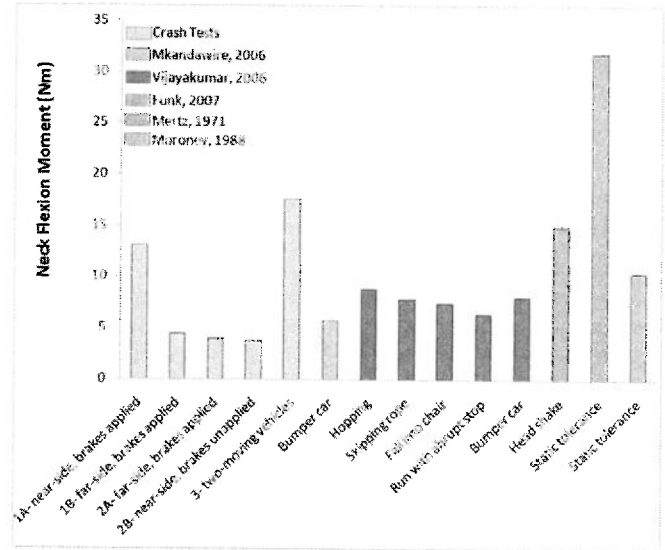


Figure 12. Peak upper neck flexion moments for crash testing and various non-injurious activities.

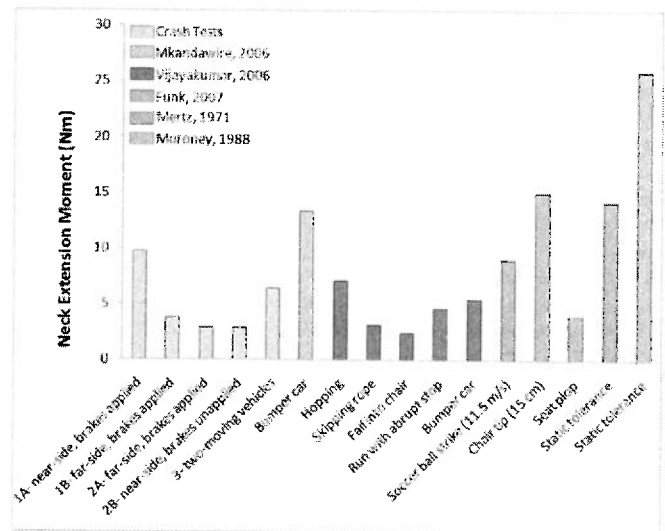


Figure 13. Peak upper neck extension moments for crash testing and various non-injurious activities.

The loading in the upper cervical spine experienced by the ATD during each of the crash tests was substantially less than the established IARVs for upper neck injury. The percentage of the IARV for each of the upper neck loading conditions was calculated for each of the crash tests, as shown in Table 9.

Table 9. Percentage of the upper neck IARVs experienced by ATD during crash testing.

Test	% of IARV			
	Compression	Tension	Extension	Flexion
1A- near-side, brakes applied	2%	3%	7%	4%
1B- far-side, brakes applied	1%	1%	3%	1%
2A- far-side, brakes applied	1%	1%	2%	1%
2B- near-side, brakes unapplied	2%	1%	2%	1%
3- two-moving vehicles	15%	12%	5%	6%

The risk of sustaining a neck injury based on N_{ij} values from each of the crash tests was calculated using [equation 4](#) and [Table 3](#). The risk of sustaining a neck injury in any of the crash tests was low: 11-13% for $AIS \geq 2$, 4-5% for $AIS \geq 3$, 6-7% for $AIS \geq 4$, and 2% for $AIS \geq 5$. Test 3 generated the greatest loads in the upper neck, but the risk of injury during this test was comparable to the risk of injury during the sideswipe impacts. It is worth noting that because the risk curves predict non-zero risk for $N_{ij} = 0$, the probability of sustaining an upper neck injury as a result of *no* loading of the upper neck is 11% for $AIS \geq 2$, 4% for $AIS \geq 3$, 6% for $AIS \geq 4$, and 2% for $AIS \geq 5$. Further, it was determined that the likelihood of sustaining an upper neck injury during the crash tests was comparable to the probability of sustaining a neck injury during non-injurious activity.

Lower back loads

The loads acting on the lumbar spine during the sideswipe collisions were one-third or less than anterior-posterior shear loads experienced by volunteers during non-injurious activities, such as amateur golfing and rowing; were one-half or less than lumbar torsional loads experienced by volunteers during amateur golfing; and were several times less than lumbar compressive loads experienced by volunteers during activities such as standing, sitting, bending forward, pushing a cart, and golfing [[11](#), [33](#), [34](#), [35](#), [36](#), [37](#), [38](#), [39](#)]. During the two-moving vehicles collision, the anterior-posterior shear and torsional loads acting on the lumbar spine were comparable to loads experienced by volunteers during non-injurious activities such as amateur golfing and the compressive loads on the lumbar spine were several times less than the loads experienced by volunteers during activities such as standing bent forward, extending one leg rearward while on both hands and one knee, pushing a cart, and amateur golfing. Lumbar loads are reported below in [Figure 14](#), [Figure 15](#), and [Figure 16](#), respectively.

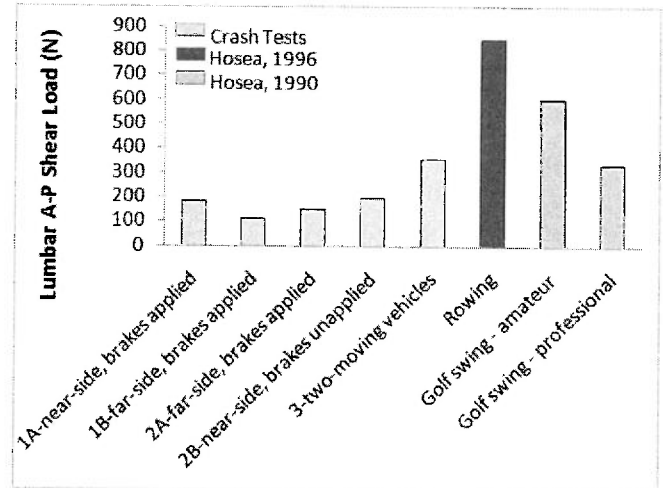


Figure 14. Peak lumbar shear loads for crash testing and various non-injurious activities.

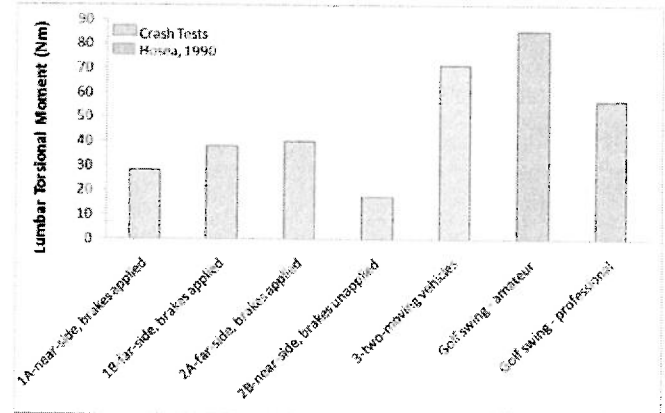


Figure 15. Peak lumbar torsional moment for crash testing and golfing.

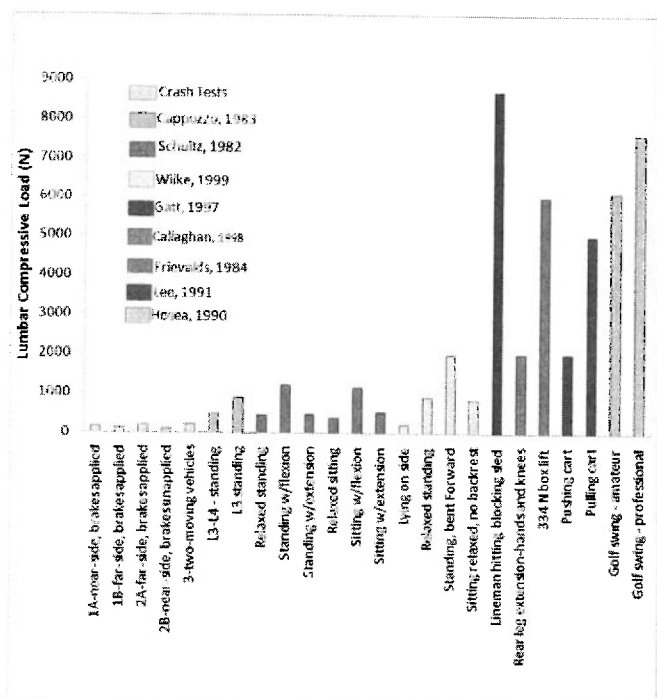


Figure 16. Peak lumbar compressive load for crash testing and various non-injurious activities.

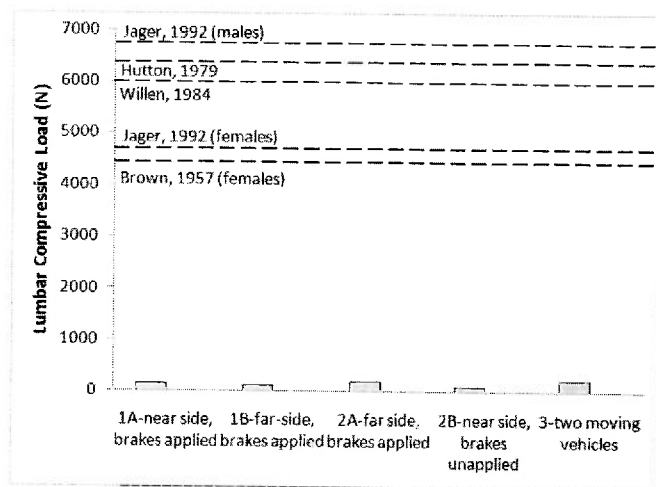


Figure 17. Peak lumbar compressive loads for crash testing in relation to reported lower limits for lumbar failure.

The loading in the lumbar spine experienced by the ATD during this testing was substantially less than failure loads previously reported in the literature for lumbar vertebrae [40, 41, 42], as shown in Figure 17. The highest compressive lumbar load of 221.2 N, experienced by the ATD driver during the two-moving vehicles collision, was less than 5% of the lowest failure load of 4448 N reported by Brown et al.

[40]. This load is also well below the NIOSH recommended compression force of 3400 N.

Femur Loads

The compressive loads in the femurs of the ATD during the crash testing were well below the IARV for the femur, as shown in Table 10.

Table 10. Percentage of the femur IARV experienced by ATD during crash testing.

Test	% of IARV	
	Left Femur	Right Femur
1A- near-side, brakes applied	1%	1%
1B- far-side, brakes applied	0%	1%
2A- far-side, brakes applied	1%	0%
2B- near-side, brakes unapplied	0%	1%
3- two-moving vehicles	0%	2%

The compressive loading in the femurs during the crash tests were a small percentage of the IARV for the femur. The IARV for the femur was established to determine the risk of injury to the leg during interaction between an occupant's knees/legs and the instrument panel in a frontal collision. During our crash tests, the knees/legs of the ATD did not contact any vehicle structures forward of its seated position. The loads measured in the femurs of the ATD were due to inertial loading. The risk of sustaining an AIS ≥ 2 injury during the sideswipe and two-moving vehicles crash tests was approximately 0.3%, computed using equation 5. Peak knee (patello-femoral joint) forces from various daily activities (in terms of multiples of body weight) were reported for squatting (6.0-7.6) [15], rising from a chair (3.1) [16], stair climbing (3.3) [17], and walking (0.5) [17]. Additionally, Mow et al. [43] performed a literature summary and reported the patello-femoral joint forces for level walking (0.5-1.7), ascending stairs (2.0-3.2), descending stairs (2.5-5.5), walking downhill (1.7-7.0), rising from a chair (3.1), jogging (7.0), and squat descent (7.6). These are greater than the compressive loads on the femur during our testing (0.1 for Tests 1 and 2 and 0.2 for Test 3).

STUDY LIMITATIONS

The Hybrid III ATD used in this study was originally designed to provide an indication of injury potential in severe frontal barrier impacts, and as such, its responses would not be expected to precisely replicate those of a living human subject in much lower severity sideswipe impacts. Also, given the long crash pulses associated with the sideswipe collisions, a human occupant might be expected to exert voluntary muscle control to partially resist the disturbances to normal seated posture. However, the Hybrid III is a valuable tool for this study in that it provides well established IARV measures which have been applied in numerous testing applications in addition to frontal impacts. For example,

comparing human volunteer and ATD responses in tip-up testing, which produced accelerations of similar magnitudes and durations to those seen in during our sideswipe testing, Yamaguchi et al. [44] found ATD excursions were greater than volunteers exhibiting voluntary postural control, but near the outer ranges of the human data. In effect, the ATD's higher passive stiffness properties helped to partially offset its lack of voluntary response. Hybrid III head/neck responses have also been proposed as injury predictors in low-speed rear impacts [45, 46]. In our study, where peak injury values often occurred at extremes of excursion, it was felt that the Hybrid III ATD, with no voluntary muscle control to limit excursion or damp out observed "bouncing" or "rocking" motions, provided a reasonably conservative estimate of human injury potential for such events.

SUMMARY/CONCLUSIONS

1. The biomechanical response of a 50th percentile Hybrid III male ATD was examined for various crash test configurations with a sedan and a tractor-semitrailer.
2. The biomechanical responses in the head, upper neck, and femur of the ATD were well below the established IARVs, with extremely low predicted injury risk.
3. The biomechanical responses in the head, upper neck, lower back, and femur of the ATD were lower than or comparable to the responses of these body regions to the loads experienced by volunteers during non-injurious activities and less than loads of static tolerance levels with the exception of Test 1A and Test 3.

REFERENCES

1. Tanner, C.B., Wiechel, J.F., and Guenther, D.A., "Vehicle and Occupant Response in Heavy Truck to Passenger Car Sideswipe Impacts," SAE Technical Paper 2001-01-0900, 2001, doi:[10.4271/2001-01-0900](https://doi.org/10.4271/2001-01-0900).
2. *Injury Criteria and Tolerance Levels*, in *Test Methodology for Protection of Vehicle Occupants against Anti-Vehicular Landmine Effects*. 2007, NATO Research and Technology Organization, RTO-TR-HFM-090.
3. Eppinger, R., Sun, E., Bandak, F., Haffner, M., Khaewpong, N., Maltese, M., Kuppa, S., Nguyen, T., Takhounts, E., Tannous, R., Zhang, A., Saul, R., *Development of Improved Injury Criteria for the Assessment of Advanced Automotive Restraint Systems-II*. 1999, National Highway Transportation and Safety Administration.
4. Mertz, H.J., Irwin, A.L., and Prasad, P., "Biomechanical and Scaling Bases for Frontal and Side Impact Injury Assessment Reference Values," SAE Technical Paper 2003-22-0009, 2003.
5. Gennarelli, T., Wodzin, E., eds. *Abbreviated Injury Scale 2005*. Rev 01/08 ed. 2005, Association for the Advancement of Automotive Medicine: Barrington, IL. 167.
6. Hayes, W. C., Erickson, M. S., Power, E. D., 2007, "Forensic Injury Bio mechanics," Annual Review of Biomedical Engineering, 9: p. 55-86.
7. Roberts, V. L., McElhaney, J. H. *Review of Head Injury Tolerance to Direct Impact*. in *International Conference on the Biokinetics of Impacts*. 1973. Amsterdam.
8. Waters, T., Putz-Anderson, V., Garg, A., *Applications Manual for the Revised NIOSH Lifting Equation*. 1994, U.S. Department of Health and Human Services, Public Health Service Centers for Disease Control and Prevention, DHHS Publication No. 94-110.
9. *Federal Motor Vehicle Safety Standard 208 Occupant Crash Protection*. 2010, National Highway Traffic Safety Administration, Department of Transportation.
10. Allen, M., Weir-Jones, I., Motiuk, D., Flewin, K., Goring, R., Kobetitch, R., Broadhurst, A., 1994, "Acceleration Perturbations of Daily Living," *Spine*, 19(11): p. 1285-1290.
11. Cappozzo, A., 1984, "Compressive Loads in the Lumbar Vertebral Column during Normal Level Walking," *Journal of Orthopaedic Research*, 1(3): p. 292-301.
12. Funk, J., Cormier, J., Bain, C., Guzman, H., Bonugli, E., *An Evaluation of Various Neck Injury Criteria in Vigorous Activities*, in *2007 International IRCOBI Conference on the Biomechanics of Injury*. 2007, International Research Council of Biomechanics of Injury: Maastricht (The Netherlands).
13. Mkandawire, C., Mazzucco, D., Vijayakumar, V., Irving, S., Heller, M., Morrison, H. *Head Kinematics and Upper Neck Loading During Simulated Low-Speed Lateral Impact Collisions*, in *FISITA 2006 World Automotive Congress*. 2006. Yokohama, Japan: International Federation of Automotive Engineering Societies Paper F2006T044.
14. Vijayakumar, V., Scher, I., Gloeckner, D.C., Pierce, J. et al., "Head Kinematics and Upper Neck Loading During Simulated Low-Speed Rear-End Collisions: A Comparison with Vigorous Activities of Daily Living," SAE Technical Paper 2006-01-0247, 2006, doi:[10.4271/2006-01-0247](https://doi.org/10.4271/2006-01-0247).
15. Dahlkvist, N. J., Mayo, P., Seedhom, B. B., 1982, "Forces during Squatting and Rising from a Deep Squat," *Engineering in Medicine*, 11(2): p. 69-76.
16. Ellis, M. I., Seedhom, B. B., Wright, V., 1979, "Forces in the Knee Joint Whilst Rising from Normal and Motorized Chairs," *Engineering in Medicine*, 8(1): p. 113-120.
17. Reilly, D. T., Martens, M., 1972, "Experimental Analysis of the Quadriceps Muscle Force and Patello-Femoral Joint Reaction Force for Various Activities," *Acta Orthopaedica Scandinavica*, 43(2): p. 126-37.
18. Fittanto, D., Bare, C., Smith, J., and Mkandawire, C., "Passenger Vehicle Response to Low-Speed Impacts Involving a Tractor Semitrailer," SAE Technical Paper 2011-01-0291, 2011, doi:[10.4271/2011-01-0291](https://doi.org/10.4271/2011-01-0291).

19. SAE International Surface Vehicle Information Report, "Sign Convention for Vehicle Crash Testing," SAE Standard J1733, Rev. Nov. 2007.
20. SAE International Surface Vehicle Recommended Practice, "Instrumentation for Impact Test-Part 1-Electronic Instrumentation," SAE Standard J211-1, Rev. Dec. 2003.
21. *Investigation of Amusement Park and Roller Coaster Injury Likelihood and Severity*. 2002, Exponent, Incorporated.
22. Fisher, J. L., Newberry, W. N., Krishnan, R., Pierce, J., Moore, T. L. A., *Late-Phase Occupant Rebound after Rear-End Impact*, in *ASME 2005 Summer Bioengineering Conference*. 2005, American Society of Mechanical Engineers: Vail, Colorado.
23. Bussone, W.R., Moore, T.L.A., Richards, D., Bove, R.T.Jr., et al., "Measurements of Non-Injurious Head Accelerations of a Pediatric Population," *SAE Int. J. Passeng. Cars - Mech Syst.* **2** (1):565-586, 2009, doi: [10.4271/2009-01-0383](https://doi.org/10.4271/2009-01-0383).
24. Bayly, P., Naunheim, R., Standeven, J., Neubauer, J., Lewis, L., Genin, G., *Linear and Angular Accelerations of the Human Head During Heading of a Soccer Ball*, in *Proceedings of the Second Joint EMBS/BMES Conference*. 2002: Houston, Texas.
25. Funk, J. R., Duma, S. M., Manoogian, S. J., Rowson, S., 2007, "Biomechanical Risk Estimates for Mild Traumatic Brain Injury," *Annual Proceedings / Association for the Advancement of Automotive Medicine*, **51**: p. 343-61.
26. Tierney, R. T., Higgins, M., Caswell, S. V., Brady, J., McHardy, K., Driban, J. B., Darvish, K., 2008, "Sex Differences in Head Acceleration during Heading while Wearing Soccer Headgear," *Journal of Athletic Training*, **43**(6): p. 578-84.
27. Schnebel, B., Gwin, J. T., Anderson, S., Gatlin, R., 2007, "In Vivo Study of Head Impacts in Football: A Comparison of National Collegiate Athletic Association Division I versus High School Impacts," *Neurosurgery*, **60**(3): p. 490-6.
28. Rowson, S., Brolinson, G., Goforth, M., Dietter, D., Duma, S., 2009, "Linear and Angular Head Acceleration Measurements in Collegiate Football," *Journal of Biomechanical Engineering*, **131**(6): p. 061016.
29. Mihalik, J. P., Bell, D. R., Marshall, S. W., Guskiewicz, K. M., 2007, "Measurement of Head Impacts in Collegiate Football Players: An Investigation of Positional and Event-Type Differences," *Neurosurgery*, **61**(6): p. 1229-35.
30. Greenwald, R. M., Gwin, J. T., Chu, J. J., Crisco, J. J., 2008, "Head Impact Severity Measures for Evaluating Mild Traumatic Brain Injury Risk Exposure," *Neurosurgery*, **62**(4): p. 789-98.
31. Mertz, H.J. and Patrick, L.M., "Strength and Response of the Human Neck," SAE Technical Paper [710855](https://doi.org/10.4271/710855), 1971, doi: [10.4271/710855](https://doi.org/10.4271/710855).
32. Moroney, S. P., Schultz, A. B., Miller, J. A., 1988, "Analysis and Measurement of Neck Loads," *Journal of Orthopaedic Research*, **6**(5): p. 713-20.
33. Callaghan, J. P., Gunning, J. L., McGill, S. M., 1998, "The Relationship between Lumbar Spine Load and Muscle Activity during Extensor Exercises," *Physical Therapy*, **78**(1): p. 8-18.
34. Freivalds, A., Chaffin, D. B., Garg, A., Lee, K. S., 1984, "A Dynamic Biomechanical Evaluation of Lifting Maximum Acceptable Loads," *Journal of Biomechanics*, **17**(4): p. 251-62.
35. Hosea, T., Gatt, C.Jr., Galli, K., Langrana, N., Zawadsky, J., *Biomechanical Analysis of the Golfer's Back*, in *Science and golf: proceedings of the First World Scientific Congress of Golf*, Cochran, A., Editor. 1990: London, United Kingdom, p. 43-48.
36. Hosea, T. M., Gatt, C. J.Jr., 1996, "Back Pain in Golf," *Clinics in Sports Medicine*, **15**(1): p. 37-53.
37. Lee, K. S., Chaffin, D. B., Herrin, G. D., Waikar, A. M., 1991, "Effect of Handle Height on Lower-Back Loading in Cart Pushing and Pulling," *Applied Ergonomics*, **22**(2): p. 117-23.
38. Schultz, A., Andersson, G., Ortengren, R., Haderspeck, K., Nachemson, A., 1982, "Loads on the Lumbar Spine. Validation of a Biomechanical Analysis by Measurements of Intradiscal Pressures and Myoelectric Signals," *Journal of Bone and Joint Surgery American volume*, **64**(5): p. 713-20.
39. Wilke, H. J., Neef, P., Caimi, M., Hoogland, T., Claes, L. E., 1999, "New In Vivo Measurements of Pressures in the Intervertebral Disc in Daily Life," *Spine*, **24**(8): p. 755-62.
40. Brown, T., Hansen, R. J., Yorra, A. J., 1957, "Some Mechanical Tests on the Lumbosacral Spine with Particular Reference to the Intervertebral Discs; A Preliminary Report," *Journal of Bone and Joint Surgery American volume*, **39-A**(5): p. 1135-64.
41. Hutton, W. C., Cyron, B. M., Stott, J. R., 1979, "The Compressive Strength of Lumbar Vertebrae," *Journal of Anatomy*, **129**(4): p. 753-8.
42. Richards, D., Carhart, M., Raasch, C., Pierce, J., Steffey, D., Ostarello, A., 2006, "Incidence of Thoracic and Lumbar Spine Injuries for Restrained Occupants in Frontal Collisions," *Annual Proceedings / Association for the Advancement of Automotive Medicine*, **50**: p. 125-39.
43. Mow, V. C., Huiskes, R., 2005, "Basic Orthopaedic Biomechanics and Mechano-Biology." Third ed. 2005, Philadelphia: Lippencott Williams & Wilkens.
44. Yamaguchi, G.T., Carhart, M.R., Larson, R., Richards, D. et al., "Electromyographic Activity and Posturing of the Human Neck during Rollover Tests," SAE Technical Paper [2005-01-0302](https://doi.org/10.4271/2005-01-0302), 2005, doi: [10.4271/2005-01-0302](https://doi.org/10.4271/2005-01-0302).

45. Kuppa, S., Saunders, J., Stammen, J., Mallory, A., *Kinematically Based Whiplash Injury Criterion*, in *19th International Technical Conference on the Enhanced Safety of Vehicles*. 2005, Paper 05-0211-O: Washington, D.C.

46. Viano, D.C., Olsen, S., Locke, G.S., and Humer, M., "Neck Biomechanical Responses with Active Head Restraints: Rear Barrier Tests with BioRID and Sled Tests with Hybrid III," SAE Technical Paper 2002-01-0030, 2002, doi:10.4271/2002-01-0030.

CONTACT INFORMATION

The authors can be contacted via the offices of Exponent Failure Analysis Associates, 23445 North 19th Avenue, Phoenix, AZ 85027, (623) 582-6949, 1011 Warrenville Rd., Suite 215, Lisle, IL 60532, (630) 743-770, or 3401 Market St., Suite 300, Philadelphia, PA, 19104, (215) 594-8800. Email addresses for the authors include the author's first initial and last name @exponent.com (e.g., krodowicz@exponent.com).

ACKNOWLEDGMENTS

The authors would like to express their sincere gratitude to the testing staff at the Exponent Test and Engineer Center for their efforts in conducting the testing that contributed to this research. Additionally, the authors would like to thank Mike Drzal and William Bussone from Exponent for their help with this document.

DEFINITIONS/ABBREVIATIONS

AIS

Abbreviated Injury Scale

ATD

Anthropomorphic Test Device

CG

Center of Gravity

FMVSS

Federal Motor Vehicle Safety Standard

HIC₁₅

Head Injury Criterion (15 ms)

HIC₃₆

Head Injury Criterion (36 ms)

IARV

Injury Assessment Reference Value

NHTSA

National Highway Traffic Safety Administration

N_{ij}

Normalized neck injury criterion

The Engineering Meetings Board has approved this paper for publication. It has successfully completed SAE's peer review process under the supervision of the session organizer. This process requires a minimum of three (3) reviews by industry experts.

All rights reserved. No part of this publication may be reproduced, stored in a retrieval system, or transmitted, in any form or by any means, electronic, mechanical, photocopying, recording, or otherwise, without the prior written permission of SAE.

ISSN 0148-7191

Positions and opinions advanced in this paper are those of the author(s) and not necessarily those of SAE. The author is solely responsible for the content of the paper.

SAE Customer Service:

Tel: 877-606-7323 (inside USA and Canada)

Tel: 724-776-4970 (outside USA)

Fax: 724-776-0790

Email: CustomerService@sae.org

SAE Web Address: <http://www.sae.org>

Printed in USA

SAEInternational

**SAE TECHNICAL
PAPER SERIES**

950352

Data and Methods for Estimating the Severity of Minor Impacts

Mark N. Bailey, Bing C. Wong, and Jonathan M. Lawrence
MacInnis Engineering Associates Ltd.

**Reprinted from: Accident Reconstruction: Technology and Animation V
(SP-1083)**

SAE *The Engineering Society
For Advancing Mobility
Land Sea Air and Space®*
INTERNATIONAL

**International Congress and Exposition
Detroit, Michigan
February 27 - March 2, 1995**

400 Commonwealth Drive, Warrendale, PA 15096-0001 U.S.A. Tel: (412) 776-4841 Fax: (412) 776-5760
EXHIBIT G

The appearance of the ISSN code at the bottom of this page indicates SAE's consent that copies of the paper may be made for personal or internal use of specific clients. This consent is given on the condition, however, that the copier pay a \$5.00 per article copy fee through the Copyright Clearance Center, Inc. Operations Center, 222 Rosewood Drive, Danvers, MA 01923 for copying beyond that permitted by Sections 107 or 108 of the U.S. Copyright Law. This consent does not extend to other kinds of copying such as copying for general distribution, for advertising or promotional purposes, for creating new collective works, or for resale.

SAE routinely stocks printed papers for a period of three years following date of publication. Direct your orders to SAE Customer Sales and Satisfaction Department.

Quantity reprint rates can be obtained from the Customer Sales and Satisfaction Department.

To request permission to reprint a technical paper or permission to use copyrighted SAE publications in other works, contact the SAE Publications Group.



GLOBAL MOBILITY DATABASE

All SAE papers, standards, and selected books are abstracted and indexed in the Global Mobility Database.

No part of this publication may be reproduced in any form, in an electronic retrieval system or otherwise, without the prior written permission of the publisher.

ISSN 0148-7191

Copyright 1995 Society of Automotive Engineers, Inc.

Positions and opinions advanced in this paper are those of the author(s) and not necessarily those of SAE. The author is solely responsible for the content of the paper. A process is available by which discussions will be printed with the paper if it is published in SAE transactions. For permission to publish this paper in full or in part, contact the SAE Publications Group.

Persons wishing to submit papers to be considered for presentation or publication through SAE should send the manuscript or a 300 word abstract of a proposed manuscript to: Secretary, Engineering Activity Board, SAE.

Printed in USA

90-1203D/PG

EXHIBIT G

950352

Data and Methods for Estimating the Severity of Minor Impacts

Mark N. Bailey, Bing C. Wong, and Jonathan M. Lawrence
MacInnis Engineering Associates Ltd.

ABSTRACT

Front, rear, lateral and side-swipe collisions were staged to correlate passenger vehicle damage to motion. Data from the staged collisions are used to develop severity-prediction methods for the four collision types. Human volunteers were present in many of the vehicles tested. Their responses, and the responses of human volunteers to staged impacts in other studies, are discussed in terms of impact severity.

For front and rear impacts, data are presented that correlate the post-impact condition of bumper systems to impact severity. These data build on data previously presented^{1,2,3}. A method for computing velocity change (ΔV) for vehicle to vehicle collisions from vehicle to barrier data is presented.

Data from staged low-speed lateral collisions correlate target and bullet vehicle damage to linear and angular velocity change (ΔV , $\Delta \omega$), impact location, pavement friction and collision force. It is shown how momentum, energy and restitution principles can be used to predict ΔV and $\Delta \omega$ from damage.

For staged side-swipe collisions, damage details are correlated to the target vehicle acceleration-time history. The vehicle motion is characterized as a vibration dose.

INTRODUCTION

Four types of "minor" collisions frequently occur. These are rear-end, front-end, lateral, and side-swipe, (Figure 1). Our previous work has concentrated on bumper properties and their relevance to "minor" rear-end impacts¹⁻³. The term "minor" is used to describe impacts where tire forces and/or restitution effects cannot be ignored. It is not used to reference vehicle damage or occupant symptoms.

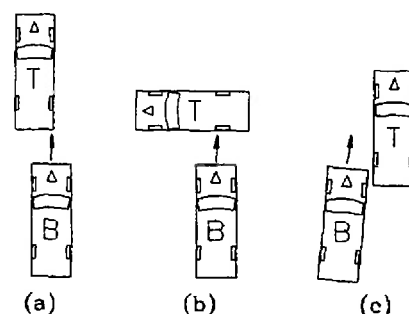


Figure 1. (a) rear and front-end; (b) lateral; (c) side-swipe
For any of the four types of collisions, the usual

question put to investigators is:

Are individuals who have experienced an apparently minor collision at risk of injury?

The diagnosis of injuries arising out of a minor collision is usually subjective. Objective clinical findings are often absent. The mechanism of a possible injury is not always well understood, so may sometimes be dismissed as being altogether absent. For example, it is unclear how neck or back symptoms occur in low-speed rear-end collisions when there is good head support. It may be, based on human volunteer tests (see McConnell et al⁴), that one possible injury mechanism is a rapid compression-tension cycle applied to the neck rather than, or in addition to, neck hyperextension. If that is the case, a neck injury mechanism can operate despite the head restraint. The type of detailed investigation that lead to that finding must

- 1) guide researchers to establish reasonable levels where symptoms can be produced,
- 2) identify injury mechanisms, and
- 3) devise safety measures to interrupt these mechanisms.

Data and methods in this paper focus on (1) above by relating levels of impact to the presence or absence of occupant symptoms. Vehicle motion, and meaningful ways to quantify it, are examined in four

types of minor collisions. The following descriptors of impact severity are discussed:

rear-end, front-end	ΔV
lateral	ΔV or $\Delta \omega$
side-swipe	$a(t)$, or $[a^4(t)dt]^{0.25}$

For staged collisions with human volunteers, impact severity is compared to the post-collision volunteer condition. Seat, posture, preparedness and physical condition are not included in the comparison. The volunteers were not instrumented, and only general details of their motion are discussed.

BACKGROUND

In collisions where a vehicle has permanent damage, for example several centimeters of frontal crush from an intersection collision, the amount of damage can be correlated to the collision severity. The method was first introduced by Campbell⁵, and has been adopted by various computer programs. An investigator attempts to quantify severity in terms of ΔV , the abrupt change in velocity of the vehicle's centre of mass from collision with another vehicle. ΔV follows directly from the crush of both vehicles. The correlation between crush and ΔV is made from a linear force-crush model, with two empirical coefficients determined from crash testing, then applying that to determine energy absorption, and finally ΔV .

Mathematically, from conservation of energy and conservation of momentum, it can be shown that for a plastic collision

$$\Delta V_1 = \sqrt{\frac{2(E_1 + E_2)(m_1 + m_2)}{m_1 m_2}} \quad (1)$$

where ΔV_1 is the velocity change of one vehicle, E_1 and E_2 is the energy absorbed by each vehicle (related to amount of damage), and m_1 and m_2 are the vehicle masses. The energy absorbed is determined from the degree of crush. In the absence of a direct correlation between energy absorption and crush, the energy absorbed is determined as follows (for the special case of uniform crush):

$$E_1 = L \left[AC + \frac{BC^2}{2} + \frac{A^2}{2B} \right] \quad (2)$$

where L is the crush width and C is the uniform crush depth. E_2 may be found similarly. The constants A and B are vehicle specific, and are different for the front, back and sides. Central to the method is the force-crush relationship, which incorporates the A and B coefficients.

$$F = A + Bx \quad (3)$$

where F is the force per unit width and x is the average crush depth. This model, while inappropriate for minor impacts, is used for higher speed impacts where there is plastic deformation. The complete energy absorption versus crush relation for a vehicle (an alternative to the force-crush model) would yield better results, though the economics are prohibitive. It should be noted that the ΔV is considered brief, on the order of 100 to 200 ms. It is implicit that any differences between duration in a barrier collision and a vehicle-to-vehicle collision do not affect the force-crush model because the structures are not strain rate sensitive at the speeds under consideration.

An important assumption of the method is that restitution effects and tire forces are small enough to be neglected. However, at lower speeds restitution is significant, and the collision force is often not small compared to available tire traction.

Another measure of severity, similar to ΔV , is the EBS (equivalent barrier speed), also referred to as the BEV (barrier equivalent velocity). Setting E_2 to zero and m_2 to infinity in Equation 1 yields the EBS. The EBS will be equal in magnitude to ΔV only in certain cases. The reader is referred to articles by Hight⁶ and Varat⁷ for further explanation. Specifically, in a plastic impact the ΔV and the EBS will be equal when the vehicle stiffnesses and masses are equal.

In attempting to estimate ΔV in minor rear-end, front-end and lateral collisions, methods analogous to the foregoing have been developed, with these additional factors included in the analysis:

- restitution is accounted for
- tire forces are accounted for
- direct energy-deformation data are used, so that a force-deformation model is unnecessary

Restitution is accounted for by including the equation for restitution with the momentum and energy equations. Tire impulse forces are accounted for with an $F\Delta t$ term in the momentum equation. A large quantity of energy-deformation data have been gathered for many vehicles in non-plastic impacts (in low-speed front or rear impacts the damage is slight or nil and the same vehicle can be tested repeatedly; several energy absorption-deformation data points can be acquired for the same vehicle). For a minor collision, it is a matter of correlating the damage with the energy absorbed, then solving the appropriate momentum, energy and restitution equations to estimate the ΔV .

An alternative method is to scale the EBS of one vehicle by a factor relating mass and stiffness of both vehicles,

$$\Delta V_1 = EBS_1 \sqrt{(m_2 / (m_1 + m_2))((k_1 + k_2) / k_2)}$$

which is only applicable for higher speed impacts. That method can make use of the force-crush model discussed above, which implies energy absorption is of the form $E = \frac{1}{2}kd^2$, where k is stiffness (force per unit crush) and d is deformation or crush. If energy versus deformation is quadratic in a bumper impact, results identical to the direct energy method can be anticipated if restitution is accounted for and tire effects are ignored.

EXPERIMENTAL PROCEDURE

All the vehicles that were tested met Canadian Motor Vehicle Safety Standards (CMVSS). As such, all vehicles had bumpers that met CMVSS 215, which stipulates that passenger cars must be free of lamp, lens and fuel tank damage and must be driveable after 8 km/h front and rear barrier impacts and 5 km/h corner impacts and 8 km/h pendulum impacts. The post-impact condition of the bumpers is exempted in the standard.

Front and rear collision data have been recorded for vehicle-to-vehicle and vehicle-to-barrier tests. For vehicle-to-vehicle tests the bullet vehicle was either driven or pushed into the stationary target vehicle. In all tests with volunteers the bullet vehicle was pushed and its engine was off. The vehicles had MEA 5th wheels attached to their sides which recorded vehicle position at 128 or 200 Hz. Some vehicles also had strain-gage type accelerometers mounted laterally and/or longitudinally on the transmission tunnel. From the 5th wheel data, time-varying velocity and acceleration can be derived. Figure 2 shows a 5th wheel velocity trace for a vehicle-to-barrier collision. Figure 3 shows acceleration derived from the same data shown in Figure 2. Acceleration from the 5th wheel is derived from a quadratic least squares moving average⁸. The acceleration compares favorably with the acceleration measured directly with an accelerometer mounted on the vehicle's transmission tunnel and from two load cells in the barrier at the bumper level.

Target/bullet vehicle pairs were usually collided several times at increasing severity and details of bumper or other damage were recorded after each individual collision. When volunteer occupants were present in the target vehicle the rear view mirrors were covered or removed so that there was no visual stimulus for the volunteer occupant to respond to. With the engine of the bullet vehicle off, there was also no audible stimulus for the volunteer. The volunteer occupants in all rear-end tests were asked to relax, but knew that an impact would occur in a

matter of minutes. Occupants in all front-end tests did not have any stimuli masked. Volunteers were asked to report any symptoms immediately after each test, and in the days following the test. For vehicle-to-barrier tests the vehicles were pushed frontwards or backwards into a rigid barrier. The barrier consists of two steel floor mounted trusses with a horizontal steel beam. The beam can be raised or lowered to accommodate varying bumper heights. A 10,000 lb (44,500 N) load cell is fitted between the horizontal beam and each vertical truss (two load cells total). Vehicles that were pushed into the barrier were fitted with an MEA 5th wheel mounted to the side. Biaxial accelerometers were also mounted to the transmission tunnels of some vehicles. Data were recorded at 128 or 200 Hz. As in the vehicle-to-vehicle tests, visual and audio stimuli were removed as much as possible for the collisions with volunteer occupants. However, a volunteer facing forward in a backward moving vehicle knows when the impact will occur due to his/her view of the surroundings and initial separation from the barrier. Initial separation from the barrier was about 10m or less for most tests.

Lateral collisions were staged on a level concrete or asphalt surface. The angle between adjacent sides of the vehicles was 90°. The bullet vehicle was equipped in each case with a 5th wheel mounted to its left or right side. In Tests 1 through 4 there were MEA 5th wheels mounted to the target and bullet vehicles to measure their forward velocities. The target 5th wheel had a pivoted rear mount to prevent damage from lateral post-impact movement. Two accelerometers were mounted on the transmission tunnel of the Toyota to measure lateral and longitudinal acceleration.

In tests 18 to 21 the bullet vehicle had two 10000 lb (44500 N) load cells mounted between its bumper beam and its bumper isolators, and an MEA 5th wheel was mounted on the target vehicle rear bumper parallel to the bumper to measure angular speed. Two uni-axial accelerometers were mounted on the target vehicle, one on the transmission tunnel and one directly above on top of the roof. The sensitive axes were oriented transverse to the vehicle's longitudinal axis to record lateral acceleration. The target vehicles were weighed to determine their overall and individual axle weights.

Side-swipe collisions 22 to 24 used the same bullet/target vehicle pair used in lateral tests 18 to 21. The lateral collisions were done on the vehicle right (passenger) side and the side-swipe tests were done on the left (driver's) side. The same instrumentation was used as in the lateral tests, except that the 5th wheel on the target vehicle was swung around parallel to the vehicle longitudinal axis and the roof. For side-swipe tests SS8 to SS19, the bullet vehicle was